

Assessment of the impact of climate change on Fraser River low flows

Aneesh Kochukrishnan

A Thesis

in

The Department

of

Building Civil and Environmental Engineering

Presented in Partial Fulfillment of the Requirements
for the Degree of Master of Applied Science (Civil Engineering) at

Concordia University

Montreal, Quebec, Canada

October 2020

© Aneesh Kochukrishnan, 2020

CONCORDIA UNIVERSITY

School of Graduate Studies

This is to certify that the thesis prepared

By: Aneesh Kochukrishnan

Entitled: Assessment of the impact of climate change on Fraser River low flows

and submitted in partial fulfillment of the requirements for the degree of

Master of Applied Science (Civil Engineering)

complies with the regulations of the University and meets the accepted standards with respect to originality and quality.

Signed by the Final Examining Committee:

_____Chair
Dr. Ali Nazemi

_____Examiner
Dr. Ketra Schmitt

_____Examiner
Dr. Ali Nazemi

_____Thesis Supervisor
Dr. S. Samuel Li

Approved by _____
Dr. Ashutosh Bagchi Chair of Department

Dr. Mourad Debbabi Dean

Date _____

ABSTRACT

Assessment of the impact of climate change on Fraser River low flows

Aneesh Kochukrishnan

During the winter season, rivers in cold regions typically carry low discharges. Long-term forecast of river low flows is of practical importance. For example, authorities need the forecast to decide on water resources allocations and permits of the maximum allowable waste-effluent discharges from the land-based industry into a receiving river. Low river flows have important implications for river water quality and the health of aquatic life. Previously, there have been many investigations of the influence of climate change on river discharge, both low and high flows. Some studies of the Fraser River in British Columbia, Canada, dealt with the influence of climate change on flow and water temperatures. However, there is a lack of studies that consider the impact on low river flows under climate change scenarios. This study aims at improving the understanding of the impact of rising temperatures due to climate change on the low flows of the Fraser River. Specially, this study will reveal how the magnitudes of historic Fraser River low flows are related to freezing temperatures and will answer the question of to what extent low flows will change in response to projected changes in atmospheric temperature. The scope of work includes statistical analyses of the correlation between historic observations of Fraser River flows and watershed air temperatures over a time period of more than 100 years. The temperature data input is derived based on averaging values from 52 stations in the Fraser River basin. The variations in flow discharge with varying temperatures show uncertainties over the years. This study considers the cumulative freezing and thawing effects of fluctuating temperatures and divides the observed winter low flows into a lower limb and an upper limb. The correlation between discharge, Q , and temperature is established on the basis of the lower limb, yielding Q as a function of cumulative temperature, τ , in terms of z scores of the two variables. Global land and ocean surface temperature anomalies in the historical data are noted in several of the historic years, but their influence is removed while establishing this Q - τ relationship. A confidence bound relationship between flow and temperature is established for the thawing days, where the flow increases from its lowest value. The Q - τ relationship is further applied for forecast of future low flows, with input of temperatures from six Global Climate models (GCMs) with Representative Concentration Pathways (RCPs) 4.5 & 8.5 of the NASA Earth Exchange Global Daily Downscaled Projections (NEX GDDP) dataset. Long term forecast of river low flows is obtained. The results show an increase in the minimum flow discharge up to 48% under high emission scenarios by the end of the 21st century. Under low emission scenarios, the minimum flow discharge can increase by 11%. The methods developed in this study can be applied to other cold region rivers. This is useful for addressing the issue of climate change impacts on river low flows, making necessary adjustments to the hydraulic design of water resources infrastructures, and planning the protection of aquatic life.

ACKNOWLEDGEMENT

I would like to express my sincere gratitude to Dr. S. Samuel Li who has supervised my research project. Thanks to him for his expert advice and guidance throughout this thesis process. It was a great honor working with him and his patience and valuable feedbacks are of paramount importance in framing out this research. Thanks to Dr. Amruthur S. Ramamurthy for his help.

I thank my parents and brother for their sacrifice, support, and appreciation during these last two years. Thanks to all my friends and colleagues who cheered and encouraged me in completing this thesis.

Contents

List of Symbols.....	vii
List of Acronyms	viii
List of Figures	ix
List of Tables	xiii
Chapter 1 Thesis Overview	1
1.1 Background	1
1.2 Objectives.....	2
1.3 Significance of this study	3
1.4 Overview of this thesis.....	3
Chapter 2 Literature Review.....	5
2.1 The Fraser River.....	5
2.2 Low flow hydrology	8
2.2.1 Factors affecting low flow	9
2.2.2 Impacts of low flow	11
2.3 Water Chemistry of the Fraser River.....	12
2.4 Sedimentation in rivers	13
2.5 Effects of low flow on aquatic ecosystem.....	16
2.6 Salinity in rivers	16
2.7 Influence of climate.....	17
2.7.1 Influence of climate on stream flow hydrology	17
2.7.2 Influence of climate on low flows	20
2.7.3 Influence of climate on snow hydrology.....	22
2.7.4 General Circulation Models (GCM).....	22
Chapter 3 Methodologies	25

3.1 Data collection	25
3.2 Data processing.....	28
3.3 Selection of temperature variable	28
3.4 Classification of Data	31
3.5 Outlier identification	32
3.6 Establishing a Functional fit	40
3.7 Application of Function to IPCC- CIMIP5 Climate Models.....	41
Chapter 4 Results and Discussion	43
4.1 Application of Functional fit.....	43
4.2 Estimation of Low Flow.....	46
4.2.1 Low flow estimation with inputs from Canada’s climate changing report.....	46
4.2.2 Low flow estimation based on NASA NEX GDDP - CMIP5 GCMs	49
4.2.3 Model ensemble forecast of low flow.....	67
Chapter 5 Conclusions and Future Studies	73
5.1 Concluding remarks.....	73
5.2 Suggestions for future research.....	75
References	76

List of Symbols

The following symbols have been used in this thesis:

Q = Projected minimum yearly discharge.

\bar{Q} = Average of minimum discharge from historic data.

σ_Q = Standard deviation of minimum discharge in historic data.

τ = Model Minimum cumulative temperature.

$\bar{\tau}$ = Average of Minimum Cumulative temperature from historic data.

σ_{τ} = Standard deviation of Cumulative temperature from historic data.

a, b are the coefficients of the fit.

$^{\circ}\text{C}$ = Centigrade

τ_{min} = Average annual minimum cumulative temperature from historic records

$\sigma_{\tau_{min}}$ = Standard deviation of annual minimum cumulative temperature from historic record

τ_Z = Standard score value of Cumulative temperature

$\tau_{min (HE)}$ = Expected increase in the cumulative temperature for the minimum flow in high emission scenario (RCP 8.5)

$\tau_{min (LE)}$ = Expected increase in the cumulative temperature for the minimum flow in low emission scenario (RCP 4.5)

List of Acronyms

GCM – General Circulation Model

IPCC - Intergovernmental Panel on Climate Change

CIMIP5 - Coupled Model Intercomparison Project 5

NEX GDDP –Earth Exchange Global Daily Downscaled Projections

RCP - Representative Concentration Pathway

BC – British Columbia

WSC – Water Survey Canada

CO₂ – Carbon dioxide

AR4 – Assessment Report 4

VIC - Variable Infiltration Capacity

ENSO- El Niño–Southern Oscillation

PDO - Pacific Decadal Oscillation

AMO - Atlantic multidecadal oscillation

SST – Sea Surface Temperature

DMD – Daily mean discharge

CWT – Cumulative watershed temperature

List of Figures

Figure 2.1 Annual extremes of Fraser River flow at Hope, B.C. (WSC, 2020).	6
Figure 2.2 A map of the Fraser River basin, modified from MacLean (2009).	7
Figure 2.3 Flow duration curves for six Canadian regions (Burn et al., 2008).	9
Figure 2.4 Four hydrological regimes in British Columbia - examples (Carver et al., 2009).	10
Figure 2.5 Fraser river basin with 11 sub-basin outlets as per WSC (Shrestha et al., 2012).	18
Figure 2.6 Representation of grids in a GCM (IPCC, 2020)	23
Figure 2.7 Expected change in the surface temperature as per IPCC report (Pachauri et al., 2015)	24
Figure 3.1 Location of climate stations in the Fraser River basin where the temperature data was obtained (Image layer taken from google maps).	26
Figure 3.2 Time series of daily mean discharge (DMD) and cumulative watershed temperature (CWT)	30
Figure 3.3 Time series of daily mean discharge (DMD) and daily watershed temperature (WT)	30
Figure 3.4 Sample division of a hydrological year into falling and rising limbs.	31
Figure 3.5 Outlier years highlighted	32
Figure 3.6 Increase of DMD with increasing CWT in terms of z scores for the hydrological year 1916.	34
Figure 3.7 Increase of DMD with increasing CWT in terms of z scores for the hydrological year 1930	34
Figure 3.8 Increase of DMD with increasing CWT in terms of z scores for the hydrological year 1931	35
Figure 3.9 Increase of DMD with increasing CWT in terms of z scores for the hydrological year 1934	36
Figure 3.10 Increase of DMD with increasing CWT in terms of z scores for the hydrological year 1941	36
Figure 3.11 Increase of DMD with decreasing CWT in terms of z scores for the hydrological year 1954	37

Figure 3.12 Increase of DMD with increasing CWT in terms of z scores for the hydrological year 1963	37
Figure 3.13 Increase of DMD with increasing CWT in terms of z scores for the hydrological year 1968	38
Figure 3.14 Increase of DMD with increasing CWT in terms of z scores for the hydrological year 1970	38
Figure 3.15 Increase of DMD with increasing CWT in terms of z scores for the hydrological year 1992	39
Figure 3.16 Increase of DMD with increasing CWT in terms of z scores for the hydrological year 2005	39
Figure 4.1 Variation of low flow with respect to standard z score of cumulative watershed temperature.	46
Figure 4.2 Location of GCM grids in the Fraser River basin where the temperature data was obtained (Image layer taken from google maps).....	50
Figure 4.3 Forecast of minimum watershed cumulative temperature for RCP 4.5 from model: CanESM2.	52
Figure 4.4 Forecast of minimum discharge for RCP 4.5, on the basis of temperature from model: CanESM2.	52
Figure 4.5 Forecast of minimum watershed cumulative temperature for RCP 4.5 from model: CCSM4.....	53
Figure 4.6 Forecast of minimum discharge for RCP 4.5, on the basis of temperature from model: CCSM4.....	53
Figure 4.7 Forecast of minimum watershed cumulative temperature for RCP 4.5 from model: CNRM-CM5.	54
Figure 4.8 Forecast of minimum discharge for RCP 4.5, on the basis of temperature from model: CNRM-CM5.....	54
Figure 4.9 Forecast of minimum watershed cumulative temperature for RCP 4.5 from model: CSIRO-Mk3-6-0.....	56
Figure 4.10 Forecast of minimum discharge for RCP 4.5, on the basis of temperature from model: CSIRO-Mk3-6-0.....	56

Figure 4.11 Forecast of minimum watershed cumulative temperature for RCP 4.5 from model: INM-CM4.	57
Figure 4.12 Forecast of minimum discharge for RCP 4.5, on the basis of temperature from model: INM-CM4.	57
Figure 4.13 Forecast of minimum watershed cumulative temperature for RCP 4.5 from model: MPI-ESM-LR.	58
Figure 4.14 Forecast of minimum discharge for RCP 4.5, on the basis of temperature from model: MPI-ESM-LR.	58
Figure 4.15 Forecast of minimum watershed cumulative temperature for RCP 8.5 from model: CanESM2.	60
Figure 4.16 Forecast of minimum discharge for RCP 8.5, on the basis of temperature from model: CanESM2.	60
Figure 4.17 Forecast of minimum watershed cumulative temperature for RCP 8.5 from model: CCSM4.	61
Figure 4.18 Forecast of minimum discharge for RCP 8.5, on the basis of temperature from model: CCSM4.	61
Figure 4.19 Forecast of minimum watershed cumulative temperature for RCP 8.5 from model: CNRM-CM5.	62
Figure 4.20 Forecast of minimum discharge for RCP 8.5, on the basis of temperature from model: CNRM-CM5.	62
Figure 4.21 Forecast of minimum watershed cumulative temperature for RCP 8.5 from model: CSIRO-Mk3-6-0.	64
Figure 4.22 Forecast of minimum discharge for RCP 8.5, on the basis of temperature from model: CSIRO-Mk3-6-0.	64
Figure 4.23 Forecast of minimum watershed cumulative temperature for RCP 8.5 from model: INM-CM4.	65
Figure 4.24 Forecast of minimum discharge for RCP 8.5, on the basis of temperature from model: INM-CM4.	65
Figure 4.25 Forecast of minimum watershed cumulative temperature for RCP 8.5 from model: MPI-ESM-LR.	66

Figure 4.26 Forecast of minimum discharge for RCP 8.5, on the basis of temperature from model: MPI-ESM-LR.	66
Figure 4.27 Forecast summary of low flow for RCP 4.5, on the basis of temperature...	68
Figure 4.28 Forecast summary of low flow for RCP 8.5, on the basis of temperature...	68
Figure 4.29 Combined model forecast of cumulative watershed temperature for RCP4.5	69
Figure 4.30 Combined model forecast of minimum discharge for RCP 4.5, on the basis of temperature.	69
Figure 4.31 Combined model forecast of cumulative watershed temperature for RCP8.5	70
Figure 4.32 Combined model forecast of minimum discharge for RCP 8.5, on the basis of temperature.	70

List of Tables

Table 2.1 Summary of processes influencing low flow, modified from Burn et al. (2008).	11
Table 3.1 List of climate stations	27
Table 3.2 List of stations along with their locations chosen for downscaled GCMs.....	41
Table 3.3 A list of GCM models used in this study. (Details obtained from Program for climate model diagnosis and intercomparison (2020).	42
Table 4.1 Variation of low flow with respect to z score values of cumulative watershed temperature, with 95% confidence interval.....	44
Table 4.2 Estimates of low flow using inputs from Canada’s Changing climate report (Bush et al., 2019).....	49

Chapter 1

Thesis Overview

1.1 Background

The quantity of low flow in rivers depends up on several factors known to us such as precipitation in the catchment area, the extent of the catchment area and the land use, geological characteristics such as ground water and soil moisture, atmospheric temperature, anthropogenic interventions and climate change, to name a few of them. Typically, low flow is a concern of countries with water shortage during summer.

Low flows are categorized into two types by the World Meteorological Organization based on the season of the event, namely summer low flow, and winter low flow. Snowfall and snow storage during sub-zero temperatures will accumulate the precipitation and reduces the winter low flow levels. Low flow estimates are useful in water resources planning, forecasting the stream flows, estimating the limits of the effluent discharge to maintain water quality, navigation, hydropower designs, irrigation system designs, protection of aquatic life (World Meteorological Organization (Geneva), 2008).

There are several types of low flow regimes described based on different applications in the industry (Gustard et al., 1992). Minimum flow is a concern for the water quality for aquatic life due to the increased concentration of pollutants due to the decreased water volume for dilution. Annual minimum flow regime is important for estimating the drought return period and preliminary design of water supply schemes (World Meteorological Organization (Geneva), 2008).

The Fraser River, also known as Salmon river, is the largest river in the Canadian Province of British Columbia, with a drainage area of approximately 217,000 km², starting from the Rocky Mountains and flowing for a length of 1370 km to the Strait of Georgia (Thomson, 1981). This river is the spawning ground for sockeye and chinook salmon species. Temperatures spanning from 20 to 24°C for several days can cause decrease in spawning rates to death of these salmons (Gilhousen, 1990).

Low flow forecasts are of notable importance in the design and management of hydraulic structures. For example, the maintenance of hydraulic structures is best done during low flows to reduce the cost and infrastructure requirements for flow diversion. Also, there will be a significant increase in sediment deposition due to low flows which reduces the efficiency of hydraulic structures. Hence, there is a need of such impact assessment in the Fraser River using probabilistic climate change information.

The future prediction of low flows involves a lot of ambiguities like errors in the observations of historical discharge, errors in temperature and precipitation observations and uncertainties due to climate forcing to name a few. Climate change is expected to disturb the river hydrology and water temperature which in turn affects the river ecosystem and water usage (van Vliet et al., 2013). There have been predictions of an increase of temperature in British Columbia up to 5.2°C by 2100 from the 1986-2005 level (Bush et al., 2019). There is a clear need to understand the expected variations in the low flow levels under the influence of this increasing temperature.

1.2 Objectives

The purpose of this research is to formulate a statistical solution for the prediction of future low flows under the influence of climate change in the Fraser River. A model is developed to predict the low flow variations till the end of this century based on the inputs from a few Global climate models and other recognized researches. The main objectives of this thesis are to:

- forecast the annual low flow of the Fraser River till the end of this century due to climate change factors;

- formulate a statistical function based on more than 100 years of historical records of Fraser River discharge and average temperatures of catchment area.

1.3 Significance of this study

The topic of low flow is of prime importance in the design of hydraulic structures and protection of the aquatic environment and a wide range of other applications. The estimate of future low flow forecast in the Fraser River under climate change scenarios is very limited. The significances of this analytical research are:

- Classification of the historical records of Fraser River flow during the cold season into two segments: an upper limb, and a lower limb, based on the decreasing and increasing discharges, respectively. It is important to identify the low flow scenarios and classify the thawing effect of river under the increasing temperature.
- Identification of outliers in annual trends of lower limb and attribution to various atmospheric oscillations as their probable cause. The outliers are to be separated to arrest their influence in the data and obtain a valid statistical solution.
- Formulation of a statistical solution (a function) for predicting the minimum flow values in the Fraser River where the temperature is given as input.
- Application of the function to the temperature increment outputs of recognized research for estimates of the expected changes in the low flow.
- Application of the function to various GCM models under two different RCP's for forecasts of the expected changes in the low flow values until 2100.

1.4 Overview of this thesis

This thesis is written in the following order to best reflect the research: Chapter 2 provides a detailed review of a wide range of literatures related to the Fraser River and

low flow. It covers sediment transport in low flow, the influence of pine beetle on the hydrology of the Fraser River, the projection of low flows under climate change, water chemistry of the Fraser River, saltwater intrusion, infauna distribution and other related literatures.

The methodologies adopted in this analytical research are explained in Chapter 3. It discusses the sources of data collection, classification of freezing & thawing limbs, separation of outlier years with probable causes linked to climatic oscillation and formulation of the statistical solution and further methods of estimation of annual minimum flow till the end of 21st century using the outputs from Canada's climate change reports.

Chapter 4 is dedicated to the presentation of the results of the forecasting of low flows by an analysis of climate models. A model ensemble-based solution is also discussed, along with the implications of the results in the future and steps to be taken to accommodate the impacts of the climate change to the hydraulic structure design and also for the protection of the aquatic environment.

Chapter 5 presents conclusions from this research, and suggestions for further studies on the topic of low flow in rivers.

Chapter 2

Literature Review

This chapter presents a review of the pertinent literature about the low flow in rivers, factors affecting low flow and its estimation, sedimentation in rivers, salinity during low flow, the chemistry of water in the Fraser River, aquatic effects due to variations in low flow and the influence of climate on snow hydrology and river runoff.

2.1 The Fraser River

The Fraser River is the largest river without a dam on the west coast of North America and it is the fourth largest river in Canada (Dashtgard et al., 2012; Krishnappan, 2000). It has a total length of 1375 km, starting from the rocky mountains and ending up in the Strait of Georgia in the Pacific Ocean (Krishnappan, 2000). The drainage area of the Fraser River is around 228,000 km² and the mean annual discharge at Hope, B.C., is 2710 m³s⁻¹. Low flow occurs in winter and it ranges around 1000 m³s⁻¹ and the peak flows range between 5130 and 15200 m³s⁻¹ (WSC, 2020). Figure 2.1 shows the annual extremes of Fraser River discharge at Hope, B.C.

The Fraser River serves as a transportation channel for the Canadian Cordillera and has a significant population of Salmon and hence is of economic and environmental importance. Large pulp and lumber mills are situated along the banks of the Fraser River and they discharge their effluents into this river. Treated municipal sewage also gets discharged into the river from several cities (Ministry of Environment, Lands, and Parks,

1997). Figure 2.2 shows the basin map of the Fraser River adapted from the map prepared by MacLean (2009).

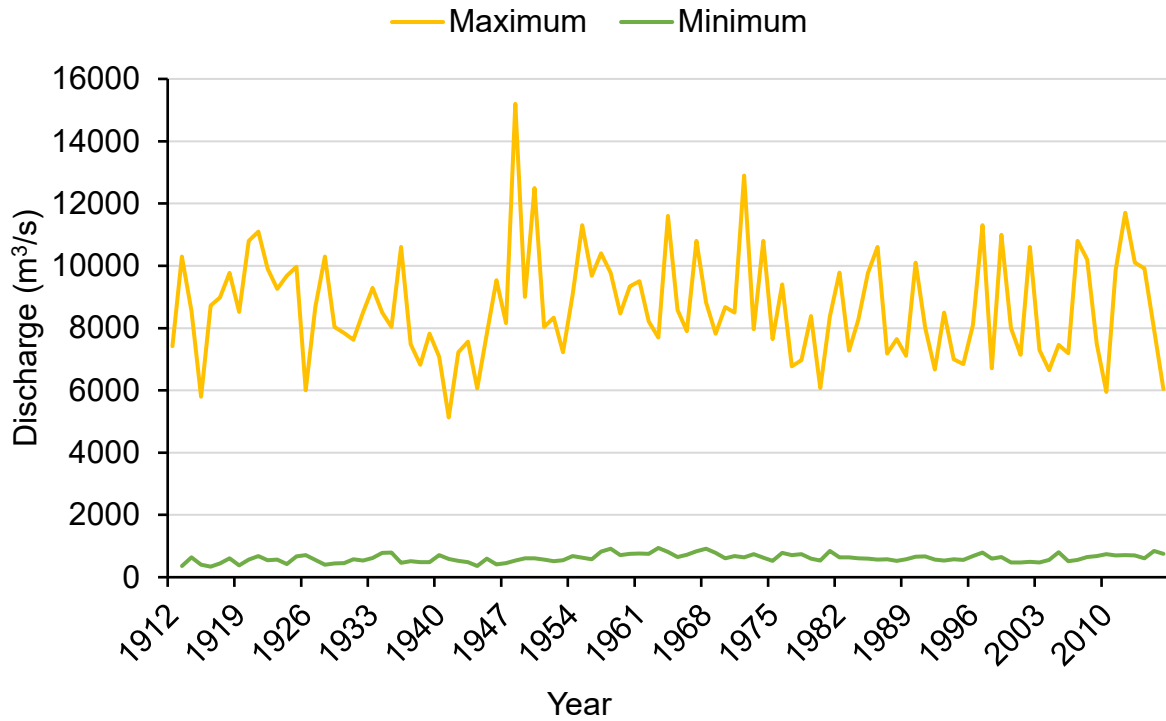


Figure 2.1 Annual extremes of Fraser River flow at Hope, B.C. (WSC, 2020).

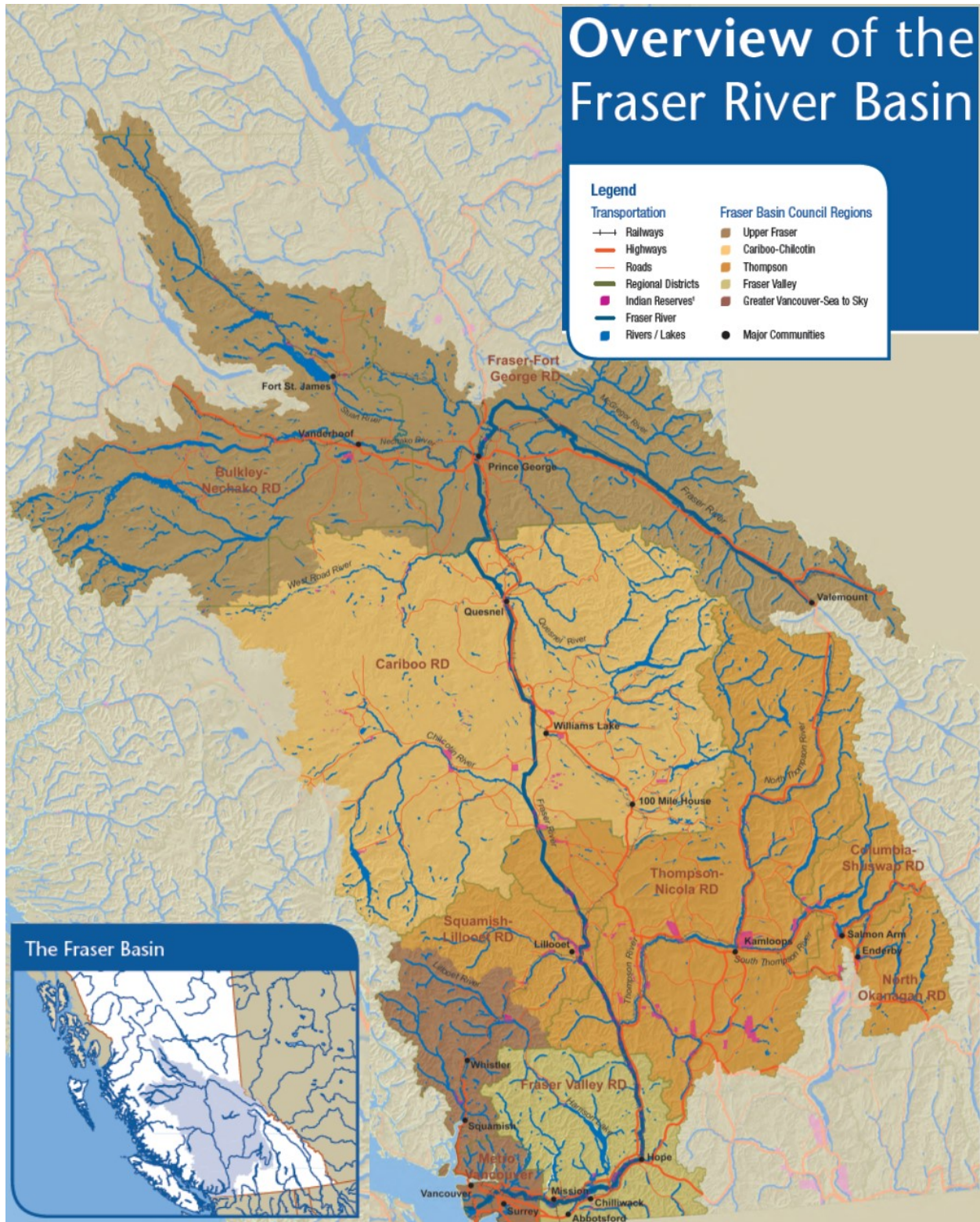


Figure 2.2 A map of the Fraser River basin, modified from MacLean (2009).

Canadian Cordillera spans from the Pacific coast to the Rocky Mountains. The altitude of these mountains range over 3000 m above the mean sea level. Their geology and geomorphology are distinct. A glacier is present in almost half of the gauged watersheds in British Columbia. It has a varying physiography and climate, and all river basins have many different bio geoclimatic zones (Burn et al., 2008).

2.2 Low flow hydrology

Low flow develops over time and its persistence creates socio-economic and environmental impacts. There are different definitions for low flow based on the interest of applications. The definition as per International glossary of hydrology is that 'low flow is flow of water in a stream during prolonged dry weather'. Low flows generally gain water from groundwater or surface discharge from lakes or melting glaciers. There are temporal and spatial components to low flow hydrology and these components are affected by climate, topography, and geology etc. A good understanding of low flow components such as the magnitude and frequency of low flow streams is essential for water resources management (Smakhtin, 2001).

The definition of low flow is to be contemplated beyond the mere concept of storage depletion and better represents the complex interactions between storages. Several preliminary works are detailed, including new methods and models for low flow predictions in catchments with no data availability (Whitfield, 2008). A detailed study is necessary to understand the effects of climate and land-use changes on low flow.

Low flows in British Columbia are mostly due to perpetual snow and winter low flows with exceptions in the low elevation rainfall systems along the coast. The span of the winter low flow depends on the fluctuations of the temperature around the freezing point. In addition to this, low flow is influenced by climate and elevations of the basin (Carver et al., 2009).

The low flow estimation methods vary from one country to another based on the risks it possesses during low flow. The most common method is use of regression analysis, mean discharge as a function of catchment properties such as annual

precipitation, drainage density, elevation etc. It can also be estimated using hydrological models with climate inputs. (Carver et al., 2009)

Figure 2.3 from Burn et al. (2008) shows the flow duration curves for six Canadian regions based on the sample inputs from 51 gauge stations .

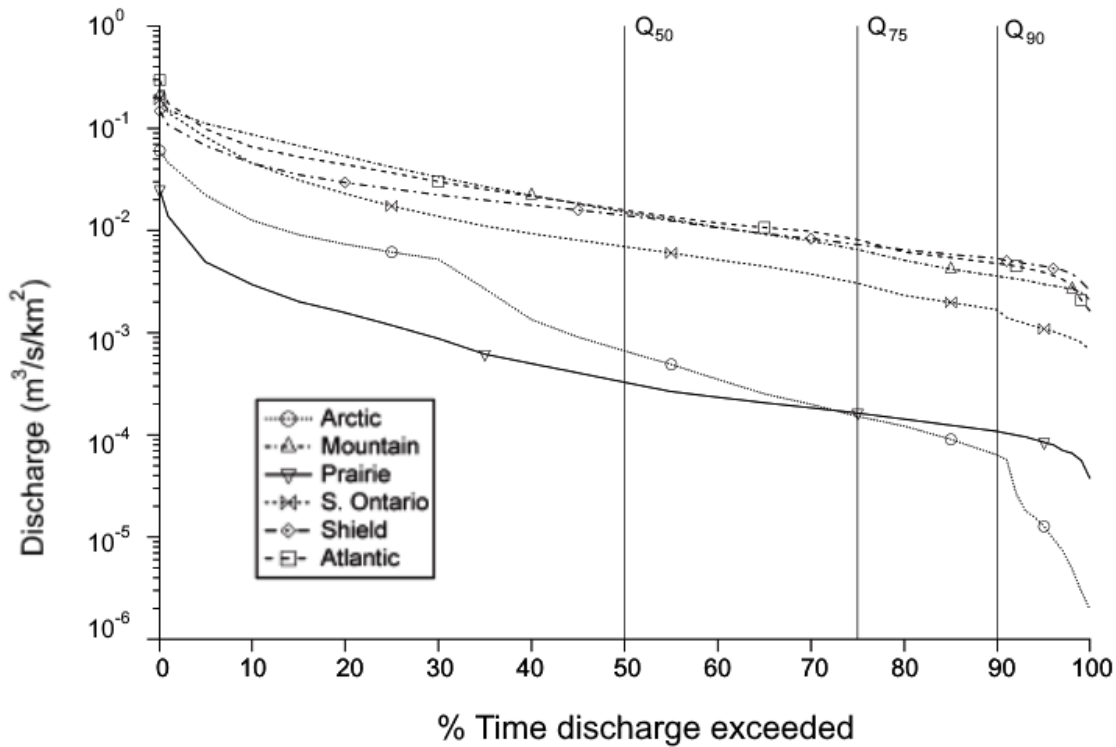


Figure 2.3 Flow duration curves for six Canadian regions (Burn et al., 2008).

2.2.1 Factors affecting low flow

Natural factors affecting low flow are: soil infiltration properties; the hydraulic characteristics and size of aquifers; the rate and frequency of recharge; evapotranspiration rates from basin, vegetation, topography; and climate. Major contribution to the low flow is from the groundwater reserves and is dependent on the characteristics of aquifers. The losses from the low flow may be caused by the transmission losses such as evapotranspiration, infiltration, and bed losses. In cold regions the low flow losses mainly occur due to the influence of permafrost on ground water contribution and low flow generally decreases with altitude. In these regions the

ivers have low flow during winter due to the accumulation of precipitation as snow (Smakhtin, 2001).

Anthropogenic factors which impact the low flow regime include groundwater abstraction, drainage of valley bottom soils for agriculture or construction, deforestation and changes to the vegetation system of the catchment area, effluent flows into rivers, discharge from agriculture, construction of river regulatory structures such as dams (Smakhtin, 2001).

Low flow magnitudes depend on the storage availability in the catchment or watershed. Prediction of low flow requires monitoring of water levels in surface and subsurface sources and soil moisture content. Augmentations in low flow may also arise from anthropogenic activities such as abstraction of water and effluent discharge, land use or land cover changes. Figure 2.4 from Carver et al. (2009) shows the examples of four hydrological regimes in British Columbia.

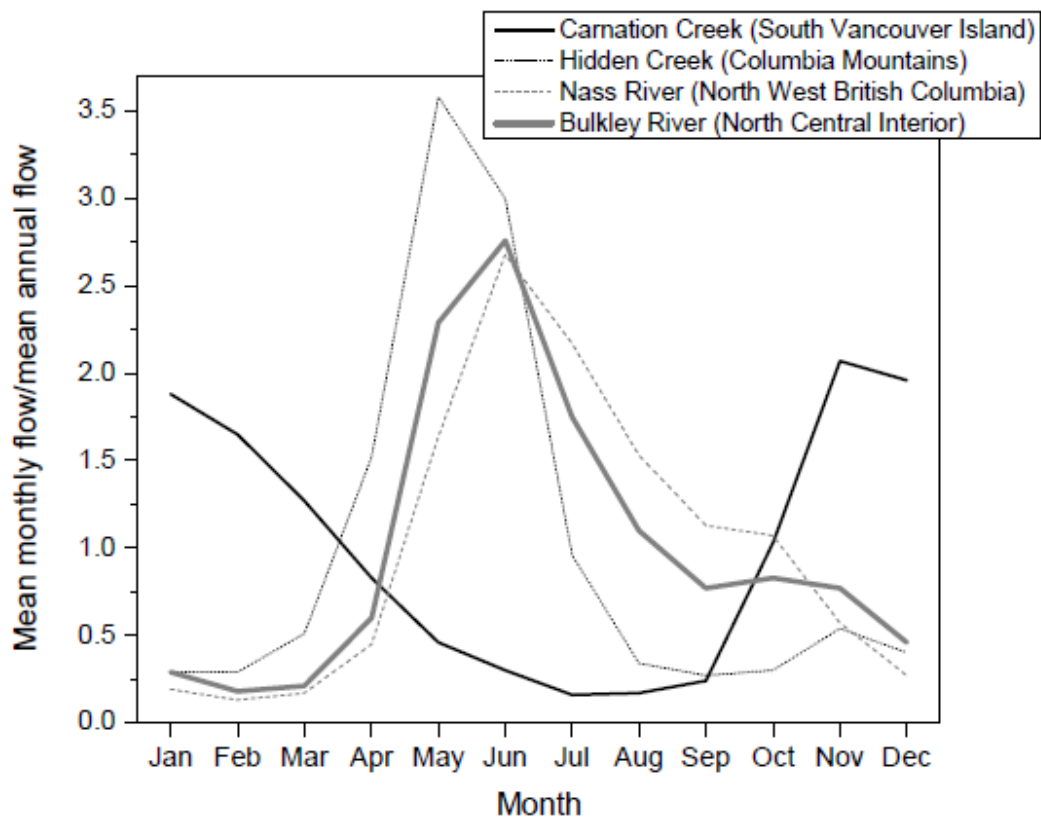


Figure 2.4 Four hydrological regimes in British Columbia - examples (Carver et al., 2009).

Table 2.1 from Burn et al. (2008) shows a summary of processes influencing low flow in six Canadian regions based on inputs from 51 gauge stations.

Process	Region					
	Arctic	Mountain	Prairie	S. Ontario	Shield	Atlantic
Low precipitation or moisture availability	•	•	•	•	•	•
Sub-freezing temperatures	•	•	•		•	•
Lake and wetland storage	•		•	•	•	•
Soil water storage and release	•		•	•	•	•
Basin size	•			•		•
Aquifer storage and hydraulic connection		•				
Snowpack, snowmelt, and glacier melt	•	•				

Table 2.1 Summary of processes influencing low flow, modified from Burn et al. (2008).

For every region in Canada the dominant processes affecting low flow are a combination of different factors. Shortage of rainfall/snowfall and moisture is a common factor in all regions. Low flow in most of the regions including Mountains, where Fraser River drainage area is present, are affected by sub-freezing temperature leading to winter low flow. Snowpack, glacier and its melting contribute to low flow in the Mountain region (Burn et al., 2008).

2.2.2 Impacts of low flow

Aquatic species generally adapt to live in the regular low flow durations. The design of water resources management system is based on the return periods of low flows of certain value. Despite of such physiological adaptation and engineering consideration,

low flow can become a hazard to the ecosystem and water management systems. The low water and deteriorated water quality pose severe threats during summer low flow than winter low flow for salmons. The operations of hydraulic structures are to be adjusted during low flows for the mobility of benthic species and this in turn could disturb the hydroelectric power generation (Carver et al., 2009).

Significant social and economic influences can be induced by changes in low stream flow. Low flow can impact fisheries and aquatic life. It's important to comprehend the processes that result in low flow for water resources management and mitigation of low stream flow hazards. Data of river discharges from 51 Water Survey of Canada (WSC) gauging stations are chosen from six regions of Canada as a sample to represent the regions and their hydrograph is plotted for a single year to find their low flow characteristics of the regions. The six regions are Artic, Mountains(British Columbia), Prairies, southern Ontario, Canadian Shield and Atlantic (Burn et al., 2008).

Warm and dry seasons pose more threat of socio-economic impacts due to low flows and poor water quality in Canadian Cordillera. This affects the ecology of cold-water species like salmonids, which form the economy and culture of many First Nations (Burn et al., 2008).

There is chance of significant hydrological impacts in the Fraser River basin due to the rescue from harvesting of pine trees. The geomorphology and scale of the Fraser River basin prevent the observation and estimation of hydrologic impacts. A low-flow hazard model was developed using the harvest scenario for Fraser River watersheds to investigate the effects of pine beetle infestation on the hydrology of the Fraser River. The hazard model is compared with the variable infiltration-capacity modeling results (Carver et al., 2009).

2.3 Water Chemistry of the Fraser River

Chlorophenol concentrations during fall low flows were compared with winter low flows to understand the impact of seasonal flow variations and sediment concentrations. Pulp mills are the important source of chlorophenolics to the aquatic environment of the

Fraser River. Measurement was taken using a continuous centrifuge during both fall and winter low flows at three sites downstream to the pulp mills and one station upstream from the mills. The winter low flow had higher concentration of three chlorophenol compounds than that in fall low flow. This brings to an inference that the higher concentrations of these compounds are due to the decrease in both river flow and suspended sediment concentration. These compounds were even traced 450 km downstream from the nearest pulp mill (Sekela et al., 1999).

To protect the socio-economic activities in and around the Fraser River, it is important to maintain the quality of its water. A study was conducted to record the chemistry of the water. Samples from 17 sites along the Fraser River and its tributaries were analysed for various chemical components like major cations, anions, 28 dissolved traces and ultras-trace elements, and isotope ratios of oxygen, hydrogen, sulphur, carbon and strontium; their sources are identified. Further, the anthropogenic additions like dissolved organic carbon and sodium chloride from pulp mills are recognized. During high flows, the Fraser River contains high levels of CO₂, which is from the decayed vegetation or from timber mills (Cameron et al., 1995).

2.4 Sedimentation in rivers

The transportation mechanism of the suspended sediment particles under low flow conditions in the Fraser River is investigated by studying the size distribution of these particles and comparing it with the size distribution of the ultrasonically dispersed sediments collected. Size distribution is a significant property which governs the transportation of sediments, and their deposition and adsorption of contaminants. The investigation showed that the suspended particles are transported after agglomeration as flocs. The study of the transport mechanism is to determine the impact of the pollutants on water quality and benthic aquatic life. Earlier studies have shown that the intrusion of saline water contributes to flocculation, and the freshwater flocculation is mainly due to organic particles and other contaminants from industries and sewage treatment plants. The size distribution data of the suspended particles were rarely available for low flow conditions for the Fraser River because the traditional methods disturb the agglomerated

sediments. Benthic organisms and water quality are affected by the resuspension of settled particles (Krishnappan, 2000).

Sediments at the low reaches of the Fraser River show the attributes of both river and tidal processes. Coarse grained sand is deposited during decreasing flows due to snow melt, and fine-grained sand is deposited during late stage of decreasing thaw flows and base flow. Trace assemblage and bioturbation are more evident when the saline water sustains for a longer duration in the bed. The benthic animal diversity reduces to 14% in intertidal sediments from fully marine flats. Sedimentological and ichnological natures of sediment deposition in the tidal-fluvial transition zone are identified. These characteristics help differentiate sediments deposited within freshwater-tidal reaches, brackish water (more saline) - tidal reaches, and mixed tidal-river distributaries. This study could be helpful to predict the quantity and duration of saltwater intrusion based on the influence of tidal and river flow in sediment deposition (Dashtgard et al., 2012).

The relationship between channel instability and sediment transport is studied between Mission and Hope, B.C., in the lower Fraser River by examining its morphological features and the historical characteristics of the channel. This macroscopic study was required to understand the future evolution of the Fraser River channel on year to decadal scale, which will be helpful in solving engineering and river management problems. It was diagnosed that erosions may happen also in seasons with low stream flow (McLean, 1990).

The transport of sediments into and out of the lower Fraser River was estimated to have a sedimentary budget. Sediment carriage to the sand-bed and delta was measured and presented as annual hydrograph. This experimental study was carried out to understand the seasonal distribution of suspended sediment flow and to compare the result with the historical data. The measured distribution was lower than the load in the observations between 1966 and 1986 by Water Survey of Canada. The annual sediment load in 2010 was around 7.2M tonnes and out of that 70% was found to be silt and clay. About 94% of the total load was transported during flows above 1000 m³/s. The interchange of sand between the channel bed and active load determines the total sediment budget of the downstream and is associated to channel stability. Prolonged

dredging activities for maintaining the shipping channel have reduced the sediment budget in the lower Fraser River (Attard et al., 2014).

The relationship between river flow, sediment transport and morphology of the river channel is used to estimate sediment transport rates and its budget. A 2-dimensional numerical model was developed, which included along-channel and cross-channel sediment transport interactions, to predict the bedload transport and channel morphology of the gravel reach of the Fraser River. The output from an existing hydrodynamic model was combined with the bedload transport calculations and the channel morphology. The gravel reach is a wandering 70 km channel located roughly between Mission and Hope, B.C. Effectiveness of gravel extraction from the aggrading zones was numerically analysed to understand the effects of channel instability in the future. The study highlighted several factors critical for the estimation of bed load appropriate for gravel-bed rivers. The process provides a basis for managing gravel such as its extraction to avoid floods or navigation issue and to conserve the ecosystem (Li et al., 2008).

Bars in rivers provide details about the sedimentation processes and they have records of the past environment. Various methods were used to analyse the geomorphology of gravel bars in the 50 km stretch of the lower Fraser River. The work analysed the depositional processes and sedimentation of river channels along with a hierarchical classification of wandering style, a description of the development of two types of bars, estimates of accumulation and erosion rates for unit and compound bars, and a description of structures of the bar strata. The connection between short term sedimentation and long term evolution of bars are shown, and the rates of morphological changes are estimated (Rice et al., 2009).

A better idea of the influence of low angle dunes on the flow is critical to predict sediment transport and channel resistance. The study inspected the sediment flow and sediment suspension events over low-angle dunes in the Fraser estuary. Bathymetry of dunes was mapped along with the river flow measurements and sediment flow measurements. Mean flow and suspension events were analysed in the unsteady flow of the Fraser estuary and their variations with tidal cycle were noticed. River flow was the highest during low tide and majority of the sediments, around 69%, were transported

during this period. At high tides, the river flow reduces drastically and a salt wedge enters the river and shifts the freshwater to the surface due to the density gradient (Bradley, 2012).

2.5 Effects of low flow on aquatic ecosystem

The Infauna distributions were compared to the trace distributions and thus the Neoichnology characteristics in the lower delta plain of the Fraser River were mapped. These regions are exposed to physical and chemical stresses such as changes in the concentration of salt content, increase in turbidity etc. The study aimed to understand the effects of these stresses in the distribution of benthic animals in lower delta plain. There is a net northward shift of sediments in the Fraser delta due to asymmetric tides. (Dashtgard, 2011)

Experiments to determine hydraulic and sedimentary variables were carried out throughout a flood cycle to observe the variations of shear velocity and substrate mobility during low flow and peak flows. This helps reveal the importance of shore zone for the refugium of benthic species during flooding events. This in turn is of greater significance in engineering alterations and other human interventions to rivers as they change the habitats (Rempel et al., 1999).

Bioassays were carried out at the site with juvenile chinook salmon with multiple samples of varying concentration of effluents and oxygen levels. Concentration dependent clastogenic damage was examined through blood tests by flow cytometry at effluent concentrations of above 4%. This study helped understand the genetic implications to the species under investigation (Easton et al., 1997).

2.6 Salinity in rivers

In the Pacific coast, saline water flows into the river for a distance up to 30 km inland during mixed semi-diurnal tidal cycle, which is common in the north Pacific coast, of up to 5.3 m in height (Dashtgard et al., 2012).

A dynamic equilibrium state is maintained by the freshwater flow from inland to the river and the saline water intruded from the ocean during high tides. This affects the ground water flow and directions as well as its geochemistry. During low flow, the tidal water can reach up to 16 km inside the river. The saline water has a concentration of 23 parts per thousand at the mouth of the Fraser River. This saline water can form a wedge and permeate into the deltaic deposits. At a particular site, there is a record of 500 m intrusion into the land at a depth of 10 m below the ground level. The authors wanted to record the properties of saline water in a confined aquifer near a particular station of the Fraser River (Neilson-Welch & Smith, 2001).

2.7 Influence of climate

Low flow in the Fraser River is sensitive to temperature variations due to the presence of accumulated snow during winter.

2.7.1 Influence of climate on stream flow hydrology

Response to the anthropogenic effects of climate change on water resources of two river basins including the Fraser River basin was investigated. An ensemble of seven GCMs and four climate change scenarios over 30 years future duration was used in the studies. The prediction inquires the response of the snow melt and river flows based on the changes in temperature and precipitation. All GCM projections showed a change in the mean annual stream flow by $\pm 10\%$, ten projections showed a decrease in the annual mean flow, and eight projections showed an increase in the annual mean flow. The Fraser River basin is expected to get warmer and there will be a decrease in the annual snow. All models have predicted seasonal changes in stream flow due to early onset of snowmelt (Kerkhoven & Gan, 2011b).

The Fraser River basin has a hydrologic system of snow accumulation and melting. The winter discharge is low, and snowmelt is the main source of water supply in the basin. A modelling study was carried out to determine the spatial and temporal variability of hydrologic changes under the influence of climate change. A macro-scale variable infiltration-capacity hydrologic model was used to assess the hydrologic response for a

large spatial extent with inputs for the future simulations from IPCC AR4 GCMs under five emission scenarios. The 11 sub-basins and three regions showed different responses based on their snow dominance to rain dominance. These hydro-climatic predictions can be used locally for the water resource management. The forecast of early snowmelt and increased winter runoff was made. The Figure 2.5 shows the location map and elevation range of the Fraser River basin with 11 sub-basins as per Water Survey of Canada (Shrestha et al., 2012).

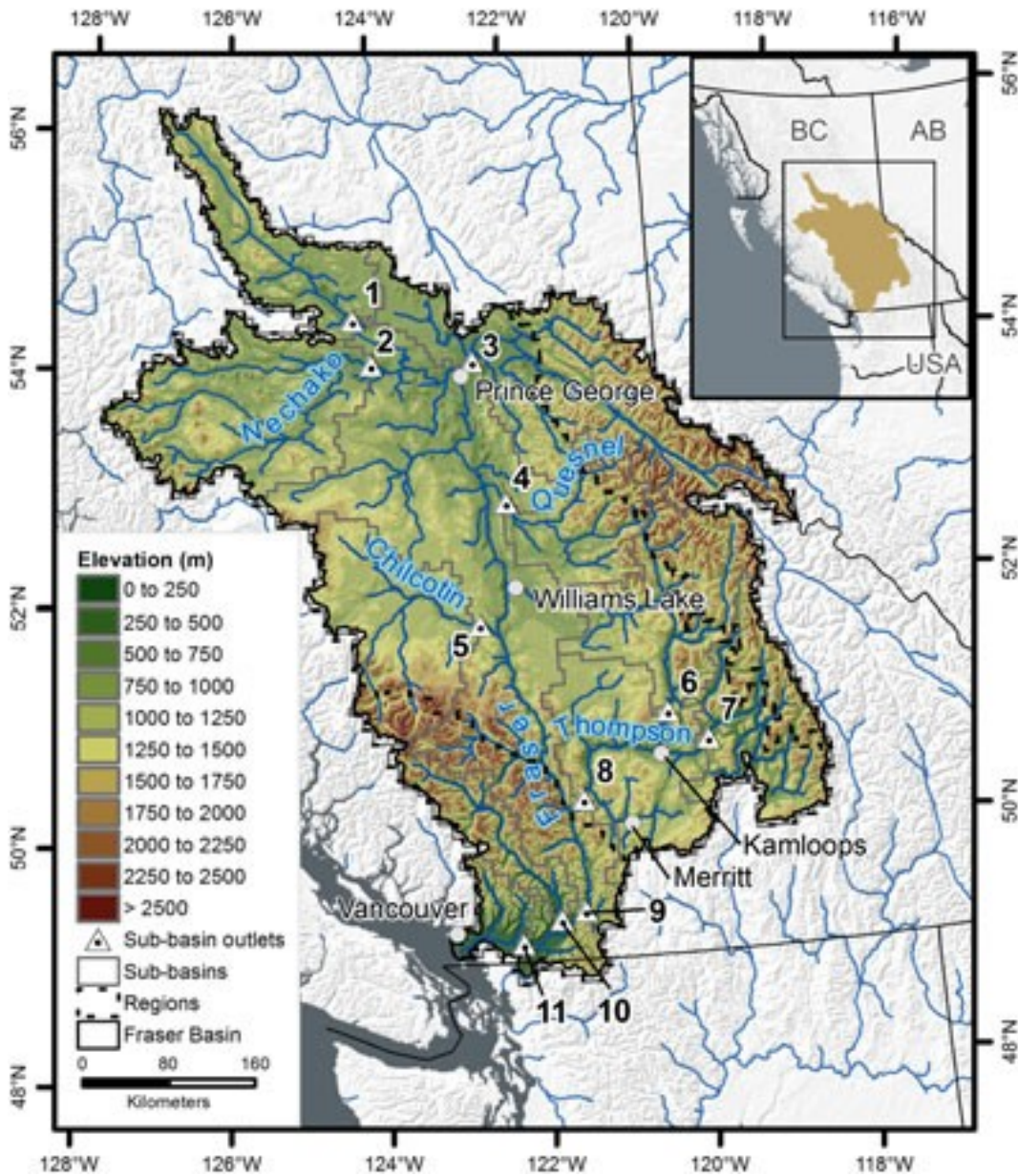


Figure 2.5 Fraser river basin with 11 sub-basin outlets as per WSC (Shrestha et al., 2012)

A study was made to calculate unconditional sample uncertainties of recorded stream flow and simulated stream flow for two rivers, one of which is the Fraser River. Multifractal properties of various simulated hydrographs were evaluated based on the predictions from GCM- climate scenarios ensembles. These properties were used to extend the time series by another model. Uncertainty estimates obtained from this multifractal method were compared with various statistical methods (Kerkhoven & Gan, 2011a).

Prediction of seasonal streamflow is critical for estimating water availability and for coping with the extremities. A study assessed the credibility of hydrologic prediction of a dynamical climate model-driven system for the Fraser River. The variable infiltration capacity (VIC) hydrologic model was used as the base for this system. The outputs from Canadian GCMs were given as an input to the hydrologic prediction system to provide the seasonal streamflow predictions (Shrestha et al., 2015).

Estimation of the climate change impacts on stream water temperature is important to understand its effects on aquatic ecosystems. The study developed a model to generate the annual fluctuations in summer water temperature in sites across Fraser River basin. This model provided necessary information for future governing of fisheries. ENSO and PDO phase changes are associated with Model simulation. Significant variations are noted in water temperature in model simulation between the extreme phase of these oscillations. Mean air temperature was observed as the primary driver of summer water temperatures in most of the sites (S Islam et al., 2019).

Hydrologic changes are estimated using CMIP5 GCMs and Variable Infiltration Capacity hydrologic model for the Liard basin located in subarctic northwestern Canada. The results of the model showed a decrease in snow water equivalent and earlier maximum snow water equivalent. Increase in annual mean and low flows are noticed. Precipitation is found to be the primary factor controlling snow water equivalent and flow variables, and temperature controls the timing of these variables. The study gave an evaluation of climate change impacts due to increased warming and variation in moisture in Liard basin (Shrestha et al., 2019).

Climate responses in three hydrologic regimes were forecasted for 2050s using a variable infiltration capacity hydrologic model and a set of eight GCM models under three emission scenarios. Snow water equivalent is expected to decline in low elevations in British Columbia and it is expected to increase in high elevations with increase in winter precipitation. A time shift in the pattern of snow flow was noticed in the forecast due to changes in snow accumulation and melting patterns. Coastal regions are observed to shift to rainfall dominated system by 2050s. The transformation of glacial-nival regime to pure nival regime was not well considered in this study (Schnorbus et al., 2014).

The study developed and calibrated a water balance model for the Yukon River basin by using precipitation & temperature data set and by comparing model estimated runoff to the actual runoff at a station. Hydrologic response to the climate change was estimated based on inputs from five IPCC GCM climate simulations. Results showed an increase in annual runoff by the end of this century for the Yukon River basin and it is influenced by precipitation. Increased temperature led to the fluctuations in snow accumulation and melting patterns (Hay & McCabe, 2010).

A five GCM model driven hydrological model under three emission scenarios were used to analyse the changes in seasonal water budget for three head water basins, Baker Creek, Ingenika and Campbell River, in British Columbia. Uncertainties in GCM response, emission scenarios and hydrologic parameters are analysed. The results showed that GCMs showed the highest uncertainty on water balance parameters, followed by emission scenarios and then by hydrologic parameterizations. Coastal regions were showed to respond higher to climate change than interior regions with snow pack storage reserves (Bennett et al., 2012).

2.7.2 Influence of climate on low flows

An increased influence on the climate on low flows was observed by Schaake and Chunzhen (1989). A recommendation for additional research on the influence of climate change on low flow for engineering and management purpose was given by Smakhtin (2001).

Precipitation is the major source of water in both surface and subsurface water regimes. It is known that any reduction in this input reduces the streamflow hydrograph resulting in low flow. Low flow conditions may result from either summer dry periods or winter snow accumulation periods. Low flow patterns are visible from climate normal, but this characteristic is impacted by the changes in the climate system (Carver et al., 2009).

Studies have concentrated on response of modeling change to global climate change. However, most of the studies have not considered the land use change and the local climate. There is a shortage of knowledge in the effects of low flows especially where there is only a little idea about the local influence of groundwater (Carver et al., 2009).

The risks caused by climate change to major assets and infrastructures were underestimated as there were few risk-based frameworks for impact assessments using probabilistic climate change information. A framework was developed by blending information from an ensemble and explored the components of uncertainty affecting projections of low flow. Daily average precipitation from a network of twelve-gauge stations were obtained. Daily potential evaporation values were calculated using a sinusoidal curve method from the obtained monthly values. River flow data was obtained from an upstream station. Using these inputs future climatic scenarios were predicted using GCM data from HadCM3 climate model. The first step involves downscaling the GCMs into regional climate change scenarios. The second step assigns weights to the uncertainty elements such as emission scenario, climate model, downscaling, hydrologic model parameter, and hydrologic model structure. The third step is Monte Carlo simulations of impacts using the scenarios and given weights. The order of uncertainty component significance for this framework from greatest to least is GCM, downscaling method, hydrological model structure, hydrological model parameters, and emission scenarios. The authors have projected the probability of summer reduction using Monte Carlo experiments. They have elucidated low flow using their framework to understand uncertainty components (Wilby & Harris, 2006).

The influences of Pacific decadal oscillation and El Niño Southern oscillation on low flow are investigated by Wang et al. (2006). Streamflow data patterns from four regions of British Columbia and southern Yukon were examined for their responses to

these two oscillations. Observations revealed the influence of PDO and ENSO in all the four regions of British Columbia. PDO influenced in these regions and its impact on low flows frequencies and magnitudes were more than that by ENSO. Occurrences of ENSO modulated the impact of PDO on low flows. Rivers in Yukon were not affected by any of these oscillations (Wang et al., 2006).

2.7.3 Influence of climate on snow hydrology

The study was carried to evaluate the impact of climate change on the snow hydrology of the Fraser River basin. Snowmelt regulates the water temperature of the Fraser River and supports the reproduction of salmon. Reduction in snow will badly affect the survival of benthic species. A combination of 24 statistically downscaled climate model scenarios and a Variable Infiltration Capacity model (VIC) simulation were used to predict the spatial snowfall hydrology changes over the Fraser River basin by year 2050. Several crucial snow hydrology variables are used to estimate snow melt-driven runoff. The total precipitation as snowfall is estimated to decline by 50% and the remaining 50% is expected to change to precipitation in the form of rain by 2050. Snow-covered areas in the Fraser River basin are expected to decrease (S Islam et al., 2017).

2.7.4 General Circulation Models (GCM)

According to Intergovernmental panel on Climate change (IPCC), GCMs are numerical models which represent the physical processes happening across atmosphere, ocean, cryosphere, and land surface. They are said to be the advanced tools for simulating the changes caused by the greenhouse gas emissions on the global climate system. They typically have a resolution between 250 and 600 km and are three-dimensional grids up to 20 vertically stacked grids in atmosphere and up to 30 vertical grids in ocean. Figure 2.6 shows the representation of horizontal and vertical grids. Different GCMs may simulate differently for same inputs because their processes, and feedbacks are modelled differently from one to another (IPCC, 2020).

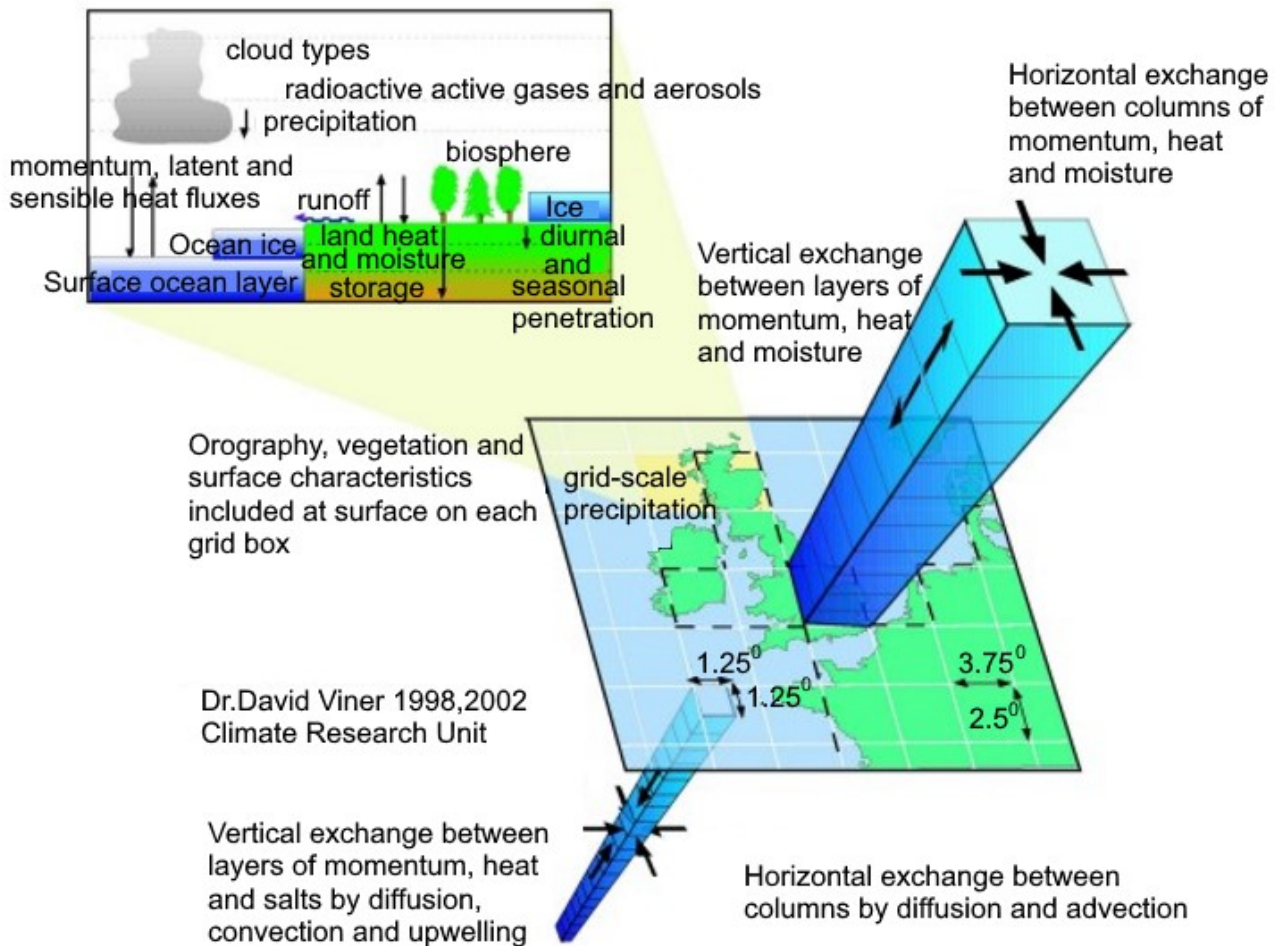


Figure 2.6 Representation of grids in a GCM (IPCC, 2020)

Representative concentration pathways (RCPs) are the scenarios with time series of emission and concentration of greenhouse gases. They give one of the many possible scenarios, which lead to that specific radioactive forcing value. They give the entire trajectory in achieving that level. Usually the pathways are until 2100 with corresponding emissions produced by the integrated assessment model. There are four major RCPs, 2.6, 4.5, 6.0, and 8.5. RCP 2.6 has a radioactive forcing of 2.6 W/m^2 , whereas RCP 8.5 has a radioactive forcing of 8.5 W/m^2 (IPCC, 2020).

The IPCC climate change report 2014 shows the expected change in the surface temperature (Figure 2.7).

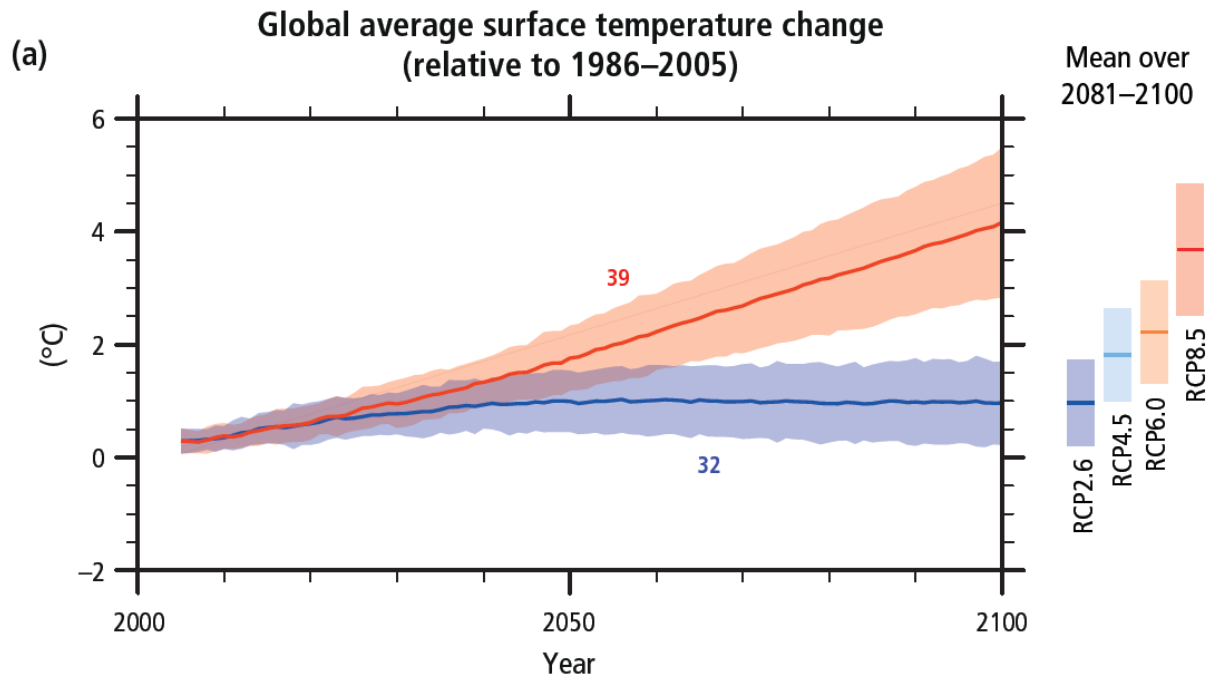


Figure 2.7 Expected change in the surface temperature as per IPCC report (Pachauri et al., 2015)

NASA provides a dataset called NASA Earth Exchange Global Daily Downscaled Projections (NEX-GDDP), which consists of downscaled climate scenarios for the globe, from GCM runs made under Coupled Model Intercomparison Project Phase 5 (CMIP5). It has a finer spatial resolution of 25 km x 25 km. The archives are downscaled projections of RCP 4.5 and RCP 8.5 and have 21 climate models with maximum and minimum temperature and precipitation values for daily scale from 1950 to 2005 (Retrospective run) and 2016 to 2099 (Prospective run) (NASA, 2020).

A study was made by combining a hydrologic model and 20 GCMs from IPCC. This was carried out to understand the impact of uncertainties in GCMs to hydrologic impact studies in the Paute River basin, Ecuador. The projections of the hydrologic model inputs with GCMs showed that the simulated discharge values could spread widely beyond the existing discharge values. Improvement in the downscaling technique and hydrologic model were suggested in this study to get better predictions for designing the adaptation actions. (Buytaert et al., 2009)

Chapter 3

Methodologies

3.1 Data collection

Historical data of Fraser River discharge from the year 1912 to 2019 is obtained from the Water Survey of Canada data (WSC, 2020). The station selected for the data is the Fraser River at Hope, which is located at the downstream of the river where most of the flow reaches from the drainage area.

The temperature records on a daily scale from 1912 to 2019 are obtained from Environment and Climate Change Canada (2011). A total of 52 stations were chosen within the basin map (MacLean, 2009) of the Fraser River and the mean values of daily temperature available in the database were obtained for analysis. The climate station locations are shown in Figure 3.1.

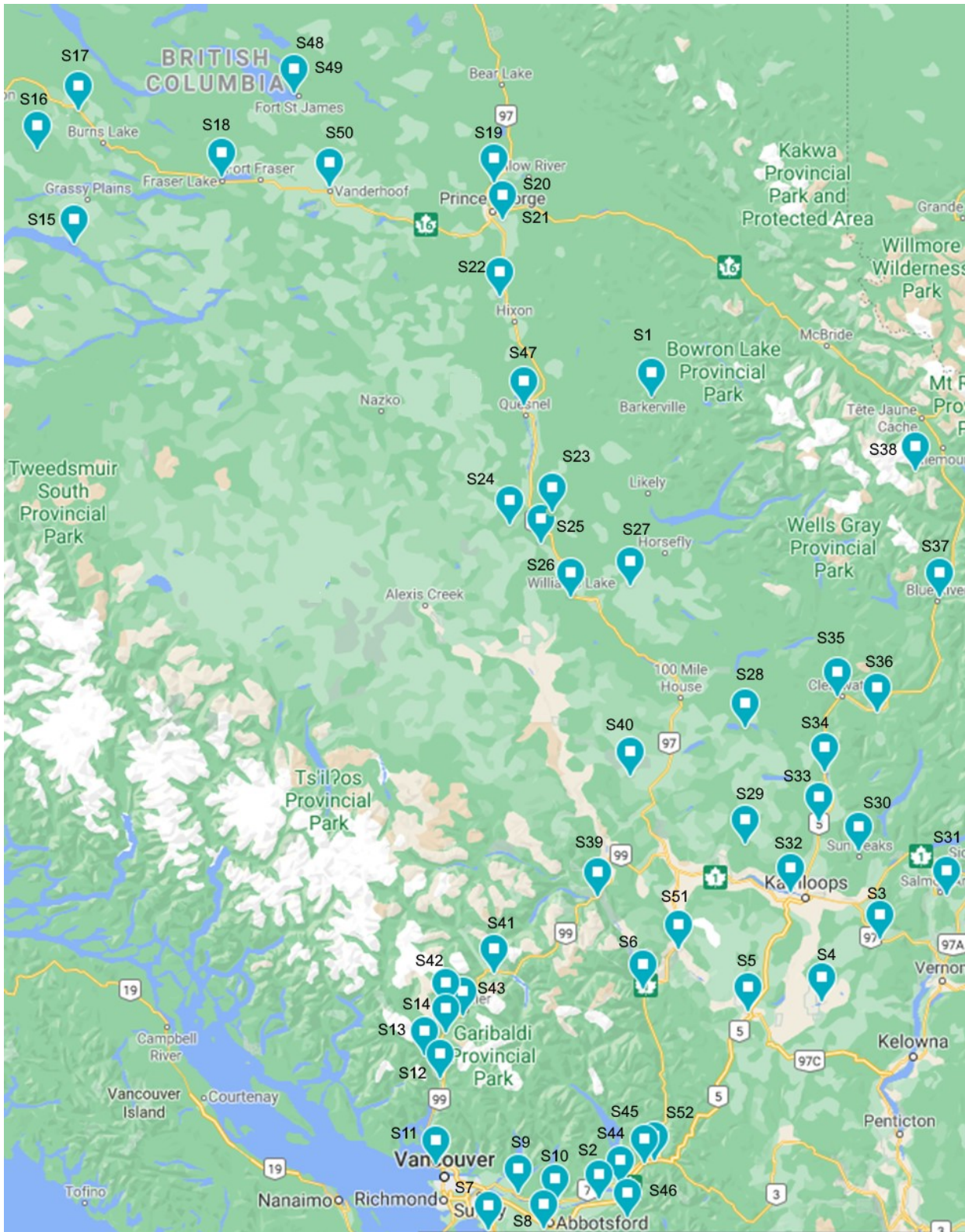


Figure 3.1 Location of climate stations in the Fraser River basin where the temperature data was obtained (Image layer taken from google maps).

Station ID	Station Name	Latitude	Longitude
S1	Barkerville	53°04'09"N	121°30'53"W
S2	Chilliwack	49°10'19"N	121°55'28"W
S3	Westwold	50°28'08"N	119°45'02"W
S4	Douglas Lake	50°09'53"N	120°11'58"W
S5	Merritt	50°06'45"N	120°46'41"W
S6	Lytton RCS	50°13'28"N	121°34'55"W
S7	White Rock Campbell scientific	49°01'05"N	122°47'02"W
S8	Abbotsford A	49°01'31"N	122°21'36"W
S9	Haney East	49°12'15"N	122°33'29"W
S10	Mission West Abbey	49°09'09"N	122°16'14"W
S11	West Vancouver AUT	49°20'49"N	123°11'35"W
S12	Squamish Airport	49°46'59"N	123°09'40"W
S13	Squamish Upper	49°53'45"N	123°16'53"W
S14	Callaghan Valley biathlon high level	50°00'32"N	123°07'07"W
S15	Ootsa Lakeskins Lake climate	53°46'18"N	125°59'48"W
S16	Equity Silver	54°11'55"N	126°16'35"W
S17	Burns Lake Decker Lake	54°22'59"N	125°57'31"W
S18	Fraser Lake north shore	54°04'42"N	124°50'50"W
S19	Prince George 15nw	54°03'11"N	122°44'09"W
S20	Prince George Airport auto	53°53'20"N	122°40'19"W
S21	Prince George STP	53°52'48"N	122°46'03"W
S22	Hixon	53°31'53"N	122°41'58"W
S23	Mcleese Lake granite mt	52°31'50"N	122°17'09"W
S24	Twan Creek	52°27'59"N	122°37'03"W
S25	Mcleese Lake Fraserview	52°22'47"N	122°22'25"W
S26	Williams Lake A	52°11'00"N	122°03'16"W

Station ID	Station Name	Latitude	Longitude
S27	Spokin Lake 4E	52°11'01"N	121°41'10"W
S28	Bridge Lake 2	51°30'13"N	120°47'36"W
S29	Red Lake	50°56'06"N	120°48'00"W
S30	Sun Peaks Mountain	50°54'10"N	119°54'40"W
S31	Salmon Arm A	50°41'08"N	119°14'01"W
S32	Kamloops A	50°42'08"N	120°26'31"W
S33	Mclure	51°02'48"N	120°13'18"W
S34	Darfield	51°17'30"N	120°10'57"W
S35	Clearwater auto	51°39'09"N	120°04'56"W
S36	Vavenby	51°34'34"N	119°46'41"W
S37	Blue River A	52°07'44"N	119°17'22"W
S38	Cariboo Lodge	52°43'10"N	119°28'18"W
S39	Lillooet	50°41'01"N	121°56'03"W
S40	Clinton A	51°15'59"N	121°41'05"W
S41	Pemberton Airport (wind)	50°18'08"N	122°44'17"W
S42	Callaghan Valley (ski jump top)	50°08'15"N	123°06'36"W
S43	Whistler Mountain timing flats	50°05'30"N	122°58'49"W
S44	Agassiz CDA	49°14'35"N	121°45'37"W
S45	Laidlaw	49°21'23"N	121°34'46"W
S46	Chilliwack R Hatchery	49°04'48"N	121°42'15"W
S47	Quesnel A	53°01'34"N	122°30'36"W
S48	Fort St James auto	54°27'19"N	124°17'08"W
S49	Fort St James	54°27'19"N	124°17'08"W
S50	Vanderhoof	54°02'00"N	124°01'00"W
S51	Spences Bridge Nicola	50°25'18"N	121°18'52"W
S52	Hope Airport	49°22'11"N	121°29'36"W

Table 3.1 List of climate stations

3.2 Data processing

Mean daily air temperatures at the 52 stations are averaged to obtain the average daily temperature for the Fraser River basin.

The daily air temperature data, which is in calendar year, is changed to hydrological year (water year), which starts from October 1st of one year and ends on September 30th of the next year (USGS, 2005).

A statistical relationship is to be established between the historical values of river basin temperature and the river discharge to understand the pattern and the influence of temperature on the river flow. Further, this relationship can be used to forecast the changes in the river flow in response to climate change. Established climate models and outputs from studies on expected variations in temperature for Western Canada can be used to forecast the expected variation in the Fraser River flow.

3.3 Selection of temperature variable

Different methods were adopted to relate the freezing effect of water with temperature drop. The following are the methods used in computing the cumulative temperature for every year in the historical data:

1. Daily temperature starting from the first day of negative temperature in a year is added in an incremental fashion for every day till the thawing temperature is reached.
2. Daily temperature starting from the first day of negative temperature in a year is added in a moving average of seven days for every day till the thawing temperature is reached.

3. Daily temperature starting from a consistent negative temperature in a year is added in an incremental fashion for every day till the thawing temperature is reached.

Of the above-mentioned methods, the third method is found to better correlate with variations in river flow discharge. The cumulative watershed temperature gives a better picture of the net freezing in the entire watershed, which causes the watershed response to reduce drastically. The patterns of cumulative watershed temperature vs river discharge during the low flow months showed better correlation than the other two variables tested.

7-day average variable was not able to give a reflection of the overall quantity of low flow since the temperature fluctuates rapidly on daily scale. The sudden increase in temperature does not necessarily increase the quantity of low flow, as the watershed response takes time to get the snow melt water to reach the streams. This delay is not well represented in this variable.

The cumulative watershed temperature calculated from the first day of negative temperature was also not successful in relating the low flow estimates. This is due to the increase in the value of this variable due to the increase in temperatures above freezing limit in the following days after the first day of negative temperature. The subsequent positive temperature gives an incorrect representation of the net freezing effect on the watershed.

A sample of the distribution of daily mean discharge with respect to cumulative watershed temperature and daily mean temperature for an example hydrologic year 1913 is shown in Figures 3.2 and 3.3 respectively.

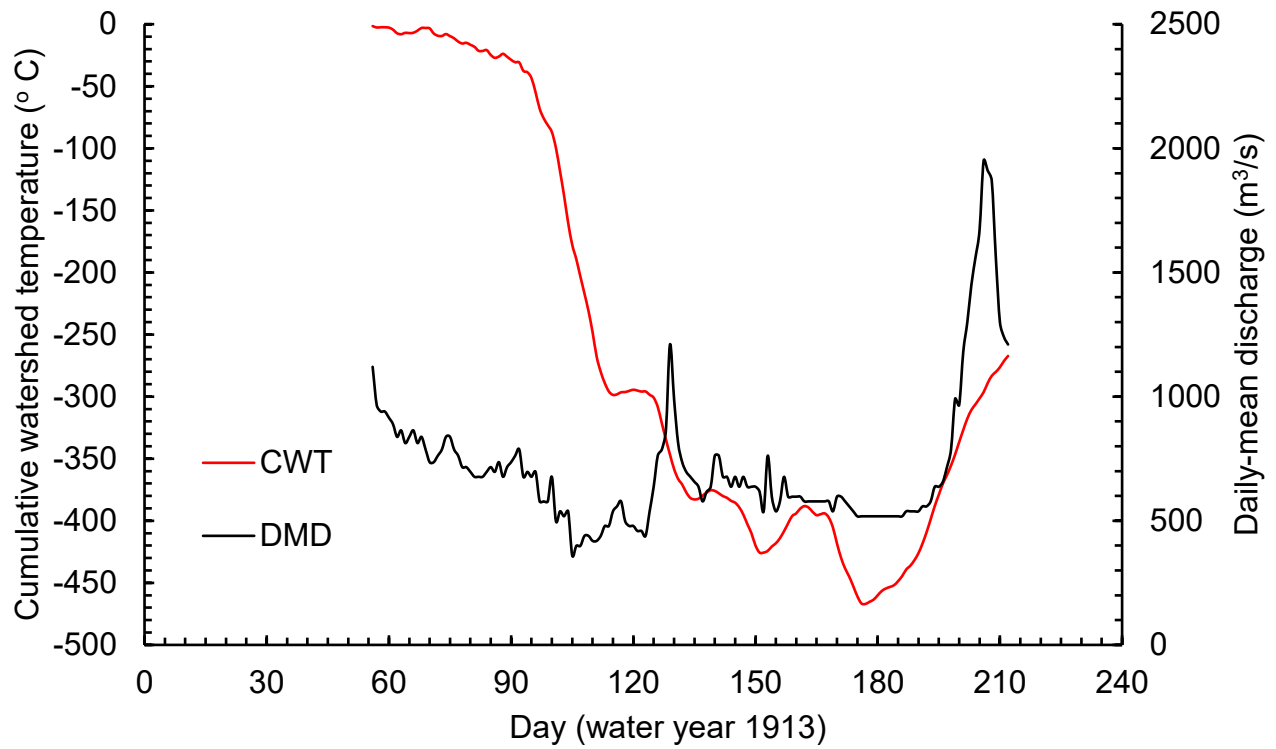


Figure 3.2 Time series of daily mean discharge (DMD) and cumulative watershed temperature (CWT)

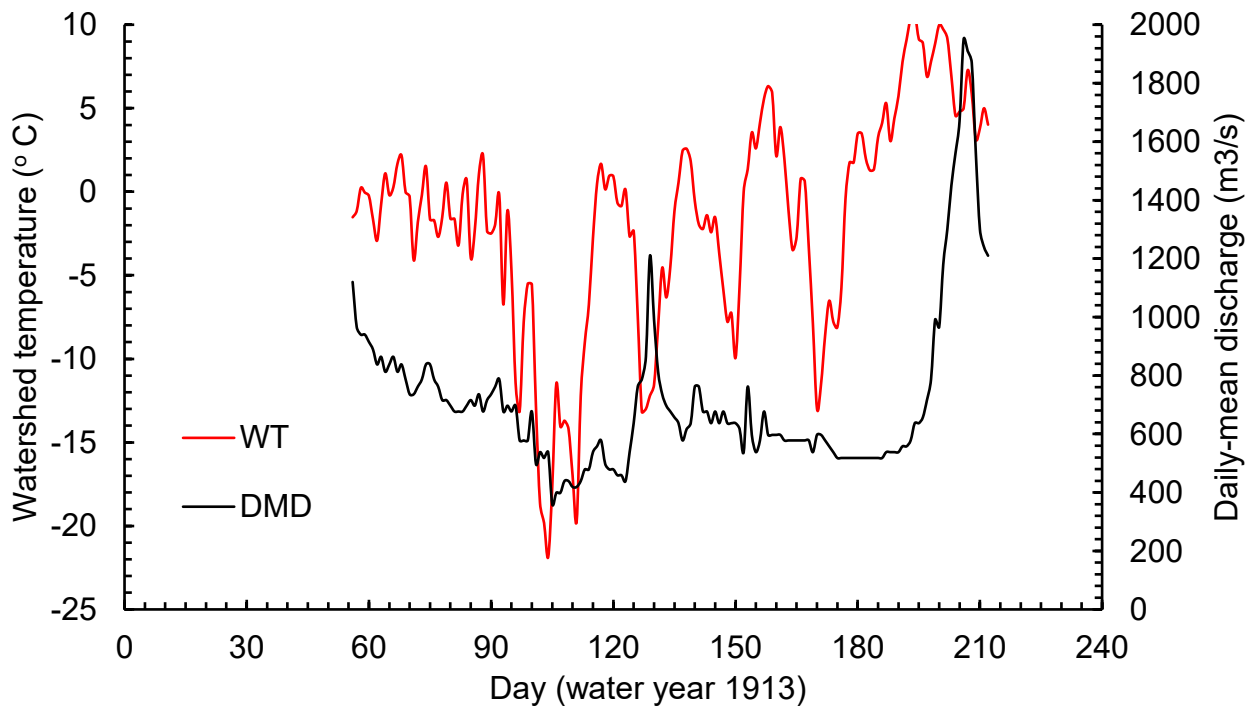


Figure 3.3 Time series of daily mean discharge (DMD) and daily watershed temperature (WT)

3.4 Classification of Data

Each year in the historical data can be classified into two limbs, the falling limb and the rising limb, based on the winter freezing and autumn thawing effect in the river. The minimum flow in the river occurs between these two limbs. In other words, the point at which the two limbs meet is the lowest flow in the river for that particular year. A typical example of this division for the water year 2016 is shown in Figure 3.4.

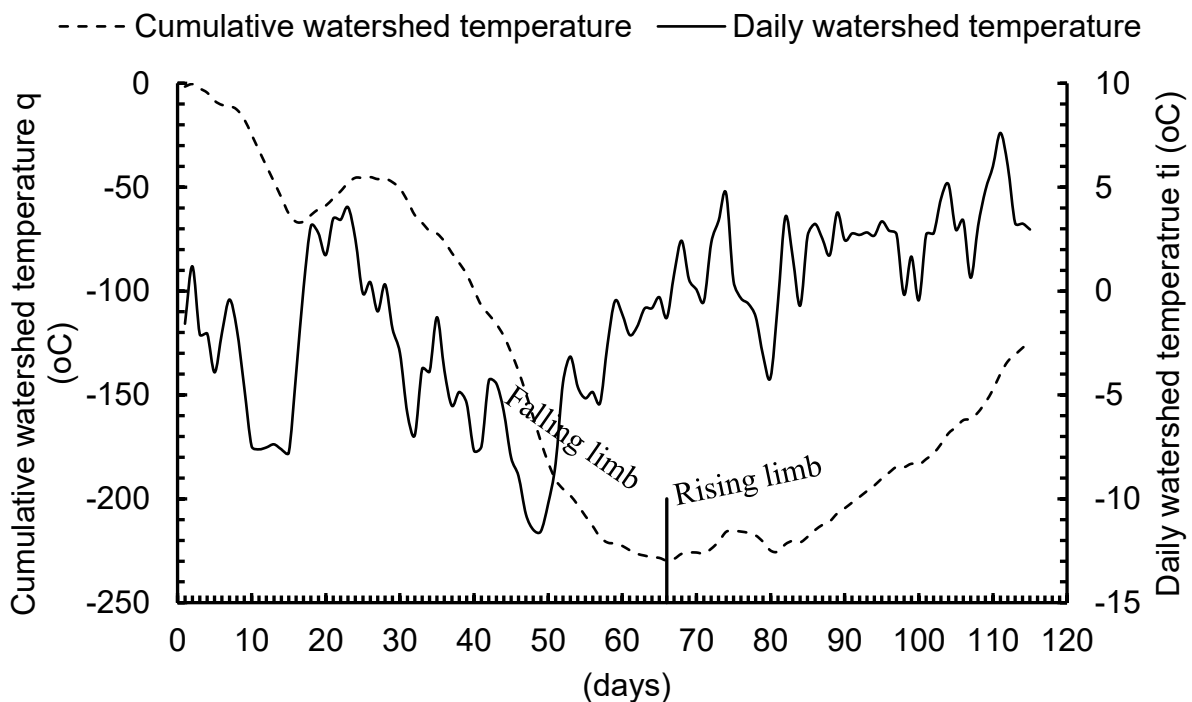


Figure 3.4 Sample division of a hydrological year into falling and rising limbs.

To understand the impact of increase (Bush et al., 2019) in temperature due to climate change, the rising limb is of interest in this study. It is required to establish a relationship to estimate the increase in discharge from its minimum value with reference to the cumulative temperature and its future increase considering the climate change factor.

3.5 Outlier identification

There are several outliers in the historical data. Outliers in the historical data are identified using a function (Eq.1) of the form

$$y = ax^b + c \quad (\text{Eq.1})$$

where y is the z score values of cumulative temperature; a , b , c are coefficients; x is the z score values of discharge.

The outlier years are highlighted in Figure 3.5

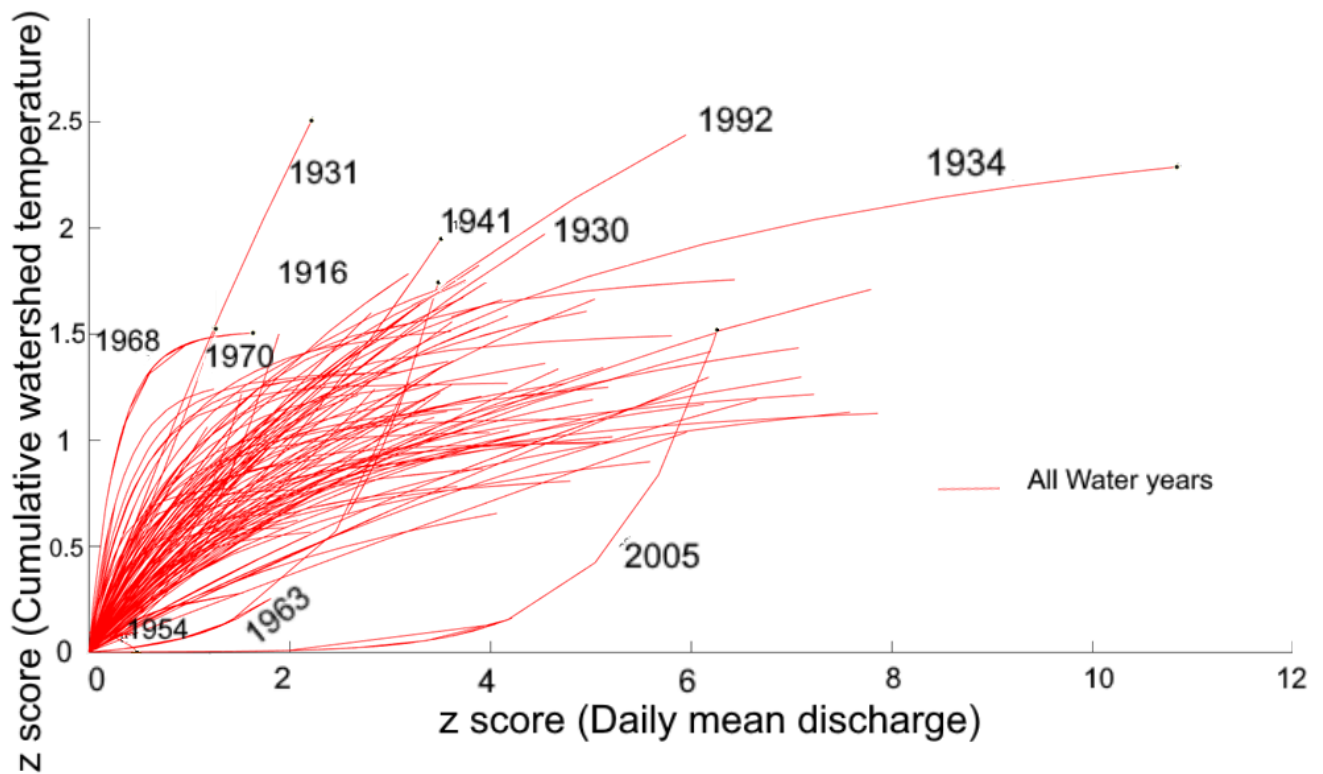


Figure 3.5 Outlier years highlighted

The identified outlier years and their possible causes for these variations from the normal trends are explained below in connection with three major climate oscillations.

El Niño is characterized by warmer atmospheric temperatures, whereas La Niña results in lower temperature. A positive Pacific decadal oscillation results in warmer sea surface temperature near the western coast of North America, and a negative PDO results in cooler SST (Bonsal & Shabbar, 2011).

The influence of these oscillations is removed from the data before establishing the relationship. This is because though the function is calibrated using the historical data, the GCM models solve a boundary value problem and they cannot guarantee to reproduce the timing of these natural climate variability (*Pacific Climate Impacts Consortium, 2020*).

Atlantic multi decadal oscillation (AMO) displayed colder phases from 1905 to 1925, 1970 to 1990 and warmer phases from 1930 to 1960(Bonsal & Shabbar, 2011).

Extended cold temperature was reported in 1916 leading to a peak cumulative temperature of -763.24° C during March of this hydrologic year. El Niño events were recorded with a standardized anomaly of around -1 prior to this year. Atlantic multidecadal oscillation displayed cold temperatures during this period. There was very impact due to Pacific decadal oscillation during this year. Figure 3.6 represents the variations during Hydrological year 1916.

La Niña peak impact reduced its intensity during 1930. Pacific decadal oscillation is recorded in the previous years. Atlantic multidecadal oscillation observed warm phase during this period. Figure 3.7 represents the variations during Hydrological year 1930.

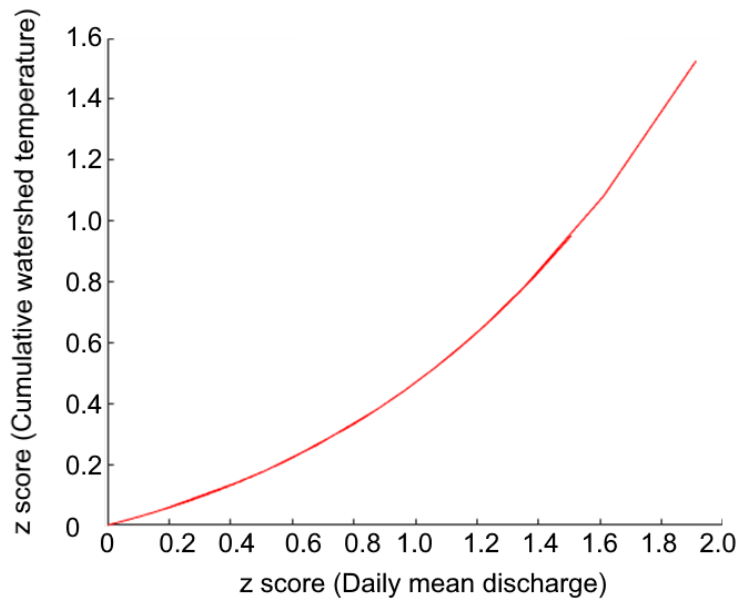


Figure 3.6 Increase of DMD with increasing CWT in terms of z scores for the hydrological year 1916.

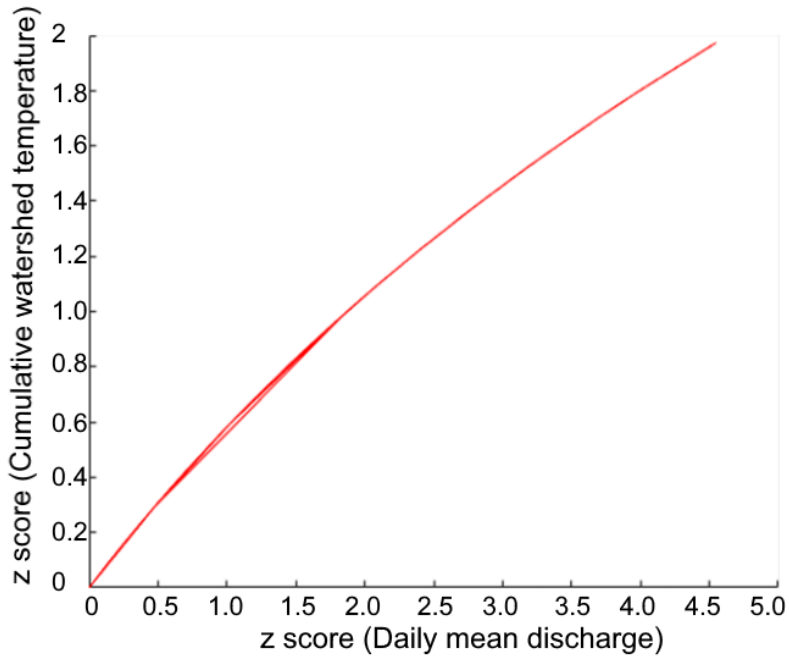


Figure 3.7 Increase of DMD with increasing CWT in terms of z scores for the hydrological year 1930

El Niño events were recorded during 1931 and positive Pacific decadal oscillation was recorded in the previous years. Warm phase was also observed in Atlantic multidecadal oscillation. Figure 3.8 represents the variations during the hydrological year 1931.

Both El Niño and La Niño were observed during 1934. Hence there is no significant impact from El Niño southern oscillation. Positive phase of Pacific decadal oscillation is observed during this year. Also, warm phase is observed in Atlantic multidecadal oscillation. Warmer temperature might be due to PDO and AMO. Figure 3.9 represents the variations during the hydrological year 1934.

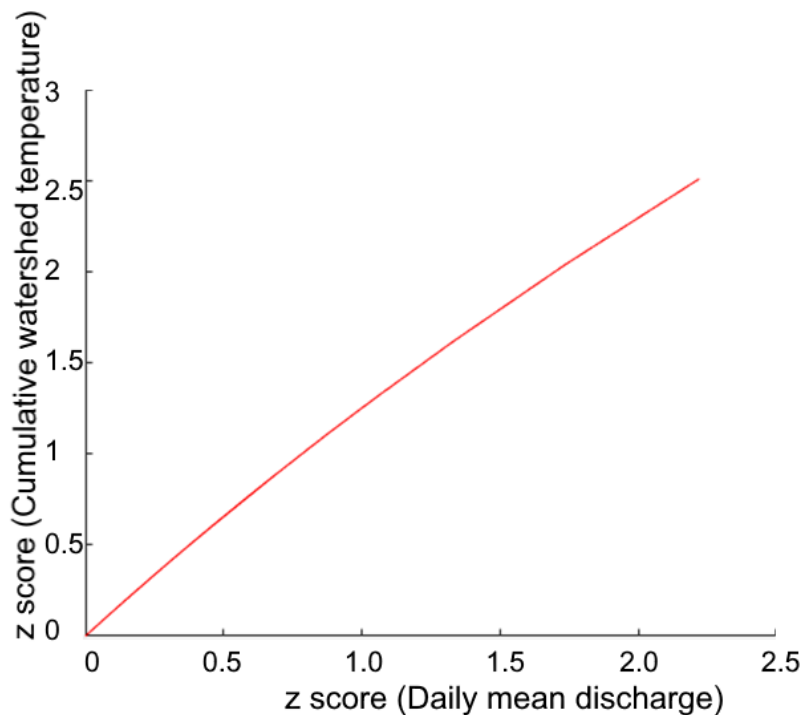


Figure 3.8 Increase of DMD with increasing CWT in terms of z scores for the hydrological year 1931

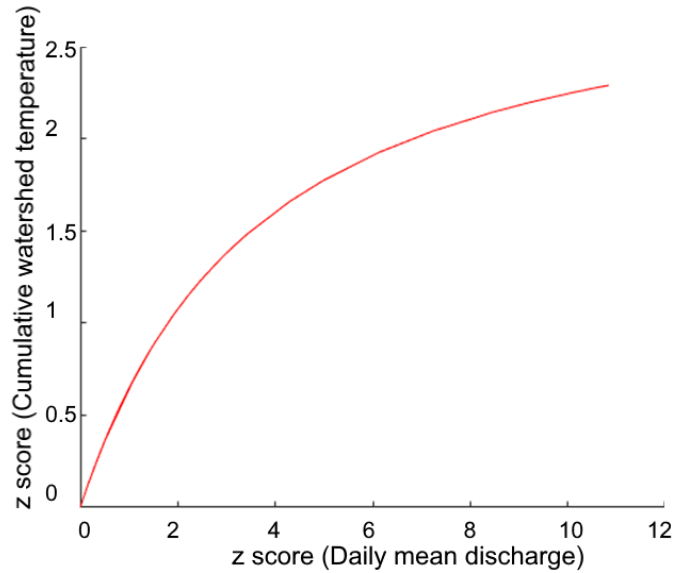


Figure 3.9 Increase of DMD with increasing CWT in terms of z scores for the hydrological year 1934

All three oscillations recorded warmer phases during Hydrological Year 1941. Figure 3.10 represents the variations during the hydrological year 1941. During hydrological year 1954, colder phase was recorded in Pacific decadal oscillation. Warmer phase was observed in Atlantic multidecadal oscillation during this period. El Niño southern oscillation showed a little impact. Figure 3.11 represents the variations during the hydrological year 1954.

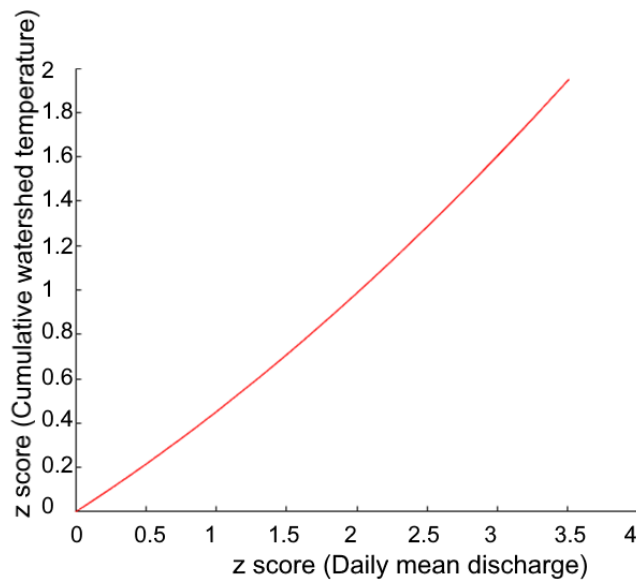


Figure 3.10 Increase of DMD with increasing CWT in terms of z scores for the hydrological year 1941

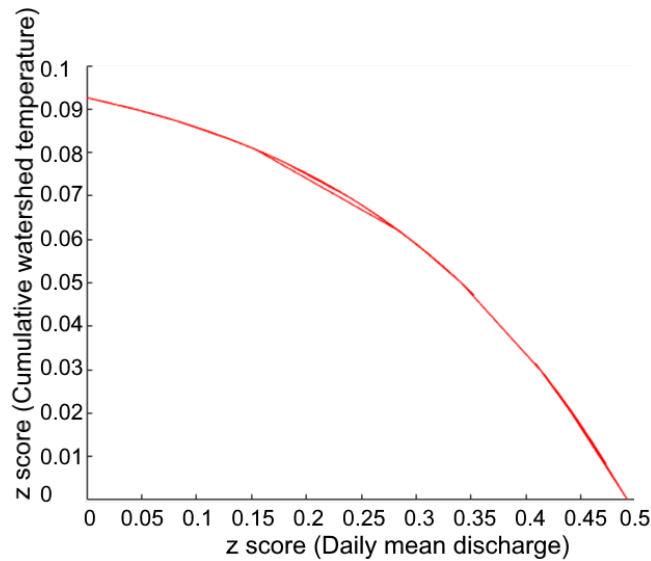


Figure 3.11 Increase of DMD with decreasing CWT in terms of z scores for the hydrological year 1954

Both El Niño Southern oscillation and Pacific decadal oscillation observed lower temperatures during hydrological year 1963. Atlantic multidecadal oscillation declined towards the cooler phase. Figure 3.12 represents the variations during the hydrological year 1963.

El Niño southern oscillation was observed around hydrological year 1968, but cooler Pacific decadal oscillation and cold phase of Atlantic multidecadal oscillation were observed during this year. Figure 3.13 represents the variations during the hydrological year 1968.

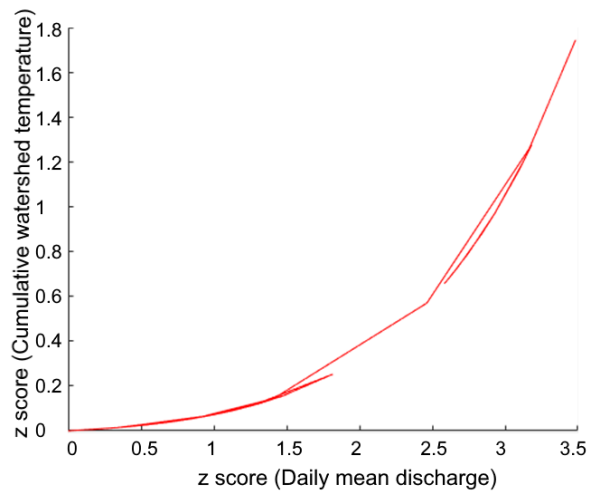


Figure 3.12 Increase of DMD with increasing CWT in terms of z scores for the hydrological year 1963

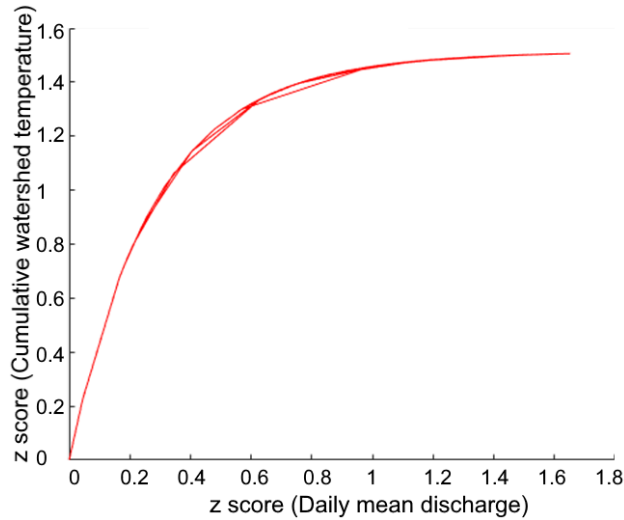


Figure 3.13 Increase of DMD with increasing CWT in terms of z scores for the hydrological year 1968

El Niño southern oscillation was recorded around hydrological year 1970. Pacific decadal oscillation did not show much effect due to net negative running average. Cold phase was observed in Atlantic multidecadal oscillation. Figure 3.14 represents the variations during the hydrological year 1970.

Record intensity of El Niño southern oscillation was recorded around hydrological year 1992 with net positive Pacific decadal oscillation. However, cold phase was observed in Atlantic multidecadal oscillation. We can clearly see the effect of this in the variation of discharge with cumulative watershed temperature

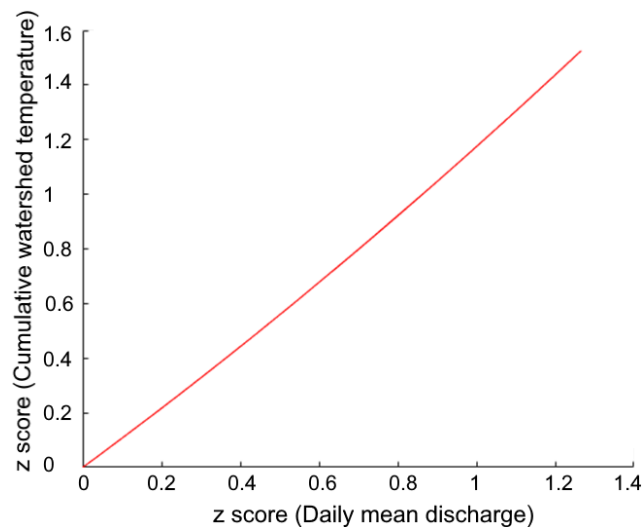


Figure 3.14 Increase of DMD with increasing CWT in terms of z scores for the hydrological year 1970

. Figure 3.15 represents the variations during the hydrological year 1992. All three oscillations showed a positive trend with weaker influence from Pacific decadal oscillation during hydrological year 2005. Figure 3.16 represents the variations during the hydrological year 2005.

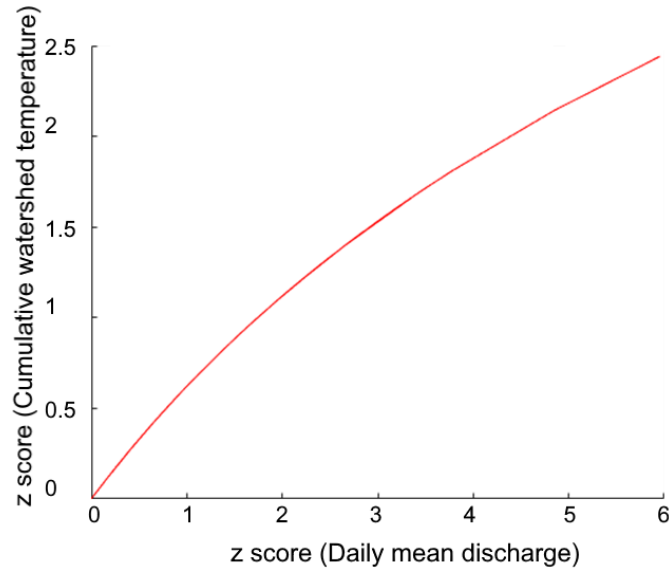


Figure 3.15 Increase of DMD with increasing CWT in terms of z scores for the hydrological year 1992

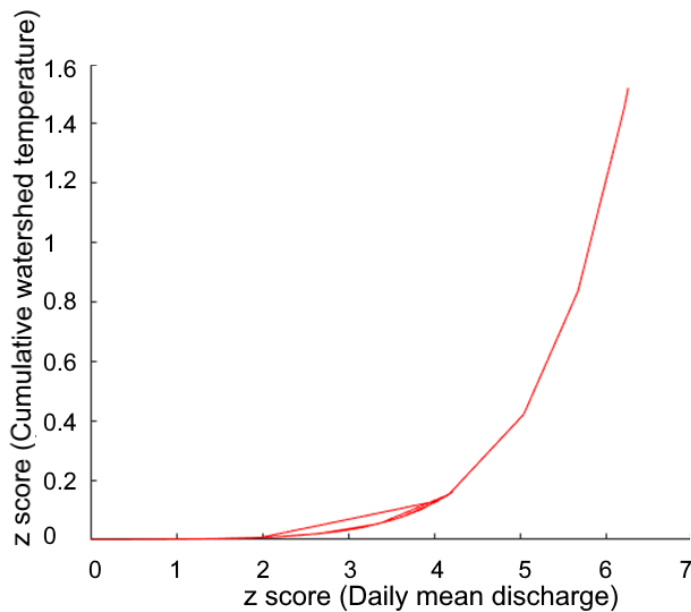


Figure 3.16 Increase of DMD with increasing CWT in terms of z scores for the hydrological year 2005

The oscillation impacts during the years mentioned above are estimated based on the graphs from Bonsal & Shabbar (2011).

3.6 Establishing a Functional fit

A relationship is established using the function (Eq. 2) below to estimate the increase in yearly minimum discharge with reference to the cumulative watershed temperature.

$$Q = \sigma_Q \left[a \left(\frac{\tau - \bar{\tau}}{\sigma_\tau} \right)^b \right] + \bar{Q} \quad (\text{Eq. 2})$$

where Q is the projected minimum yearly discharge; \bar{Q} is the average of minimum discharge from historic data; σ_Q is the standard deviation of minimum discharge in historic data; τ is the model Minimum cumulative temperature; $\bar{\tau}$ is the average of minimum cumulative temperature from historic data; σ_τ is the standard deviation of cumulative temperature from historic data; a and b are the coefficients of the fit.

The values of coefficients are obtained by fitting the historic data, and the forecast of discharge is estimated for the increasing standard deviation of cumulative temperature.

The function (Eq. 3) is used

$$y = ax^b \quad (\text{Eq. 3})$$

where y is the z score values of discharge; a and b are coefficients; x is the z score values of cumulative temperature.

3.7 Application of Function to IPCC- CIMIP5 Climate Models

In the Fraser River basin, 25 locations were selected to download a set of six general circulation models (GCM) from NASA NEX GDDP dataset. The stations' locations are shown in Figure 4.2 Location of GCM grids in the Fraser River basin where the temperature data was obtained (Image layer taken from google maps).and listed in Table 3.4. A set of six GCM models was selected to estimate the changes in low flow of the Fraser River. The CMIP5 GCM models are listed in Table 3.5. The spatial resolution of this dataset is 25 km x 25 km (NASA, 2020).

SI. No.	Location	Latitude	Longitude
1	Hope	49°22'48"N	121°26'24"W
2	Lytton	50°13'59"N	121°34'53"W
3	Lillooet	50°41'10"N	121°56'14"W
4	High Bar	51°06'14"N	121°59'43"W
5	Churn Creek	51°26'43"N	122°16'31"W
6	Alkali Lake	51°47'21"N	122°23'42"W
7	William Lake	52°09'53"N	122°15'30"W
8	Kersley	52°49'07"N	122°25'06"W
9	Hixon	53°24'57"N	122°34'59"W
10	Prince George	53°55'00"N	122°44'58"W
11	Aleza Lake	54°06'59"N	122°02'00"W
12	Penny	53°50'34"N	121°17'34"W
13	Mcbride	53°18'04"N	120°10'06"W
14	Tete Jaune Cache	52°57'56"N	119°25'47"W
15	Brule Hill	52°36'43"N	118°27'53"W
16	Nechako	53°24'42"N	126°34'05"W
17	Stellaco River	53°47'35"N	124°52'42"W
18	Mount Blanchet	55°17'58"N	125°50'49"W
19	Mt McClinchy	52°08'13"N	124°51'05"W
20	Mt Farrow	51°06'04"N	124°06'13"W
21	Hendrix Lake	52°05'31"N	120°47'36"W
22	Clearwater	51°39'09"N	120°04'56"W
23	Sun peaks mountain	50°54'10"N	119°54'40"W
24	Douglas Lake	50°09'53"N	120°11'58"W
25	Bakerville	53°04'09"N	121°30'53"W

Table 3.2 List of stations along with their locations chosen for downscaled GCMs.

Sl. No.	Modeling Centre	Model	Institution
1	CCCma	CanESM2	Canadian Centre for Climate Modelling and Analysis
2	NCAR	CCSM4	National Center for Atmospheric Research
3	CNRM-CERFACS	CNRM-CM5	Centre National de Recherches Meteorologiques / Centre Europeen de Recherche et Formation Avancees en Calcul Scientifique
4	CSIRO-QCCCE	CSIRO-Mk3-6-0	Commonwealth Scientific and Industrial Research Organisation in collaboration with the Queensland Climate Change Centre of Excellence
5	INM	INM-CM4	Institute for Numerical Mathematics
6	MPI-M	MPI-ESM-LR	Max Planck Institute for Meteorology (MPI-M)

Table 3.3 A list of GCM models used in this study. (Details obtained from Program for climate model diagnosis and intercomparison (2020).

The selected list is a subset of climate models classified based on statistical analysis by Cannon (2015) for the region Western North America. These models are said to give large range in modelling future climates according to Pacific Climate Impact consortium (2020). These GCMs are also used in an impact assessment studies on water resources in British Columbia by Jose et al. for BC Hydro (2013).

Recent studies of Climate change impacts on snow and water resources in the Fraser River basin by S Islam et.al. (2017) used the set of 12 GCMs obtained from Cannon (2015). The same set of 12 GCMs are used in an another climate change impact assessment study on waterborne disease by Chhetri et al. (2019).

Chapter 4

Results and Discussion

4.1 Application of Functional fit

A 95% confidence bound forecast is developed further using the obtained coefficients from the functional fit (Eq. 2) and the average annual minimum discharge obtained from the historical data. Table 4.1 and Figure 4.1 show the forecasted discharge values at increasing z score values of cumulative temperature.

The average value of annual minimum discharge from the historical data is found to be 827.4 m³/s with a standard deviation of 263.45 m³/s.

Table 4.1 Variation of low flow with respect to z score values of cumulative watershed temperature, with 95% confidence interval

τ_z	Minimum discharge (m ³ /s)	Minimum discharge: upper limit (m ³ /s)	Minimum discharge: lower limit (m ³ /s)
0	827.40	827.40	827.40
0.25	833.33	833.34	832.78
0.1	828.21	828.08	828.27
0.15	829.35	829.18	829.35
0.2	831.04	830.91	830.85
0.25	833.33	833.34	832.78
0.3	836.22	836.55	835.14
0.35	839.74	840.57	837.93
0.4	843.90	845.46	841.14
0.45	848.73	851.27	844.77
0.5	854.24	858.03	848.83
0.55	860.44	865.77	853.31
0.6	867.34	874.55	858.22
0.65	874.95	884.38	863.55
0.7	883.29	895.30	869.31
0.75	892.36	907.34	875.49
0.8	902.17	920.53	882.09
0.85	912.74	934.89	889.12
0.9	924.06	950.46	896.57
0.95	936.15	967.25	904.44

τ_z	Minimum discharge (m ³ /s)	Minimum discharge: upper limit (m ³ /s)	Minimum discharge: lower limit (m ³ /s)
1	949.02	985.30	912.74
1.05	962.67	1,004.62	921.45
1.1	977.10	1,025.25	930.59
1.15	992.34	1,047.19	940.15
1.2	1,008.37	1,070.48	950.14
1.25	1,025.21	1,095.13	960.55
1.3	1,042.87	1,121.17	971.37
1.35	1,061.35	1,148.61	982.63
1.4	1,080.65	1,177.48	994.30
1.45	1,100.78	1,207.79	1,006.39
1.5	1,121.75	1,239.56	1,018.91
1.55	1,143.56	1,272.81	1,031.84
1.6	1,166.22	1,307.57	1,045.20
1.65	1,189.73	1,343.83	1,058.98
1.7	1,214.09	1,381.63	1,073.18
1.75	1,239.32	1,420.99	1,087.81
1.8	1,265.41	1,461.90	1,102.85
1.85	1,292.37	1,504.41	1,118.31
1.9	1,320.20	1,548.50	1,134.20
1.95	1,348.91	1,594.22	1,150.51
2	1,378.50	1,641.56	1,167.23

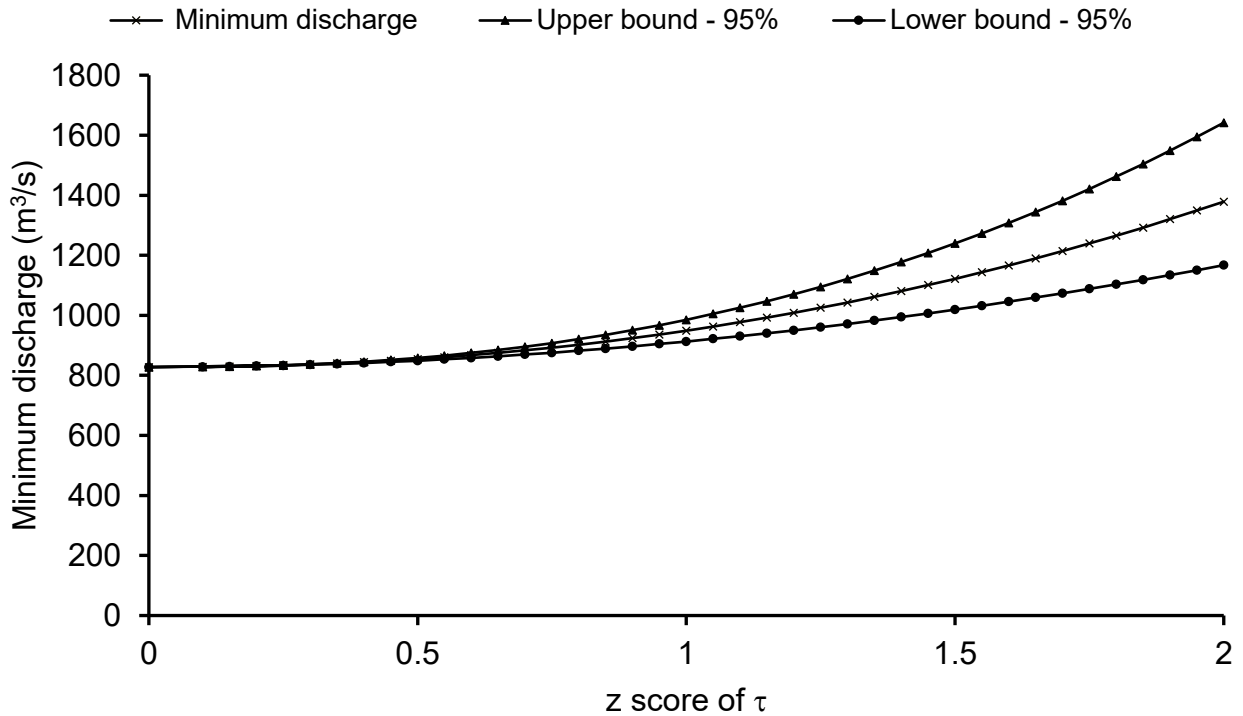


Figure 4.1 Variation of low flow with respect to standard z score of cumulative watershed temperature.

4.2 Estimation of Low Flow

4.2.1 Low flow estimation with inputs from Canada’s climate changing report

There is an expected increase in air temperature by 5.2° C by late 21st century under the high emission scenario of RCP 8.5 and a 1.6° C increase in air temperature by 2100 under the low emission scenario of RCP 2.6. (Table 4.2, (Bush et al., 2019))

The average annual minimum cumulative watershed temperature from the historic records is

$$\tau_{min} = - 357.84^{\circ} \text{ C} \quad (\text{Eq. 4})$$

The standard deviation of the annual minimum cumulative temperature from historic record is

$$\sigma_{\tau_{min}} = 215.34^{\circ} C \quad (\text{Eq. 5})$$

The expected increase in the cumulative temperature for the minimum flow under the high emission scenario (RCP 8.5),

$$\tau_{min (HE)} = \tau_{min} + (1/2) \sum_{k=0}^{96} (5.2 + 5.2k) \quad (\text{Eq. 6})$$

$$\tau_{min (HE)} = -357.84^{\circ} C + 254.8^{\circ} C \quad (\text{Eq. 7})$$

$$\tau_{min (HE)} = -103.04^{\circ} C \quad (\text{Eq. 8})$$

The expected increase in the cumulative temperature for the minimum flow under the low emission scenario (RCP 2.6) is

$$\tau_{min (LE)} = \tau_{min} + (1/2) \sum_{k=0}^{96} (1.6 + 1.6k) \quad (\text{Eq. 9})$$

$$\tau_{min (LE)} = -357.84^{\circ} C + 78.4^{\circ} C \quad (\text{Eq. 10})$$

$$\tau_{min (LE)} = -279.44^{\circ} C \quad (\text{Eq. 11})$$

Note that k ranges from 0 to 96 days since the average annual minimum flow occurs on March 7th as seen in the historical data. The 0th day is taken as December 1st as the consistent negative temperature begins around this time.

$$\tau_{Z(HE)} = \frac{[\tau_{\min(HE)} - \tau_{\min}]}{\sigma_{\tau_{\min}}} \quad (\text{Eq. 12})$$

$$\tau_{Z(HE)} = \frac{[-103.04^{\circ}\text{C} - (-357.84^{\circ}\text{C})]}{215.34^{\circ}\text{C}} \quad (\text{Eq. 13})$$

$$\tau_{Z(HE)} = 1.18 \quad (\text{Eq. 14})$$

$$\tau_{Z(LE)} = \frac{[\tau_{\min(LE)} - \tau_{\min}]}{\sigma_{\tau_{\min}}} \quad (\text{Eq. 15})$$

$$\tau_{Z(LE)} = \frac{[-279.44^{\circ}\text{C} - (-357.84^{\circ}\text{C})]}{215.34^{\circ}\text{C}} \quad (\text{Eq. 16})$$

$$\tau_{Z(LE)} = 0.36 \quad (\text{Eq. 17})$$

Discharge values under both emission scenarios are estimated using the function (Eq. 2) below and tabulated in Table 4.2

$$Q = \sigma_Q \left[a \left(\frac{\tau - \bar{\tau}}{\sigma_{\tau}} \right)^b \right] + \bar{Q} \quad (\text{Eq. 2})$$

	τ_z	Minimum discharge	Upper bound – 95% Confidence	Lower bound – 95% Confidence
		m ³ /s	m ³ /s	m ³ /s
High Emission (RCP 8.5)	1.18	1,002.91	1,062.53	946.75
Low Emission (RCP 2.6)	0.36	840.84	841.86	838.79

Table 4.2 Estimates of low flow using inputs from Canada’s Changing climate report (Bush et al., 2019)

4.2.2 Low flow estimation based on NASA NEX GDDP - CMIP5 GCMs

NASA Earth exchange global daily downscaled projections for RCP 4.5 and RCP 8.5 are used to forecast the changes in minimum discharge values under climate change scenario.

Six different GCM models for 25 grids located within the Fraser River basin (Figure 4.2) are obtained, and the mean temperature is calculated by averaging the daily minimum and maximum values. All the GCM models are combined using the averaging procedure.

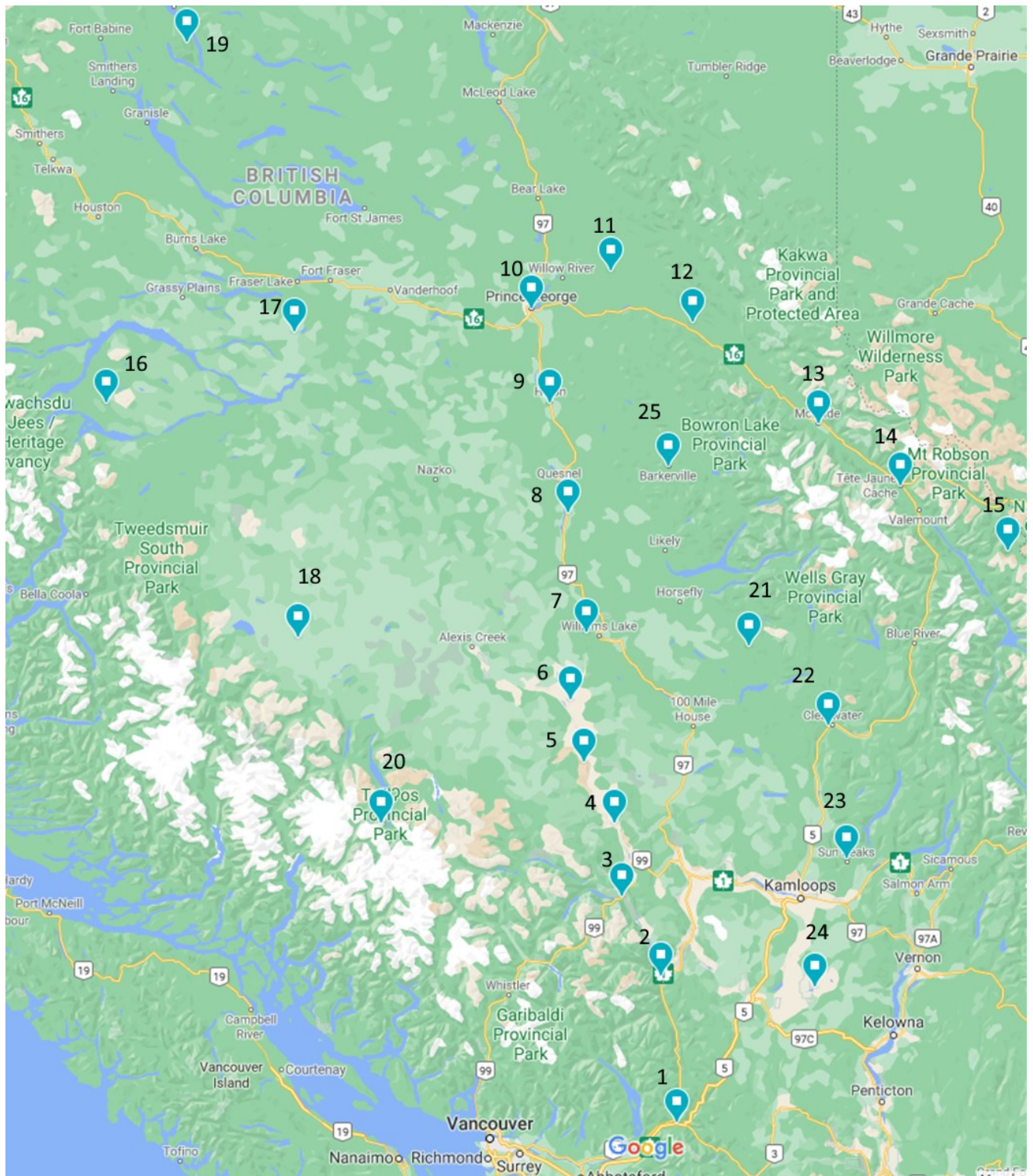


Figure 4.2 Location of GCM grids in the Fraser River basin where the temperature data was obtained (Image layer taken from google maps).

The results from the model CanESM2 under trajectory of RCP4.5, forecast a net increase in cumulative watershed temperature by the end of 21st century, from its present average value of -357.84 °C to -92.14 °C. Highest value of minimum discharge forecast is 1178.86 m³/s from its present average of 827.4 m³/s. The lowest value of discharge is forecasted up to zero, resulting in no flow condition, in the first half of this century. However, a positive trend is displayed in an overall variation of minimum discharge by the year 2100, and the trend shows an average increase up to 950 m³/s. The forecast results for this model are shown in Figure 4.3 & Figure 4.4.

The results from CCSM4, a GCM model, under trajectory of RCP4.5, forecast an insignificant increase in the trend. Highest value of minimum discharge forecast is 1346.51 m³/s from its present average of 827.4 m³/s. This is higher than the one predicted by CanESM2. The lowest value of discharge is forecasted up to 324.74m³/s during the second half of this century. The overall trend of minimum discharge is very different from the CanESM2. This model shows almost a horizontal trend with highest forecasted low discharge is around 970 m³/s. Even though there are some extreme events of high and low discharges, the trend remains mostly unaffected. The forecast results for this model are shown in Figure 4.5 & Figure 4.6.

The results from the model CNRM-CM5 under trajectory of RCP4.5, forecast a positive trend. The net cumulative watershed temperature is expected to increase up to -59.5 °C, which is similar to the expected value under CanESM2. Highest value of minimum discharge forecast is 1218.59 m³/s from its present average of 827.4 m³/s. This is similar to the expected value under CanESM2. There is a certain extreme event of no flow is forecasted in the short term and it goes up to 727.52 m³/s by the end of 21st century. The overall trend of minimum discharge is similar to CanESM2. This model shows a positive trend of low flow with highest forecasted low flow is around 970 m³/s. The forecast results for this model are shown in Figure 4.7 & Figure 4.8.

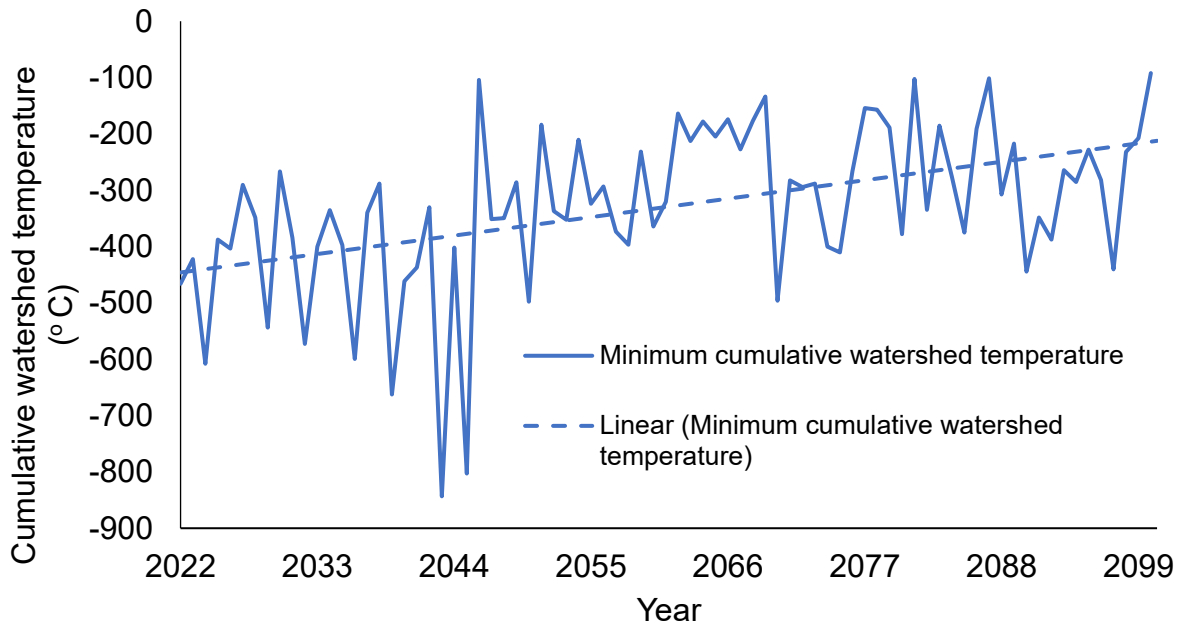


Figure 4.3 Forecast of minimum watershed cumulative temperature for RCP 4.5 from model: CanESM2.

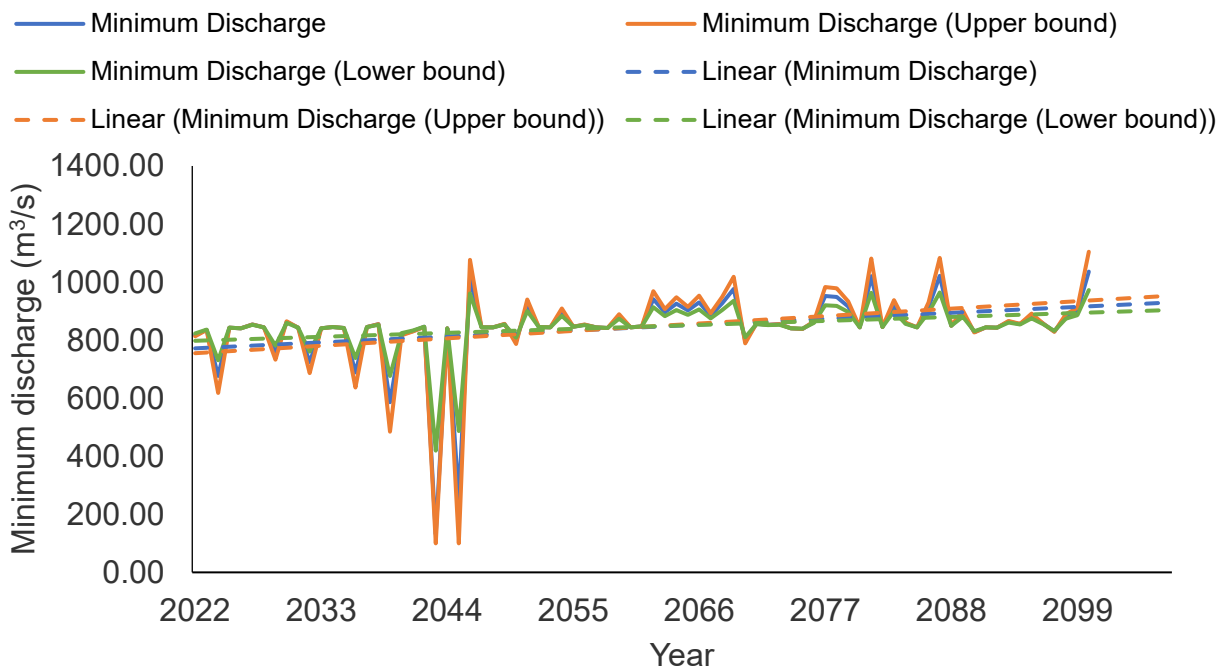


Figure 4.4 Forecast of minimum discharge for RCP 4.5, on the basis of temperature from model: CanESM2 (Predicted minimum discharge below 100 m³/s has been discarded).

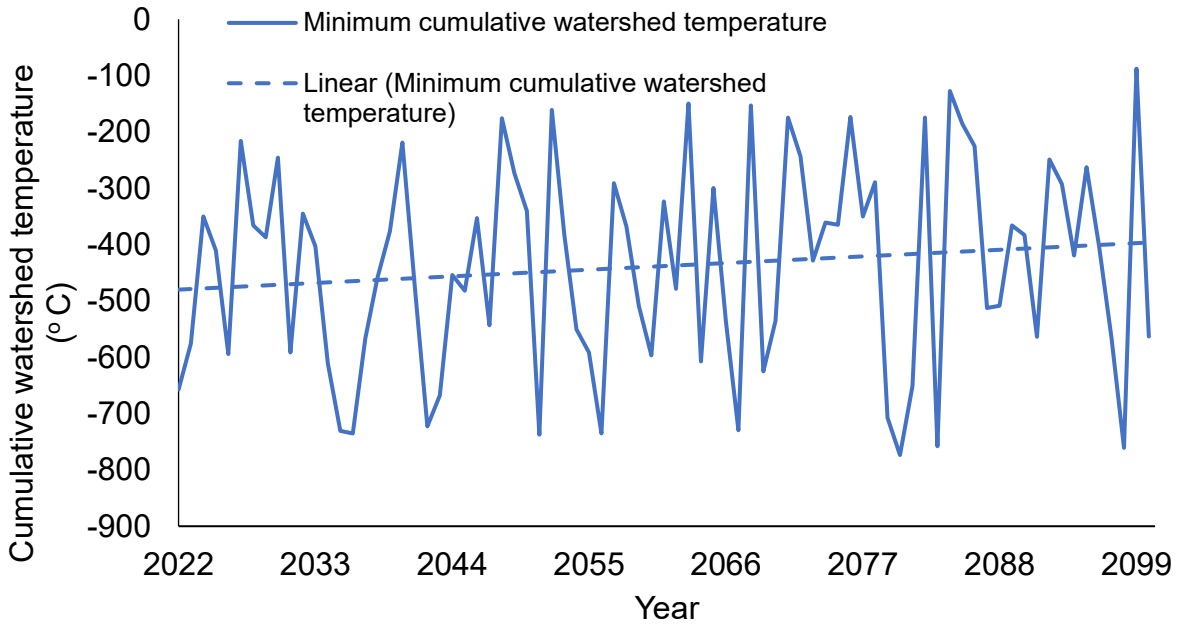


Figure 4.5 Forecast of minimum watershed cumulative temperature for RCP 4.5 from model: CCSM4.

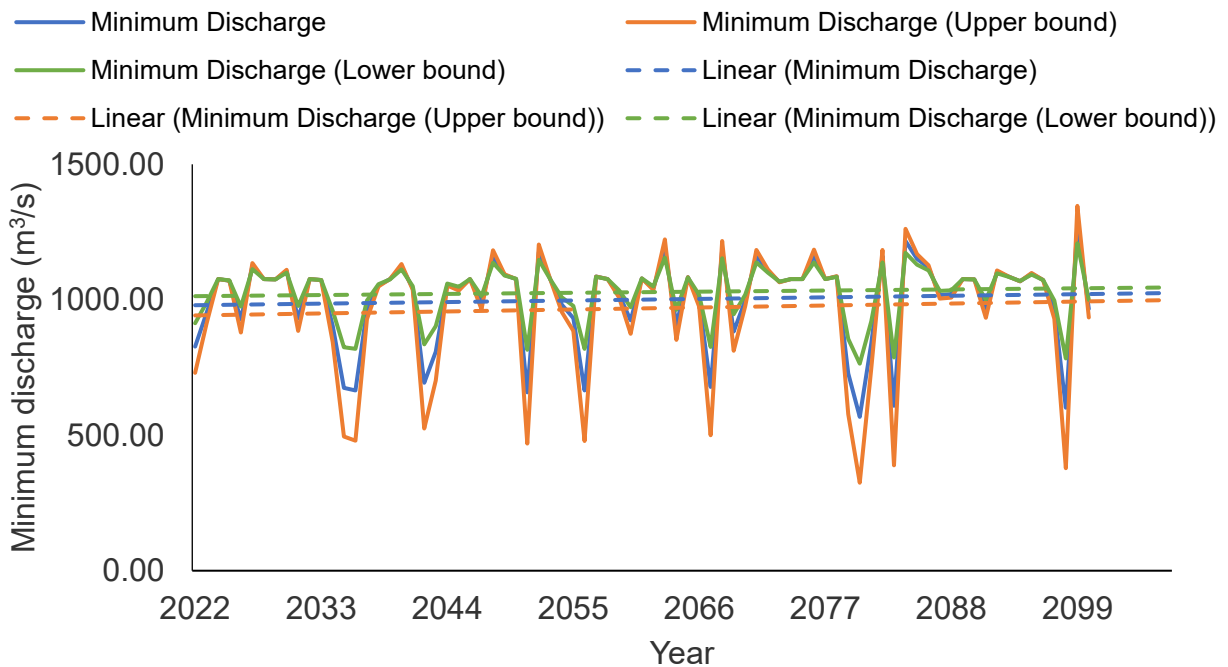


Figure 4.6 Forecast of minimum discharge for RCP 4.5, on the basis of temperature from model: CCSM4.

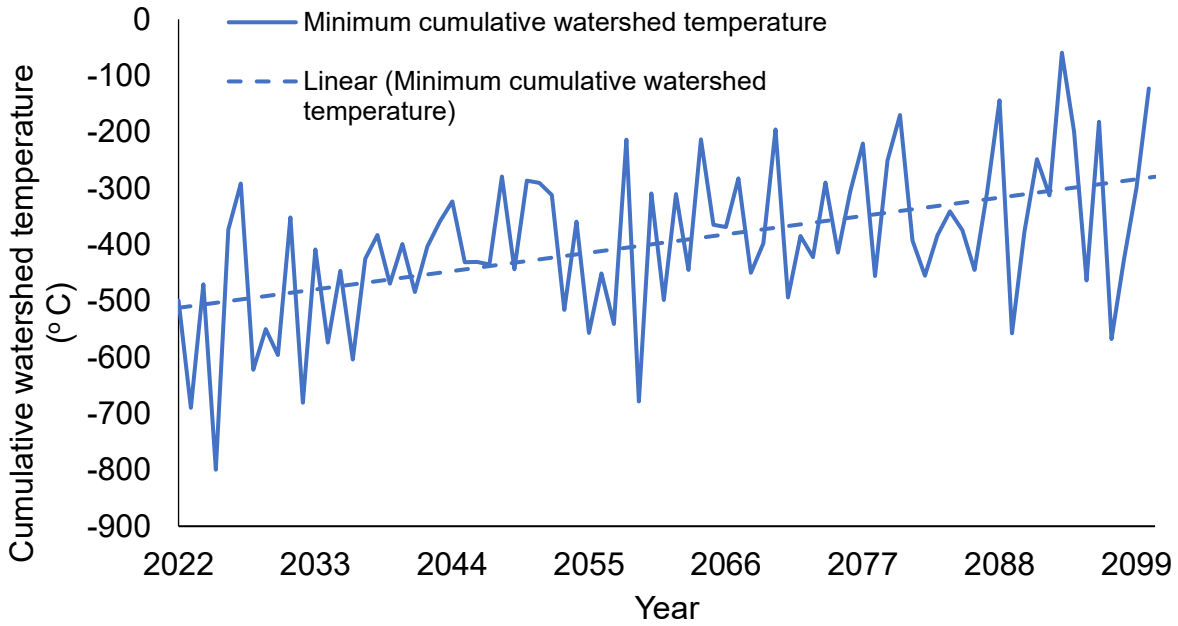


Figure 4.7 Forecast of minimum watershed cumulative temperature for RCP 4.5 from model: CNRM-CM5.

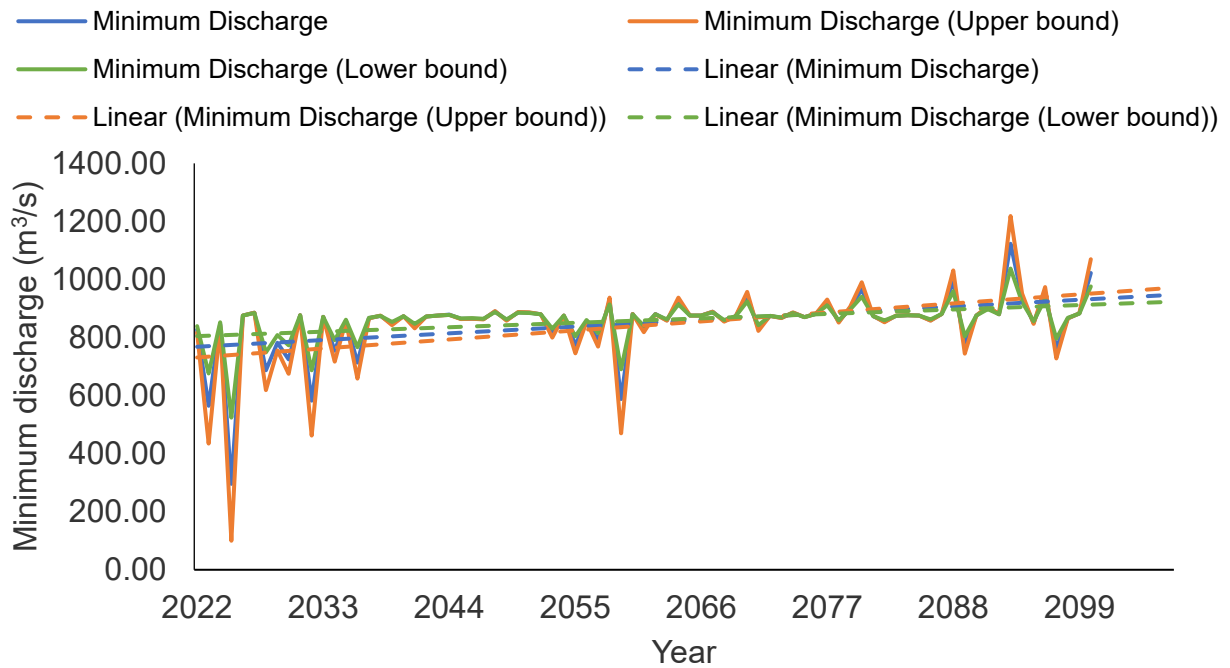


Figure 4.8 Forecast of minimum discharge for RCP 4.5, on the basis of temperature from model: CNRM-CM5 (Predicted minimum discharge below 100 m³/s has been discarded).

The results from the model CSIRO-Mk3-6-0 under trajectory of RCP4.5, forecast a positive trend of cumulative watershed temperature towards end of 21st century. Highest value of minimum discharge forecast is 1255.89m³/s from its present average of 827.4 m³/s. This is near to the one predicted by CNRM-CM5. There is a no flow condition predicted in the near future. However, a positive trend is displayed in overall variation of minimum discharge by the year 2100, and the trend shows an average increase up to 1100 m³/s, which is the higher than all the above predictions. The forecast results for this model are shown in Figure 4.9 & Figure 4.10.

The results from INM-CM4, a GCM model, under trajectory of RCP4.5, forecast a slight increase in the trend, from its present average value of -357.84 °C to -211.66 °C. Highest value of minimum discharge forecast is 1400.31 m³/s from its present average of 827.4 m³/s. This is nearer to the one predicted made by CCSM4. There is a no flow forecasted during the second half of this century. This model shows a minute positive trend with highest forecasted low discharge is around 1000 m³/s. There are some extreme events of high and low discharges expected under this model. The forecast results for this model are shown in Figure 4.11 & Figure 4.12.

The results from the model MPI-ESM-LR under trajectory of RCP4.5, forecast a horizontal trend. This is different from all the above predictions which showed an increase in the cumulative watershed temperature. Highest value of minimum discharge forecast is 1192.56 m³/s from its present average of 827.4 m³/s. The lowest value of discharge is forecasted up to 221.15 m³/s by the end of 21st century. Trend forecasts low discharge of around 830 m³/s, which is almost equal to the present average of 827.4 m³/s. There are many extreme events forecasted in this model. The forecast results for this model are shown in Figure 4.13 & Figure 4.14.

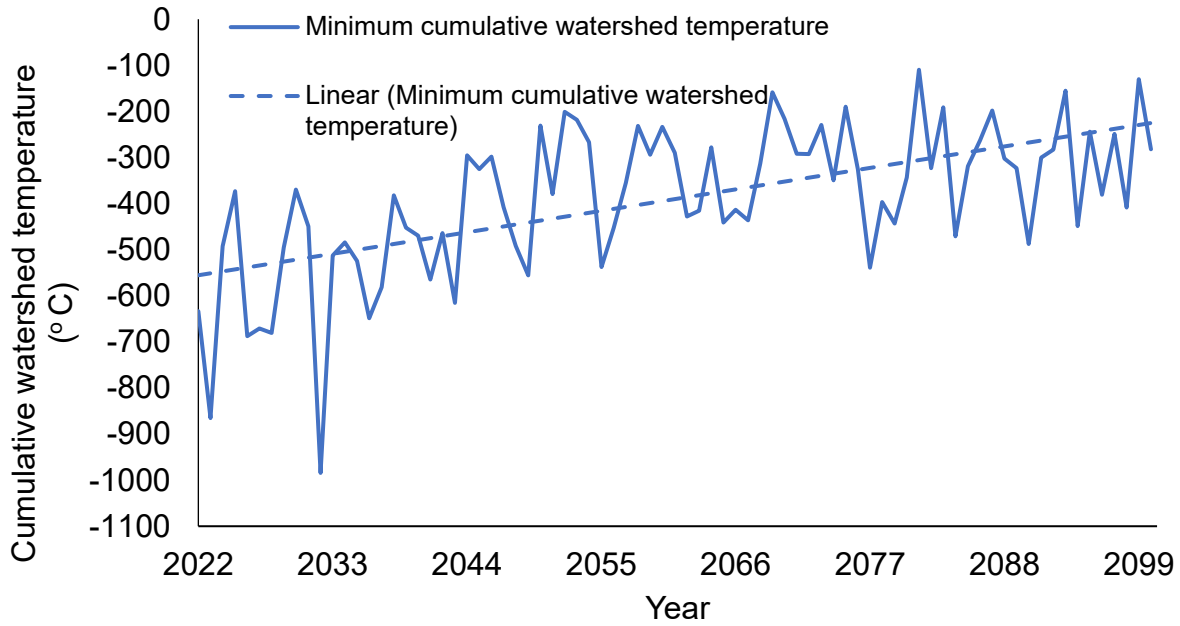


Figure 4.9 Forecast of minimum watershed cumulative temperature for RCP 4.5 from model: CSIRO-Mk3-6-0.

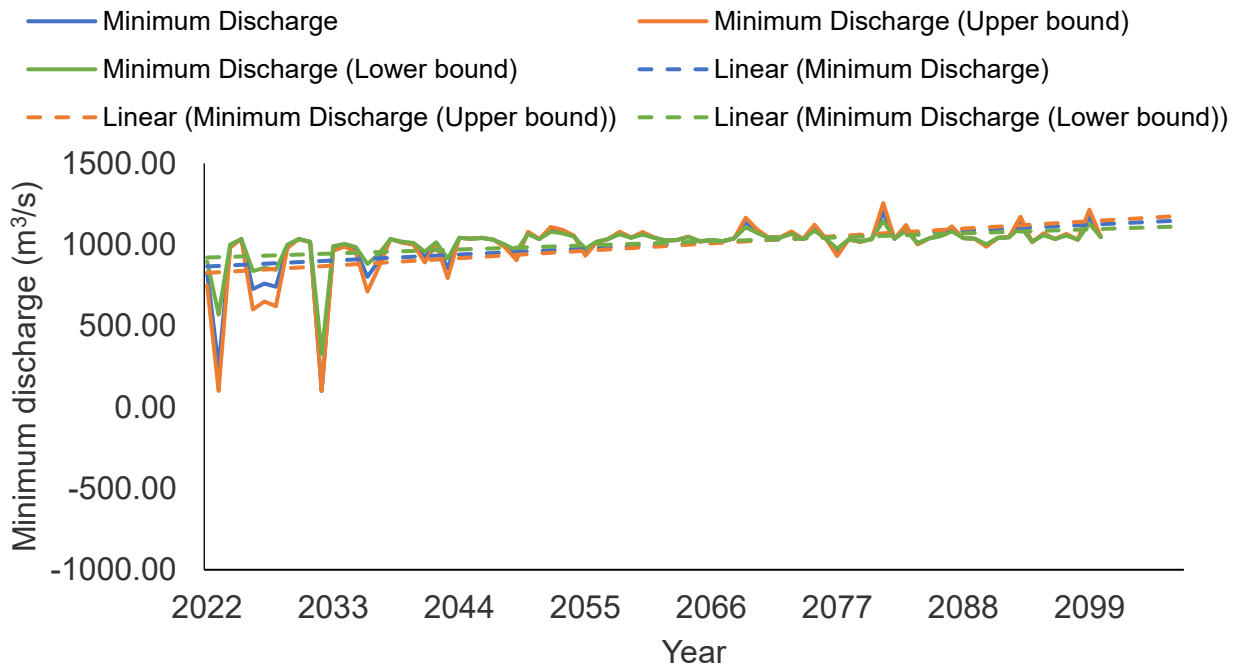


Figure 4.10 Forecast of minimum discharge for RCP 4.5, on the basis of temperature from model: CSIRO-Mk3-6-0 (Predicted minimum discharge below 100 m³/s has been discarded).

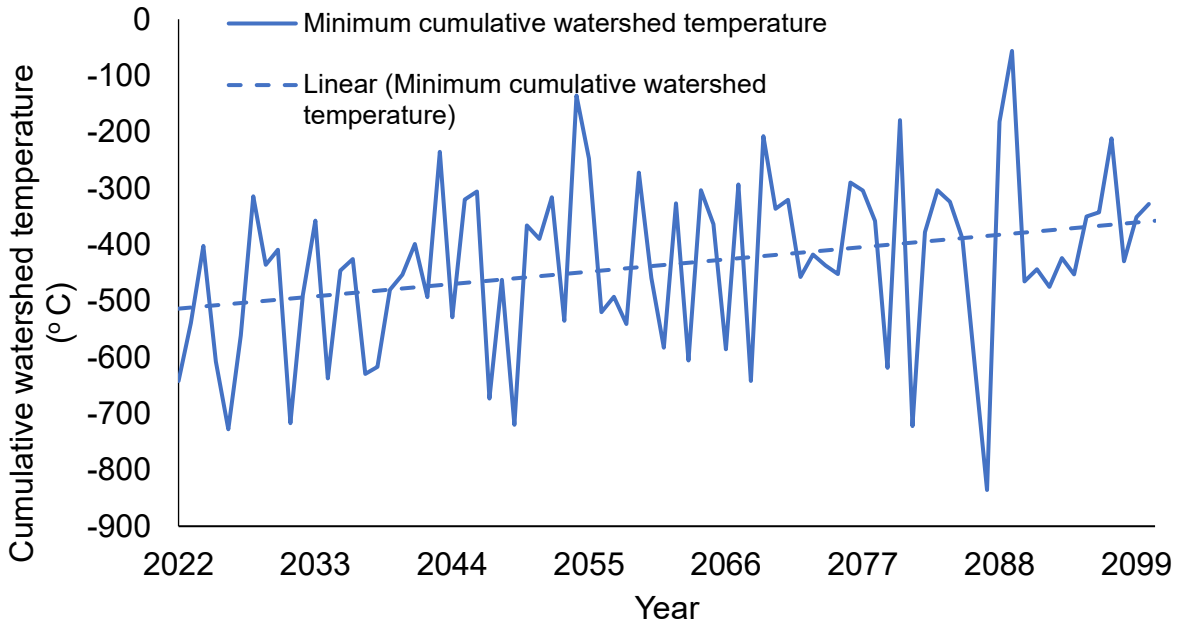


Figure 4.11 Forecast of minimum watershed cumulative temperature for RCP 4.5 from model: INM-CM4.

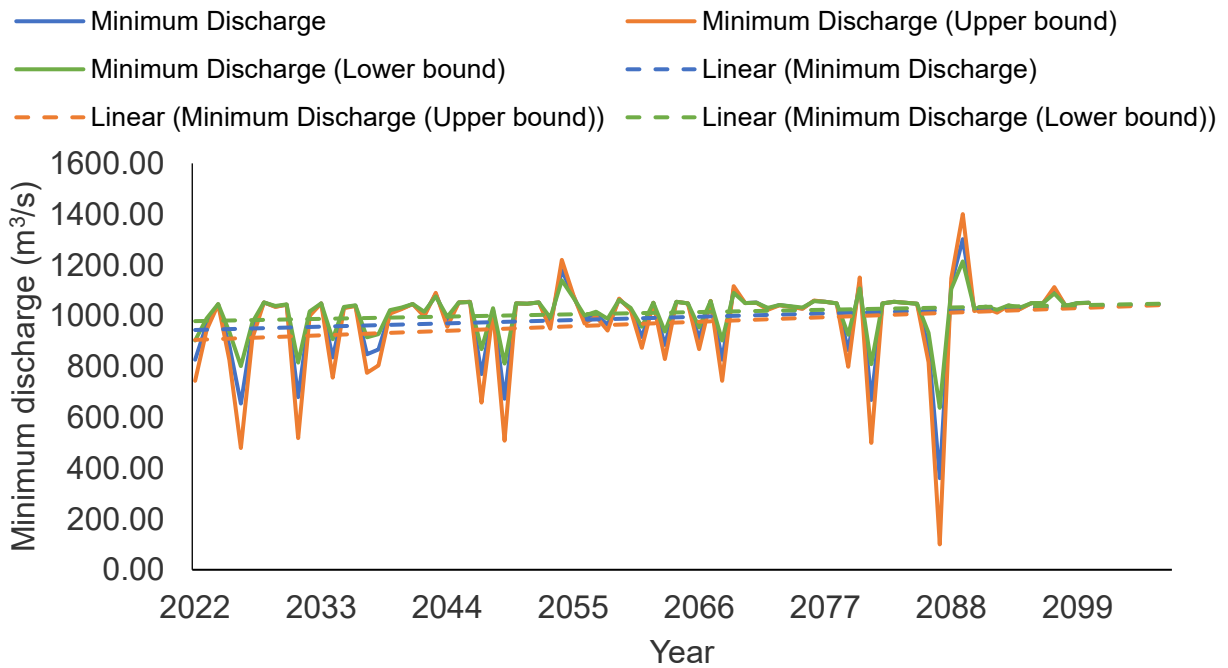


Figure 4.12 Forecast of minimum discharge for RCP 4.5, on the basis of temperature from model: INM-CM4 (Predicted minimum discharge below 100 m³/s has been discarded) .

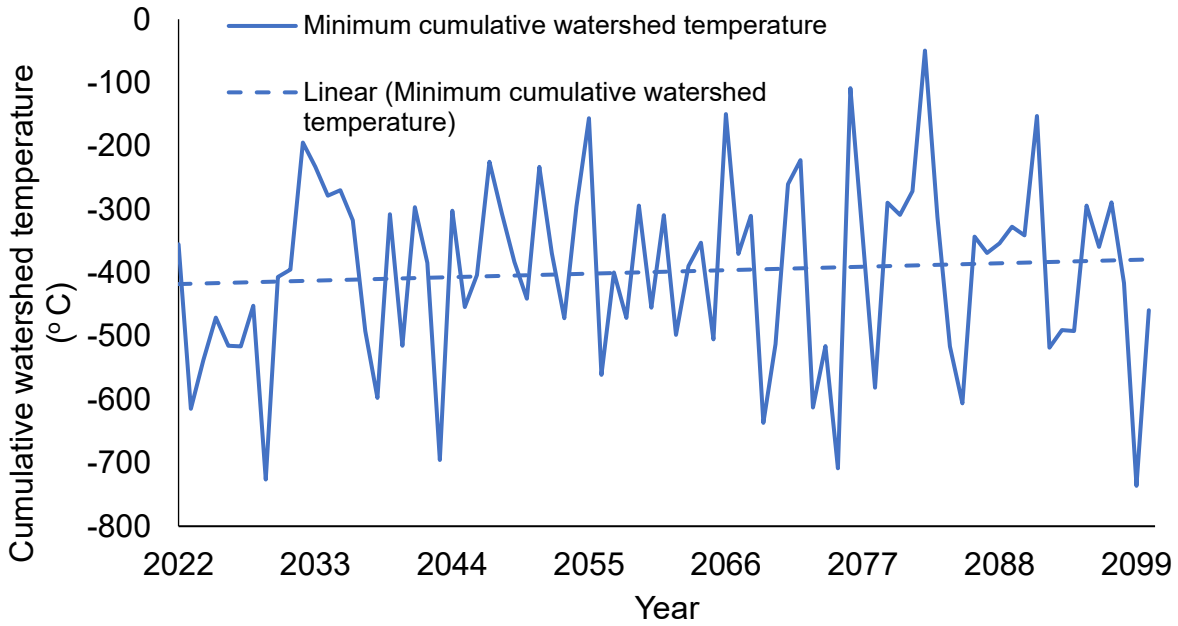


Figure 4.13 Forecast of minimum watershed cumulative temperature for RCP 4.5 from model: MPI-ESM-LR.

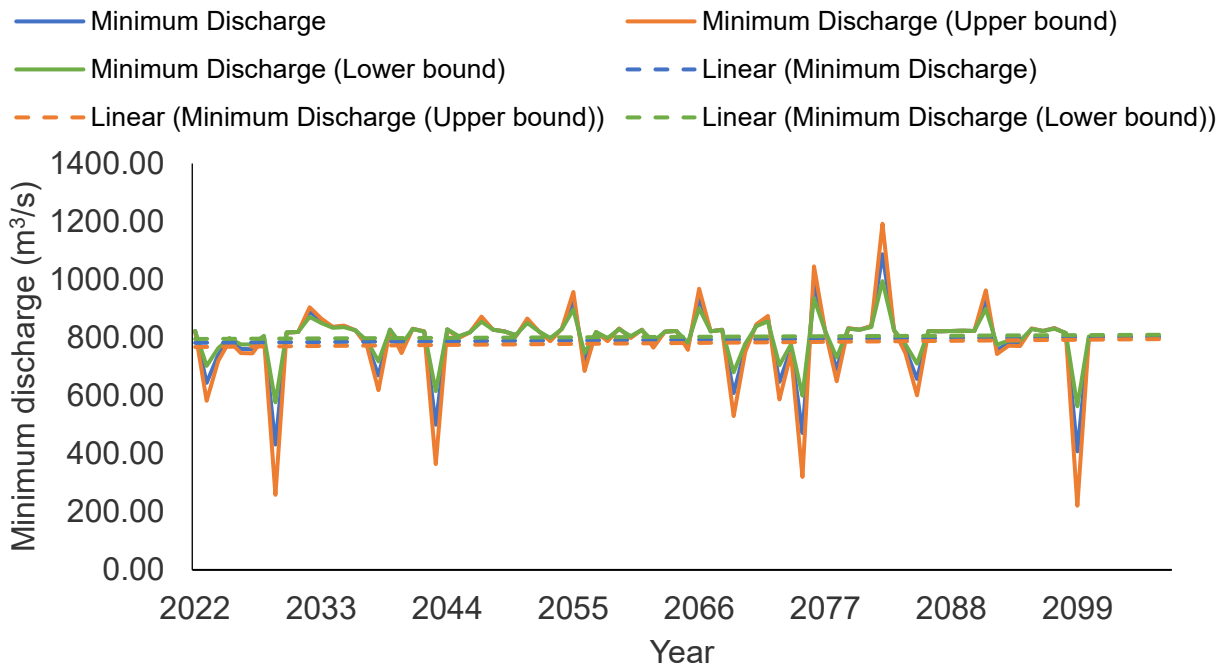


Figure 4.14 Forecast of minimum discharge for RCP 4.5, on the basis of temperature from model: MPI-ESM-LR.

The results from the model CanESM2 under trajectory of RCP8.5, forecast a net increase in cumulative watershed temperature by the end of 21st century, from its present average value of -357.84 °C to -9.82 °C. Highest value of minimum discharge forecast is 1315.62 m³/s from its present average of 827.4 m³/s. The lowest value of discharge is forecasted up to 833.16 m³/s by the end of this century. However, a positive trend is displayed in overall variation of minimum discharge by the year 2100, and the trend shows an average increase up to 1200 m³/s. The forecast results for this model are shown in Figure 4.15 & Figure 4.16.

The results from CCSM4, a GCM model, under trajectory of RCP8.5, forecast a positive trend of cumulative watershed temperature. Highest value of minimum discharge forecast is 1392.8 m³/s from its present average of 827.4 m³/s. This is higher than the one predicted by CanESM2. Model forecast no flow condition in the near future, but by the end of 21st century the lowest expected value is predicted to be 754.63 m³/s. This model shows almost a positive trend with a forecasted average of 1300 m³/s by the end of this century. The forecast results for this model are shown in Figure 4.17 & Figure 4.18.

The results from the model CNRM-CM5 under trajectory of RCP8.5, forecast a positive trend of cumulative watershed temperature and low flow, which is similar to the trend of above two models. Highest value of minimum discharge forecast is 1377.21 m³/s and the lowest is 828.81 m³/s by the end of 21st century. This model shows a positive trend of low flow with average forecasted low flow is around 1300 m³/s by year 2100. The forecast results for this model are shown in Figure 4.19 & Figure 4.20.

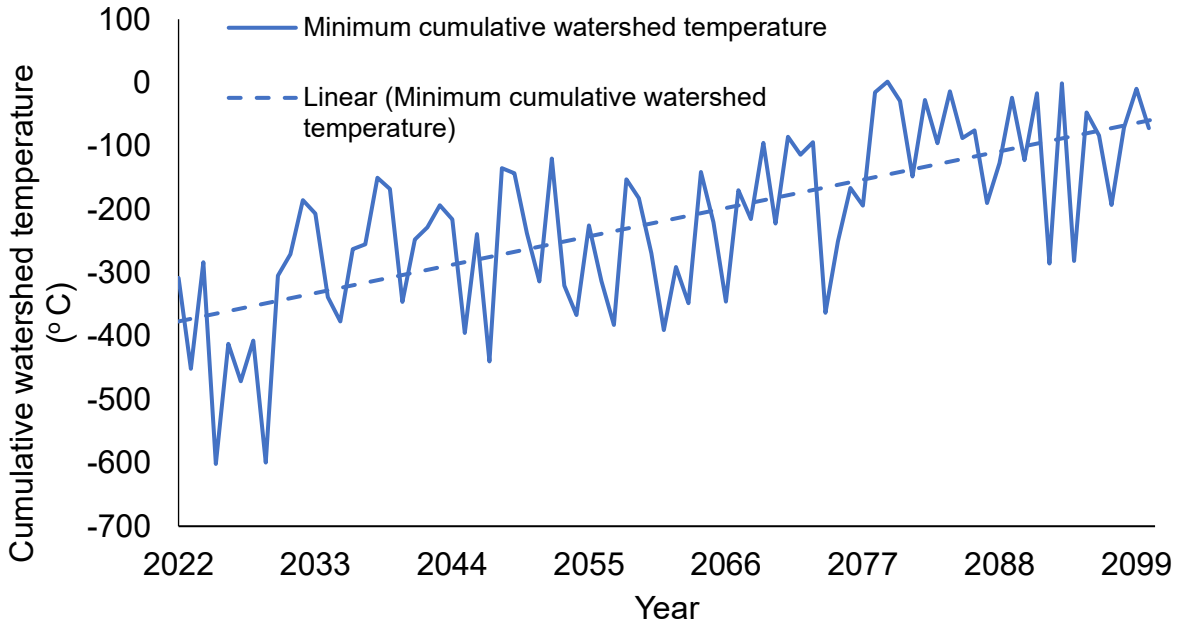


Figure 4.15 Forecast of minimum watershed cumulative temperature for RCP 8.5 from model: CanESM2.

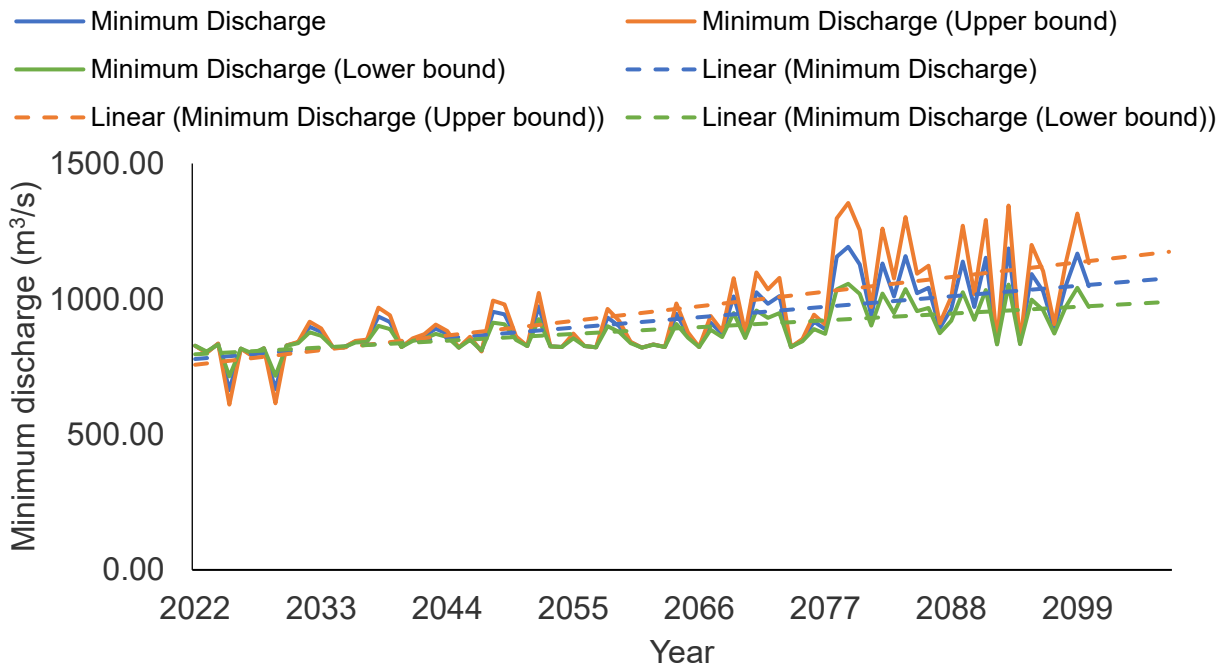


Figure 4.16 Forecast of minimum discharge for RCP 8.5, on the basis of temperature from model: CanESM2.

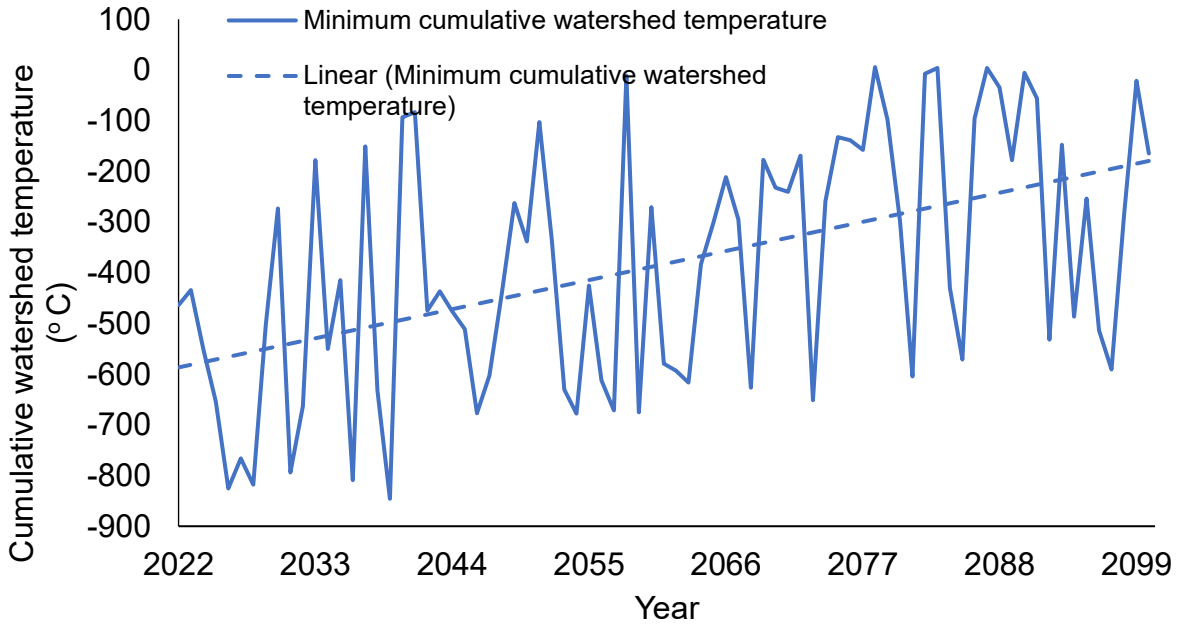


Figure 4.17 Forecast of minimum watershed cumulative temperature for RCP 8.5 from model: CCSM4.

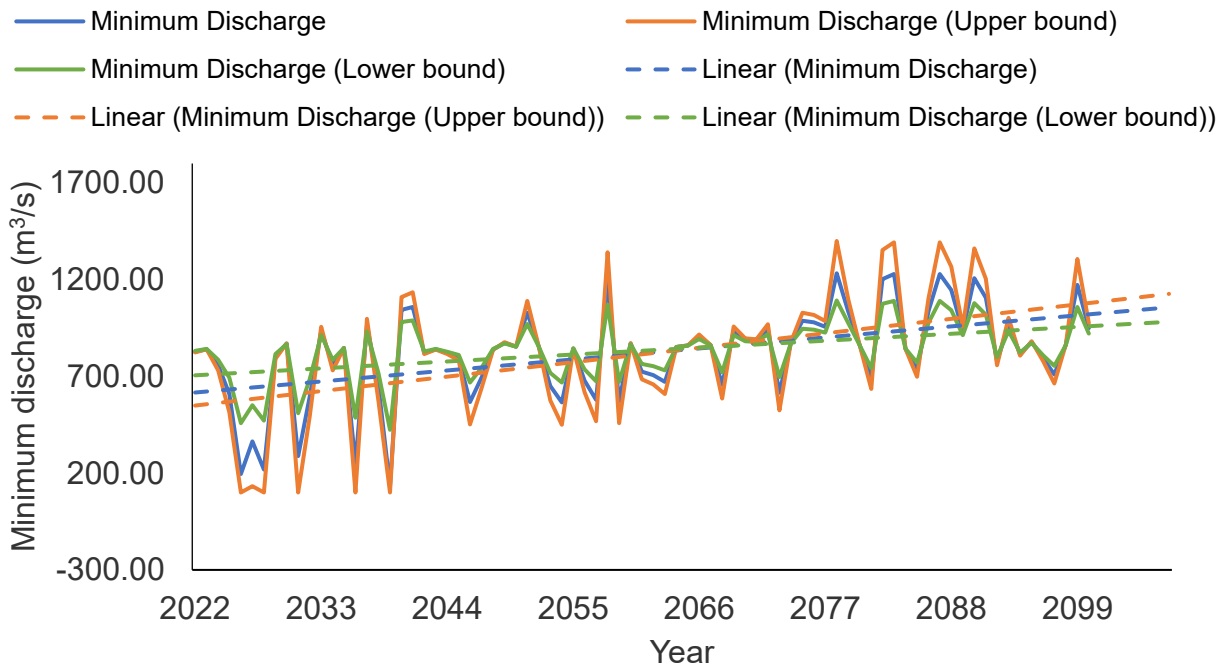


Figure 4.18 Forecast of minimum discharge for RCP 8.5, on the basis of temperature from model: CCSM4 (Predicted minimum discharge below 100 m³/s has been discarded).

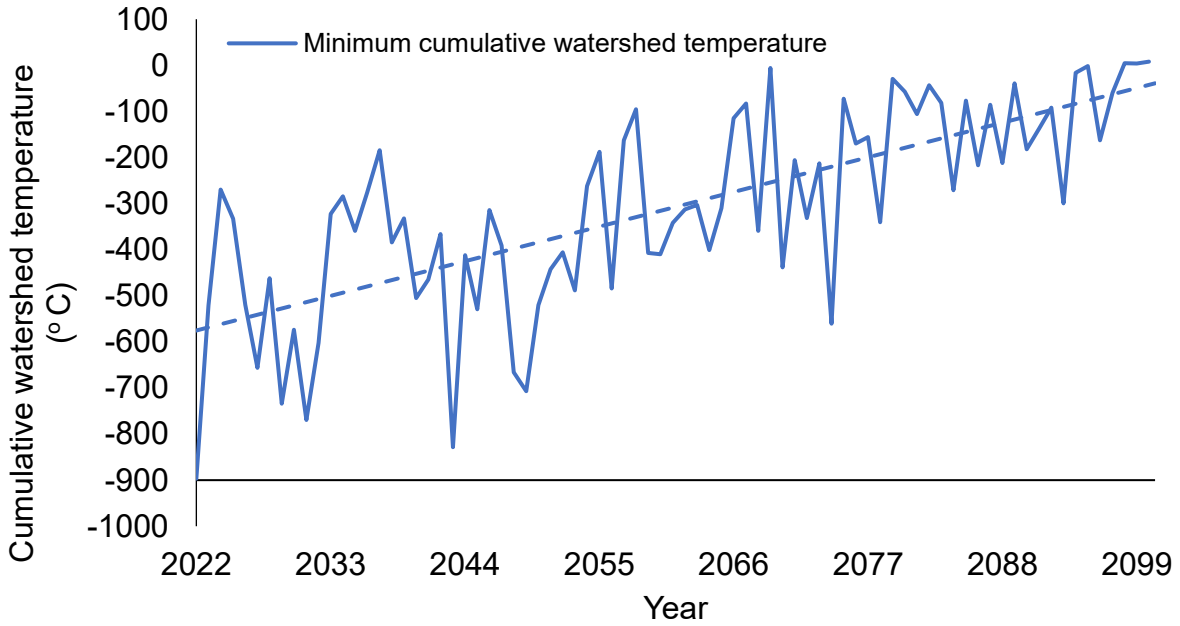


Figure 4.19 Forecast of minimum watershed cumulative temperature for RCP 8.5 from model: CNRM-CM5.

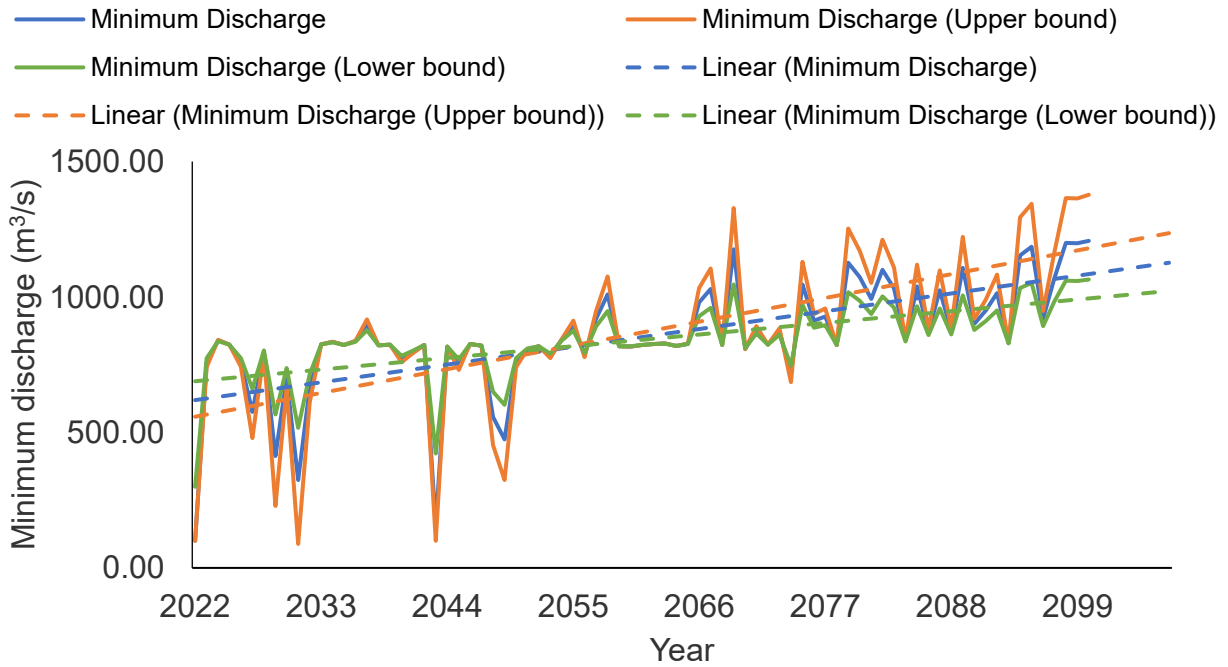


Figure 4.20 Forecast of minimum discharge for RCP 8.5, on the basis of temperature from model: CNRM-CM5 (Predicted minimum discharge below 100 m³/s has been discarded).

The results from the model CSIRO-Mk3-6-0 under trajectory of RCP8.5, forecast a positive trend of cumulative watershed temperature towards end of 21st century. Highest value of minimum discharge forecast is 1367.97 m³/s from its present average of 827.4 m³/s. This is also in the range of predictions made by above four models. There is a no flow condition predicted in the near future as an extreme event. However, a positive trend is displayed in overall variation of minimum discharge by the year 2100, and the trend shows an average increase up to 1140 m³/s, which is lower than all the above four model predictions. The forecast results for this model are shown in Figure 4.21 & Figure 4.22.

The results from INM-CM4, a GCM model, under trajectory of RCP8.5, forecast a positive increase in the trend, from its present average value of -357.84 °C to -109.77 °C. Highest value of minimum discharge forecast is 1141.23 m³/s from its present average of 827.4 m³/s. This is lower than all other RCP8.5 models. The lowest value of discharge is forecasted up to 921.65 m³/s during the second half of this century, but there are some extreme no flow events predicted in the first half of this century. The average low flow is around 1150 m³/s by the end of year 2100. There are a few extreme events of low discharges expected under this model. The forecast results for this model are shown in Figure 4.23 & Figure 4.24.

The results from the model MPI-ESM-LR under trajectory of RCP8.5, forecast a positive trend. Highest value of minimum discharge forecast is 1391.05 m³/s from its present average of 827.4 m³/s. The lowest value of discharge is forecasted up to 871.64 m³/s by the end of 21st century. Trend forecasts an average low discharge of around 1400 m³/s. The forecast results for this model are shown in Figure 4.25 & Figure 4.26.

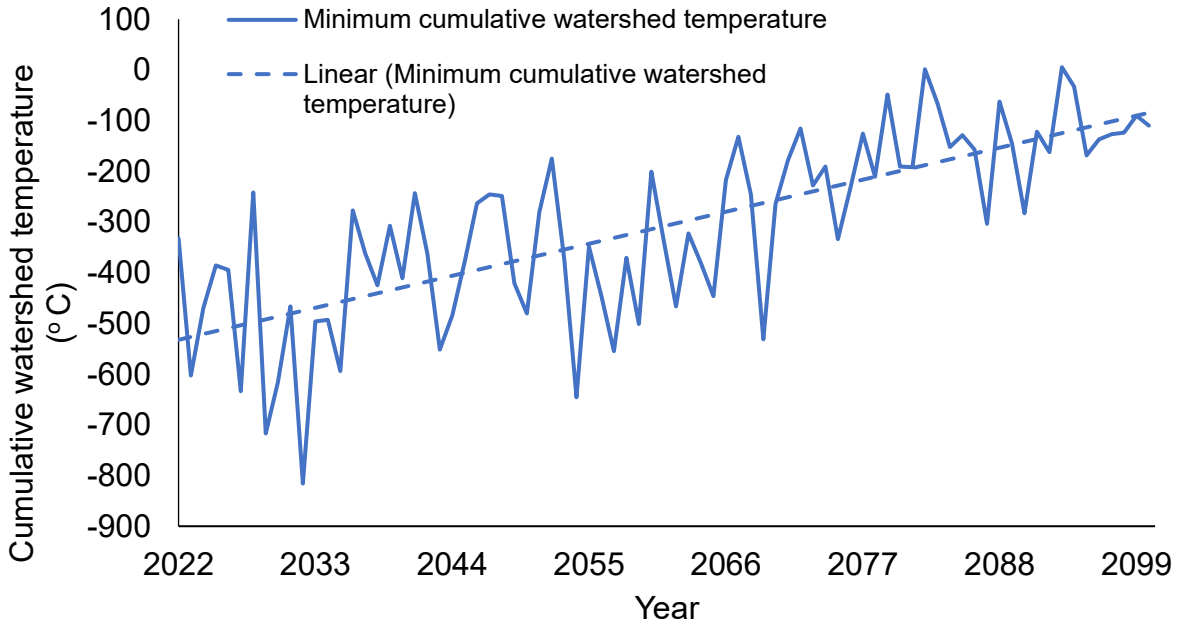


Figure 4.21 Forecast of minimum watershed cumulative temperature for RCP 8.5 from model: CSIRO-Mk3-6-0.

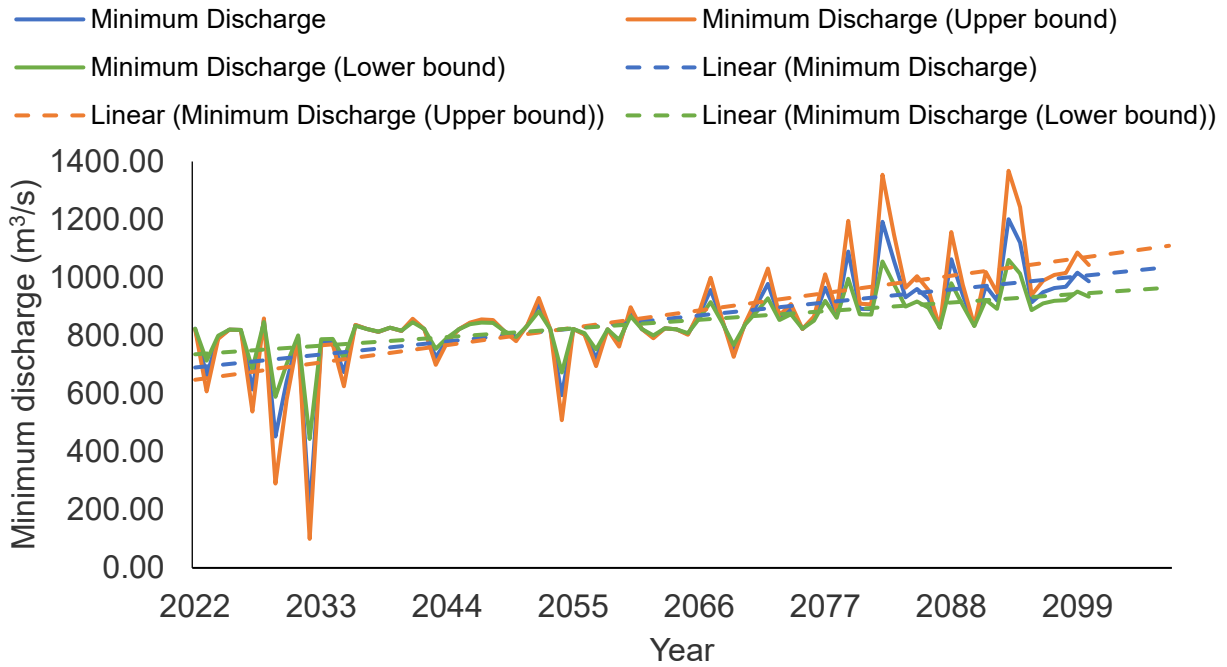


Figure 4.22 Forecast of minimum discharge for RCP 8.5, on the basis of temperature from model: CSIRO-Mk3-6-0 (Predicted minimum discharge below 100 m³/s has been discarded).

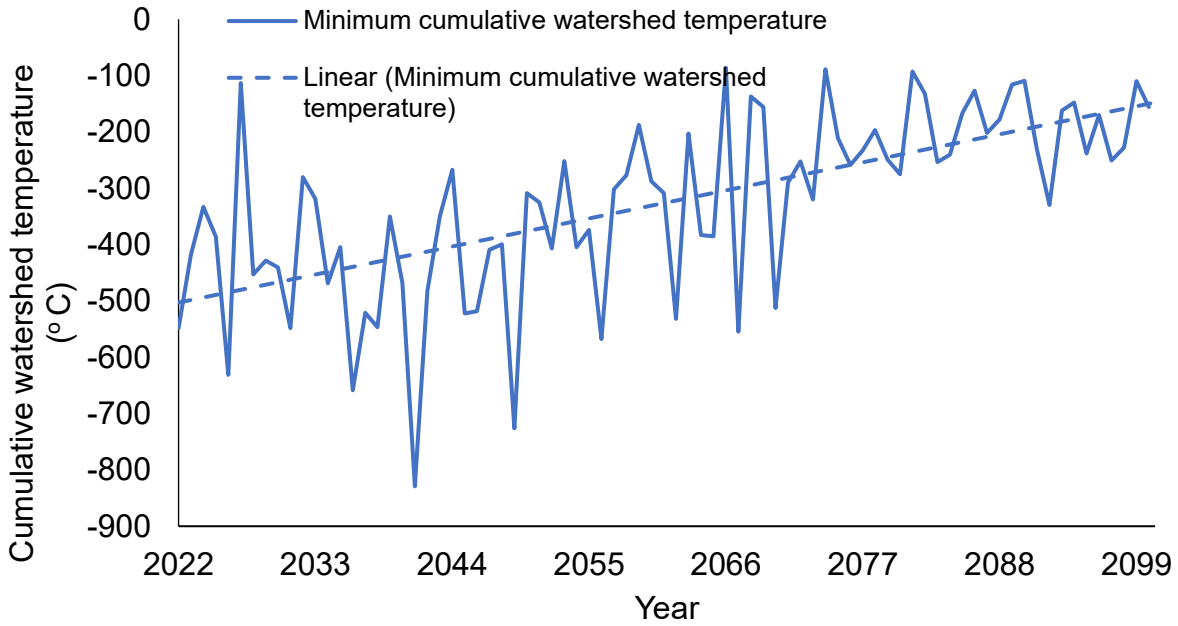


Figure 4.23 Forecast of minimum watershed cumulative temperature for RCP 8.5 from model: INM-CM4.

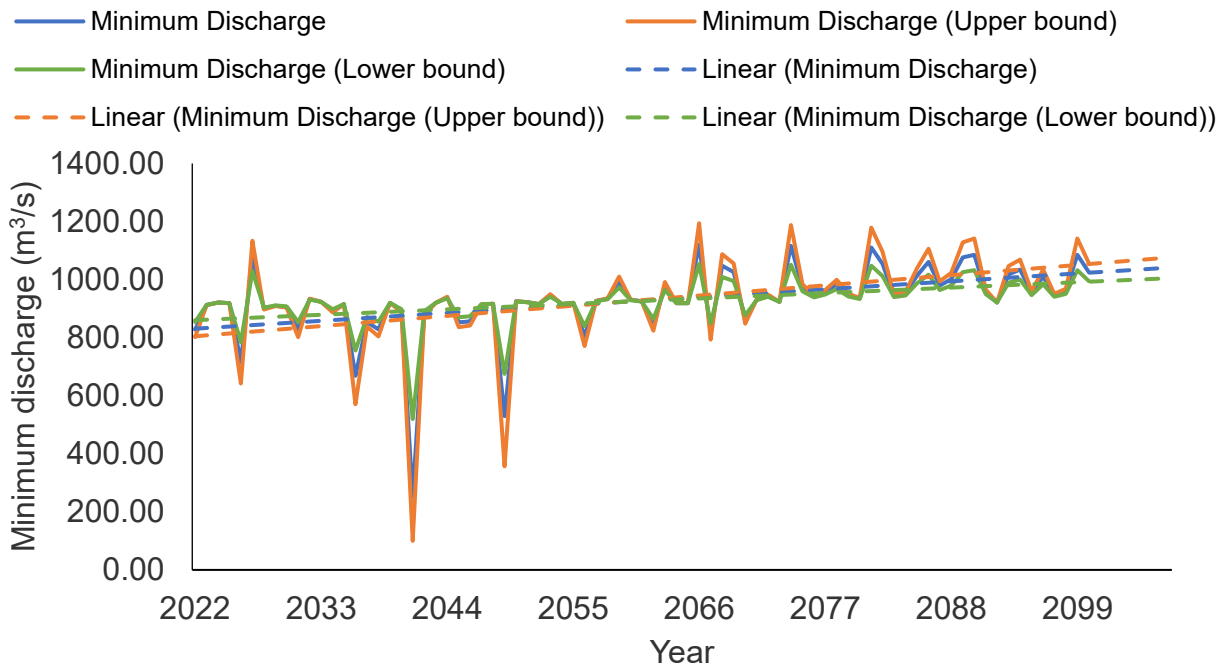


Figure 4.24 Forecast of minimum discharge for RCP 8.5, on the basis of temperature from model: INM-CM4 (Predicted minimum discharge below 100 m³/s has been discarded) .

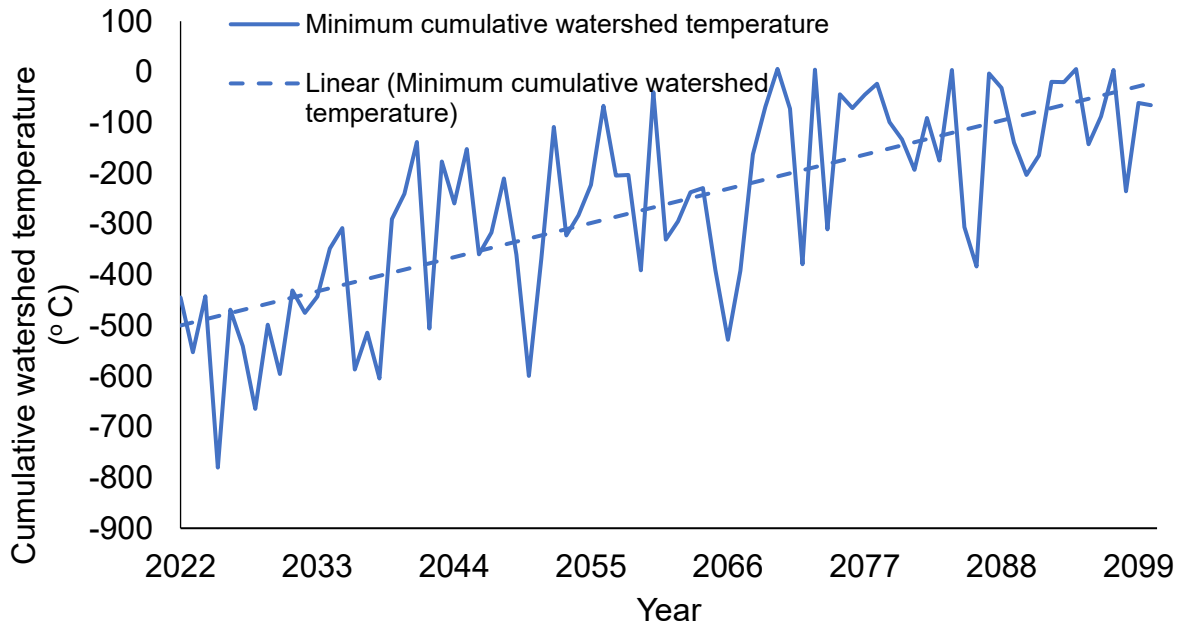


Figure 4.25 Forecast of minimum watershed cumulative temperature for RCP 8.5 from model: MPI-ESM-LR.

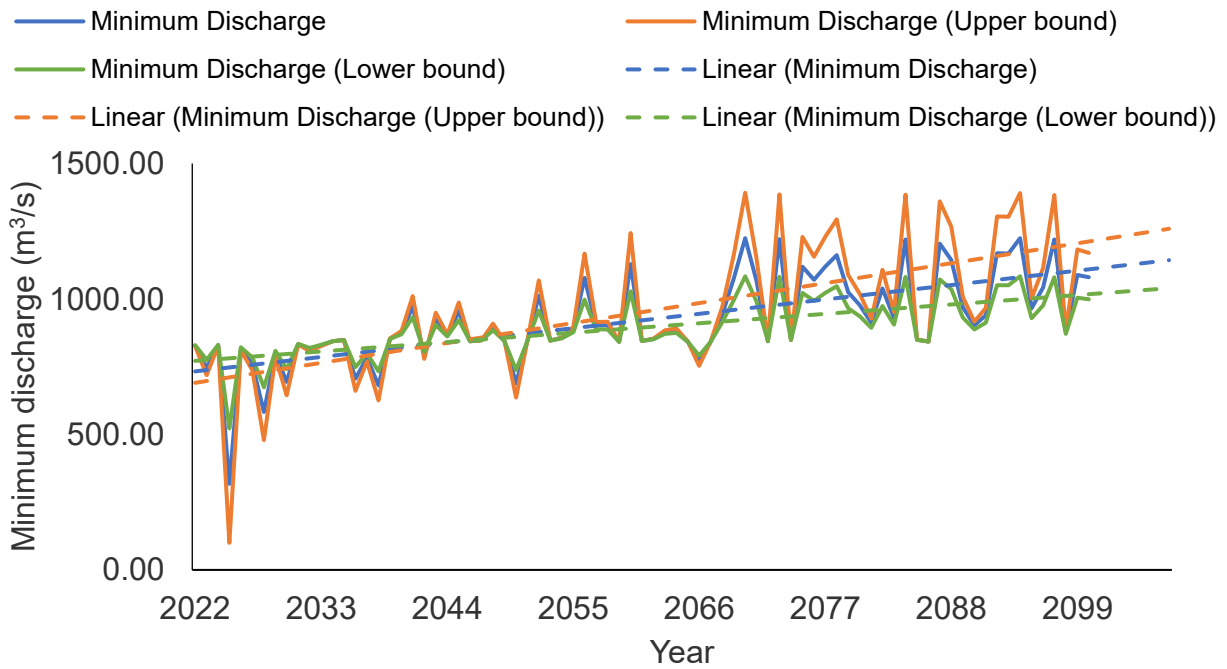


Figure 4.26 Forecast of minimum discharge for RCP 8.5, on the basis of temperature from model: MPI-ESM-LR (Predicted minimum discharge below 100 m³/s has been discarded).

Average low flow forecasted by the end of 21st century under RCP8.5 is larger than that forecasted under RCP4.5, which is the case for all the six models.

The average low flow discharge ranges from 950 to 1100 m³/s for most of the RCP4.5 models except MPI-ESM-LR. MPI-ESM-LR showed a horizontal trend in the low flow without any significant changes. The average low flow under RCP8.5 ranges between 1140 to 1400 m³/s.

A peculiar feature noticed in the GCM predictions, apart from the overall positive trend is the occurrences of extreme events of no flow during certain years. CanESM2 under RCP4.5, CNRM-CM5 under RCP4.5, CSIRO-Mk3-6-0 under RCP4.5 , INM-CM4 under RCP4.5, CCSM4 under RCP8.5, CNRM-CM5 under RCP8.5, CSIRO-Mk3-6-0 under RCP8.5, and INM-CM4 under RCP8.5 showed a few extreme events of no flow predictions.

There is not enough evidence available for the occurrence of this uncertainty. This might be due to the uncertainties in downscaled temperatures in the GCMs. A mitigation approach to avoid this uncertainty in individual models is a model ensemble forecasting procedure.

4.2.3 Model ensemble forecast of low flow

A comparison is made between all the six models to reveal how the general trend of the low flow changes. The comparison for all RCP 4.5 models is shown in Figure 4.27. The comparison for all RCP 8.5 models is shown in Figure 4.28. It is evident from the figures that under RCP8.5 the low flow value by end of this century is expected to increase more than RCP4.5. It has also been observed that uncertainties exist in different models such as occurrence of extreme events. To reduce these effects on the forecast of low flow, a model ensemble is approach is used.

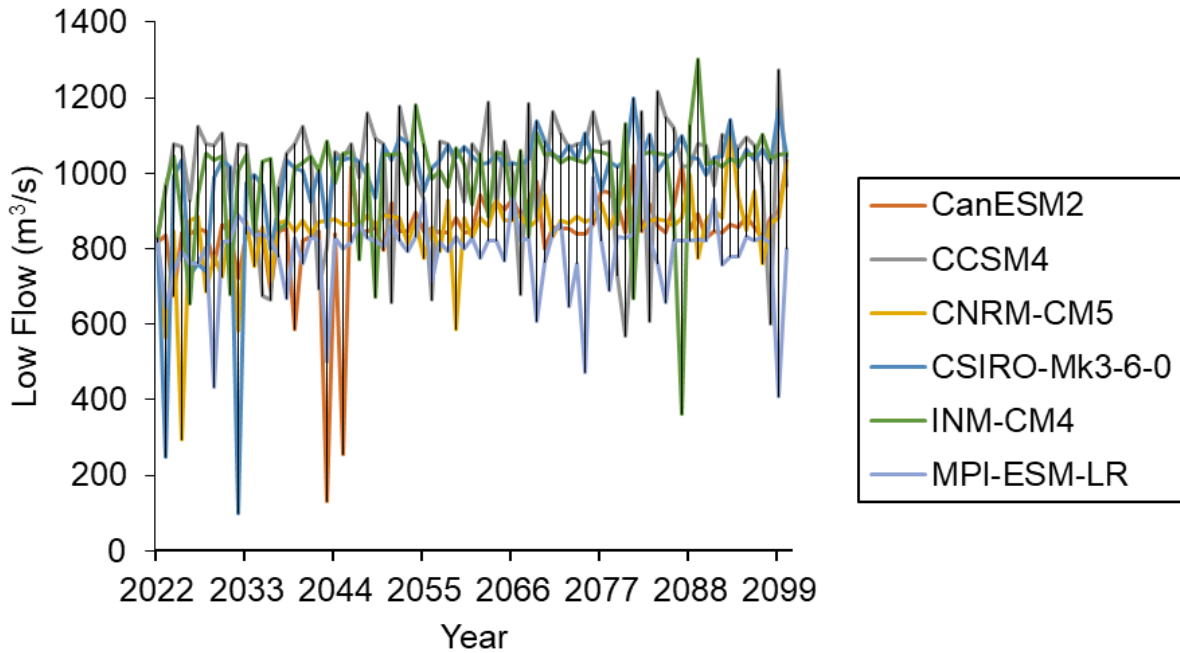


Figure 4.27 Forecast summary of low flow for RCP 4.5, on the basis of temperature (Predicted minimum discharge below 100 m³/s has been discarded).

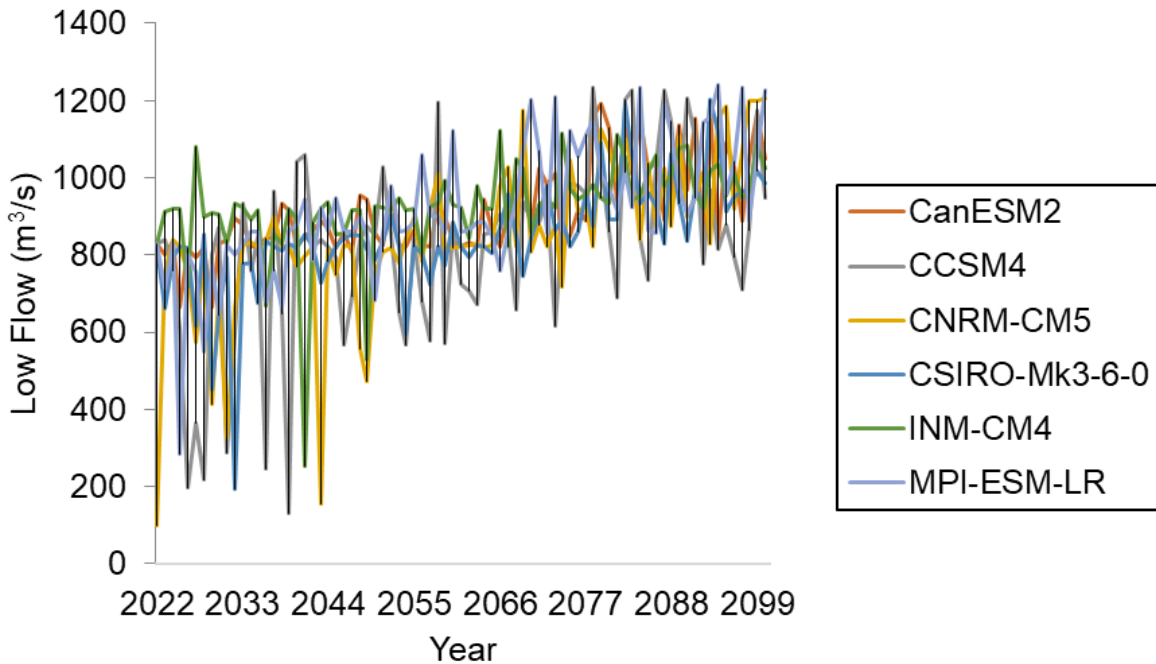


Figure 4.28 Forecast summary of low flow for RCP 8.5, on the basis of temperature (Predicted minimum discharge below 100 m³/s has been discarded).

Combined model forecast results under RCP 4.5 are shown in Figure 4.29Figure 4.30.

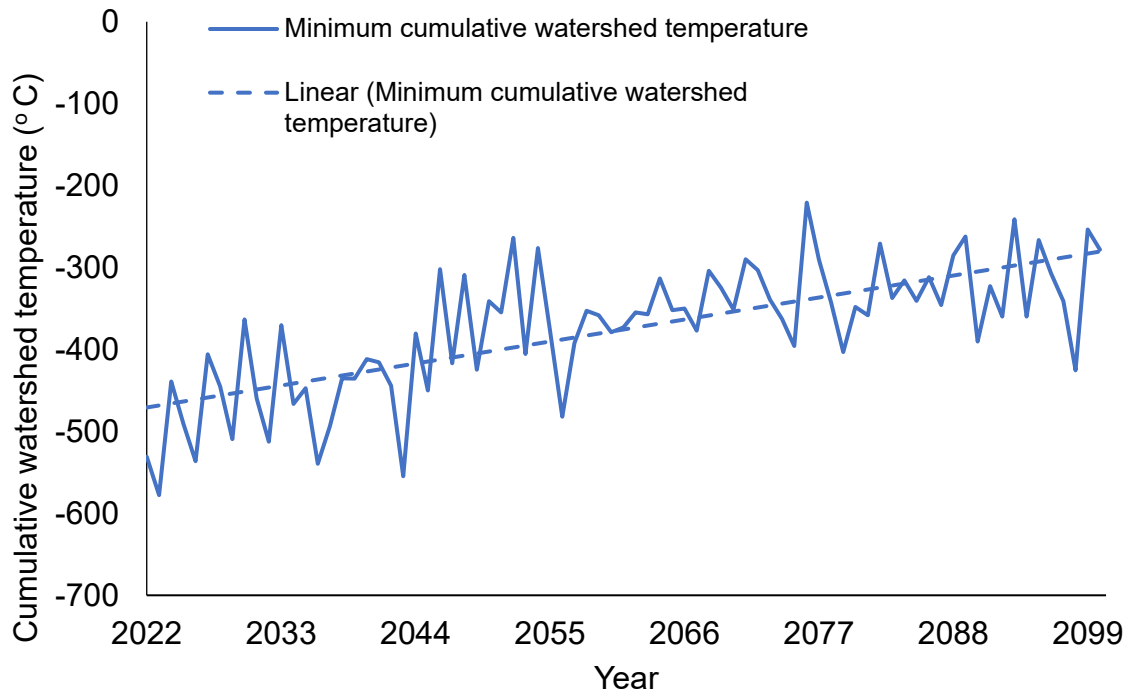


Figure 4.29 Combined model forecast of cumulative watershed temperature for RCP4.5

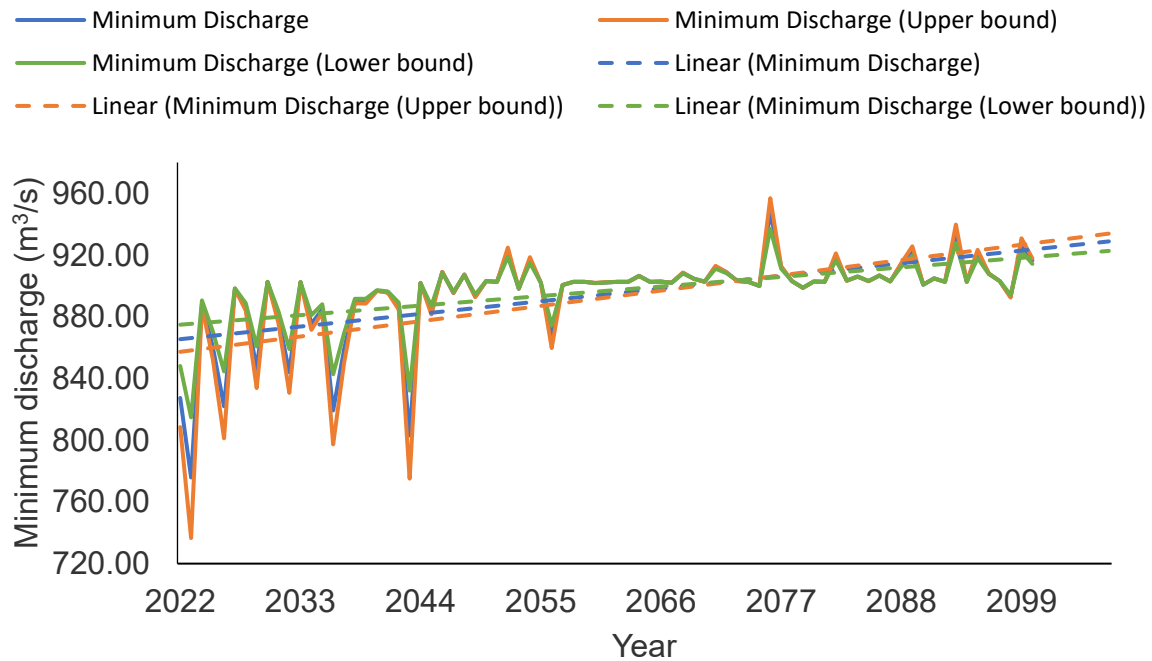


Figure 4.30 Combined model forecast of minimum discharge for RCP 4.5, on the basis of temperature.

Combined model forecast results under RCP 8.5 are shown in Figure 4.31Figure 4.32

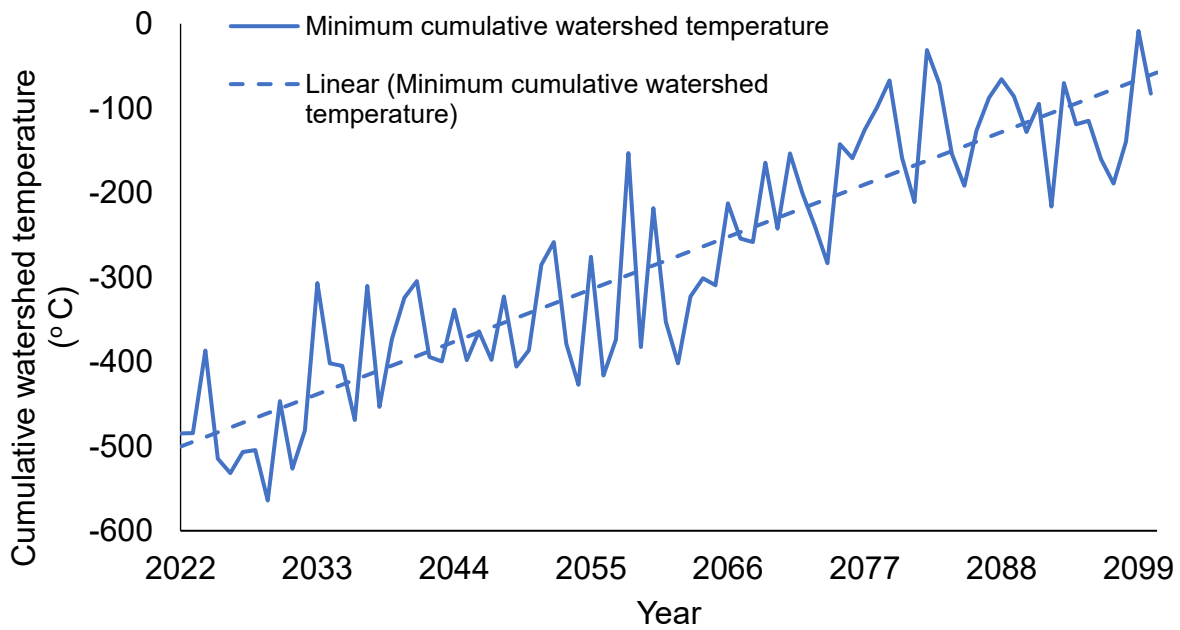


Figure 4.31 Combined model forecast of cumulative watershed temperature for RCP8.5

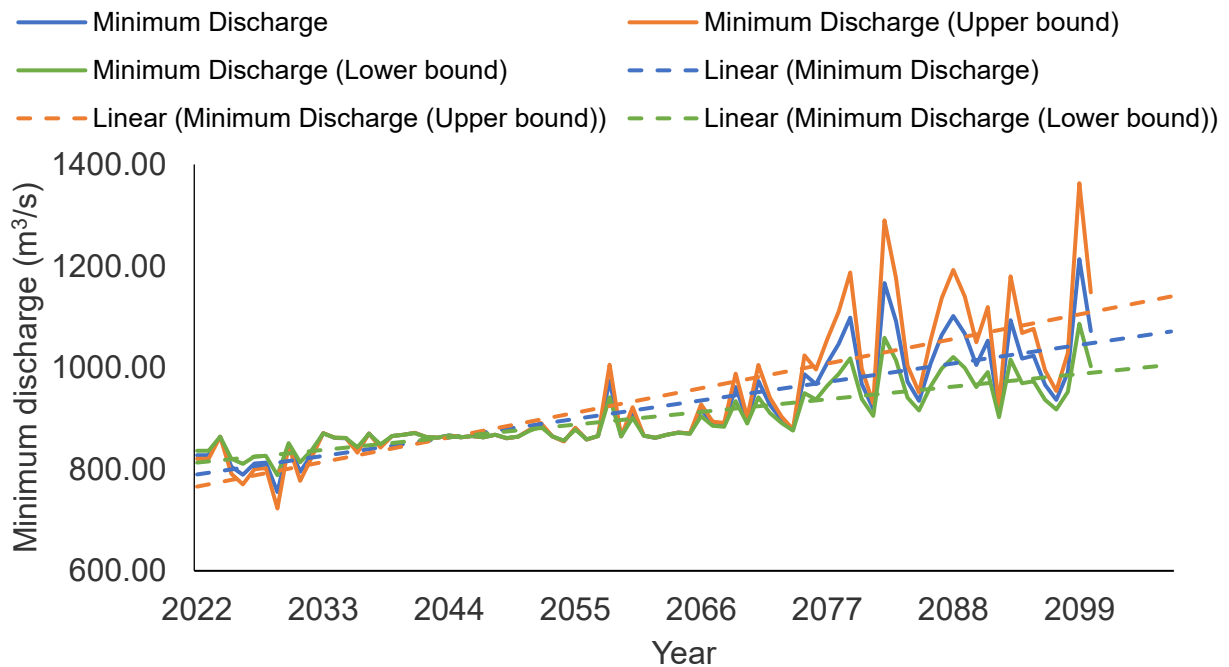


Figure 4.32 Combined model forecast of minimum discharge for RCP 8.5, on the basis of temperature.

The combined model forecast under RCP4.5 shows an increase in the low flow by a range of 95 m³/s to 100 m³/s from the historic average annual minimum values. This is around a 11% increase in total discharge of the river in response to the increased temperature. There are a few extreme discharge events on a higher side. The maximum value of the extreme event is 956.84 m³/s by the second half of the 21st century, which is around 16% increase in the low flow. There are a few decrements in the low flow are also forecasted and the lowest being 775.01 m³/s, which is around 6% lower than the historical average of low flow.

The combined model forecast under RCP8.5 shows an increase in the low flow by a range of 172.6 m³/s to 394.6 m³/s from the historic average annual minimum value. This is around a 21% to 48% increase in total discharge of the river in response to the increased temperature. The range is based on 95% confidence interval. The maximum extreme event value of low flow forecasted is 1363.09 m³/s by the end of 21st century, which is around 65% increase in the low flow. The lowest forecasted value of low flow by the end of 21st century is 917.54 m³/s, which is around 11% higher than the historic average annual minimum value.

It is recommended to consider this increase in low flow in the upcoming years in the design of hydraulic structures in the Fraser River. An increase of 39% in the future low flow suggests the necessity of considering this in the future design of river structures. Dredging and other activities related to the navigation in the Fraser River can benefit from this increase in low flow, whereas the life of aquatic species, especially salmon, may have to adapt to this changing low flow or their spawning season is affected. Further studies are needed to have a better understanding on the influence of this increasing low flow on the aquatic species. Discharges of waste water, for example, treated sanitary sewage from the Village of McBride, Village of Upper Fraser, the City of Prince George etc. (Ministry of Environment, Lands, and Parks, 1997) have to undergo regulatory changes based on the new low flow limits. It will be a similar case with industrial wastewater discharge regulations.

Wilby & Harris (2006) assessed the uncertainties in climate impact to low flows in River Thames, UK, and forecasted that summer low flows decrease by 2080. A 70%

chance of decrease in low flows (Q95) was estimated. This study was conducted to understand the impact of climate change to the public water supply, which was already facing deficit and drought was a hazard during summer. de Wit et al. (2007) forecasted the impact of climate change in the Meuse River, Europe and calculated the total discharge deficit of 292 Million m³/year. This was made to estimate the river water extraction to the canals during low flow. Also, the discharge during low flow was affected by the operation of weirs and reservoirs.

Ryu et al. (2011) conducted a climate change impact assessment on local hydrology and low flow frequency in the Geum River, Korea. There is a complex climate system which made it difficult to give concise climate and hydrologic estimates. There were other water issues in fish flow requirements, water quality control and public water supply. The forecast predicted an extreme low flow of 0.03 m³/s from the historic 1.54 m³/s during summer by the end of this century. This is 98% decrease in the summer low flow.

Forecast for the Fraser River shows 11% increase in low flows by the end of 21st century under low emission scenario of RCP4.5. An increase from 21% to 39% is forecasted under high emission scenario under RCP8.5 by the end of this century.

Forecast of low flow is made based on temperature inputs from General circulation models (GCM). GCMs are susceptible to uncertainties while forecasting future climate. This is because of the complexity in modelling physical processes, for example those associated to clouds. Errors in temperature in GCMs influences the forecast output as the low flow is estimated as a function of cumulative watershed temperature. There are uncertainties in feedback mechanisms, for example, water vapour and warming, clouds and radiation, ocean circulation and ice and snow albedo. (IPCC, 2020). Precipitation in wetter eastern coast mountains, below Texas creek, with winter rainfall will further increase the low flow (Ministry of Environment, Lands, and Parks, 1997).

Chapter 5

Conclusions and Future Studies

5.1 Concluding remarks

This research has developed analytical methods to determine the impacts of climate change on low flows of the Fraser River in British Columbia. The methods can be applied to other rivers in a cold region, where freezing temperatures and snowmelt play an important role in stream flow changes. The analyses presented in this thesis use of century long historic records of Fraser River discharges from Water Survey of Canada, and air temperatures from Environment and Natural Resources Canada. The following conclusions have been reached:

1. There exists a strong relationship between Fraser River low flows and cumulative watershed temperatures in the winter season. During the cold time period of the year, freezing effects and rising-temperature-induced snowmelt control the magnitude of the river low discharges. The established relationship describes discharge, Q , as a function of cumulative watershed temperature, τ .
2. The functional form contains empirical coefficients, whose values for the case of the Fraser River are reported in this thesis. One may obtain values for the coefficients applicable to other rivers in cold regions. With air temperature as its argument, this function is practical and convenient to use for the assessment of the impact of global warming on low discharge. The function is formulated in terms of z scores of

discharges and temperatures, making it easy for applications to other cold region rivers.

3. To quantify the influence of freezing temperatures on the river low flow, it is appropriate to add the consecutive daily mean temperatures from the first day of consistent sub-zero temperature until the thawing temperature is reached. Historical data of low flows should be split into two limbs: 1) falling limb of discharges associated with winter freezing; 2) rising limb of discharges due to subsequent thawing. The lowest flow of the year occurs at the intersection of these two limbs. The rising limb facilitates the assessment of the impact of climate change on river low flows.
4. It is important to remove outliers of flow data points from the rising limb for reliable assessment. This research identifies the outliers as possible deviations from the general patterns in temperature variations, caused by climatic oscillations of typical return periods.
5. Using the expected temperature increase reported for the British Columbia by the end of the 21st century, this research provides forecast of the variations in low flow of the Fraser River. The issue of uncertainties is dealt with by combining six GCM models from NASA NEX GDDP dataset of temperatures. Data from most of the six models leads to a significant increase in low flows. Data from CCSM4, INM-CM4 and MPI-ESM-LR gives almost negligible increment in low flows under RCP 4.5. The six-model ensemble gives an increase in low flow with increasing temperature due to climate change. The low emission scenario of RCP 4.5 causes a 11% increase in low flow by the year 2100, whereas the high emission scenarios of RCP 8.5 causes an increase from 21% to 48%.

5.2 Suggestions for future research

River low flows are an important topic. Further studies should consider the following directions:

1. The methods adopted in this study is exclusively for the forecast of future low flows in the Fraser River. The methods can be modified to accommodate other cold region rivers.
2. This study has taken into account the influence of air temperature on river low flow. Future studies should include other climate factors which affect river low flow such as variations in precipitation and atmospheric pressure due to climate change.
3. The established function for forecasting low flow is based on air temperature as the input variable. The coefficients in this function, a & b reflect the relationship between air temperature and low flow. As the discharge depends up on various sources of water like availability of snowpack, permafrost, and precipitation, these coefficients must be adjusted to include the influence of these sources of water for low stream flow. Also, with climate change, as the precipitation in the form of rain is expected to increase in parts of British Columbia, it will change the availability of snowpack and underlying permafrost that contribute to the low flow.

References

- Attard, M. E., Venditti, J. G., & Church, M. (2014). Suspended sediment transport in Fraser River at Mission, British Columbia: New observations and comparison to historical records. *Canadian Water Resources Journal / Revue Canadienne Des Ressources Hydriques*, 39(3), 356–371. <https://doi.org/10.1080/07011784.2014.942105>
- Bennett, K. E., Werner, A. T., & Schnorbus, M. (2012). Uncertainties in Hydrologic and Climate Change Impact Analyses in Headwater Basins of British Columbia. *Journal of Climate*, 25(17), 5711–5730. <https://doi.org/10.1175/JCLI-D-11-00417.1>
- Bonsal, B., & Shabbar, A. (2011). *Large-Scale climate oscillations influencing Canada, 1900-2008*. Canadian Councils of Resource Ministers. http://publications.gc.ca/collections/collection_2011/ec/En14-43-4-2011-eng.pdf
- Bradley, R. W. (2012). *Coherent flow structures and suspension events over low-angle dunes: Fraser River, Canada* [Thesis, Environment: Department of Geography]. <http://summit.sfu.ca/item/12417>
- Burn, D. H., Buttle, J. M., Caissie, D., MacCulloch, G., Spence, C., & Stahl, K. (2008). The Processes, Patterns and Impacts of Low Flows Across Canada. *Canadian Water Resources Journal*, 33(2), 107–124. <https://doi.org/10.4296/cwrj3302107>
- Bush, E., Lemmen, D. S., Canada, & Environment and Climate Change Canada. (2019). *Canada's changing climate report*. http://publications.gc.ca/collections/collection_2019/eccc/En4-368-2019-eng.pdf
- Buytaert, W., Célleri, R., & Timbe, L. (2009). Predicting climate change impacts on water resources in the tropical Andes: Effects of GCM uncertainty. *Geophysical Research Letters*, 36(7). <https://doi.org/10.1029/2008GL037048>
- Cameron, E. M., Hall, G. E. M., Veizer, J., & Krouse, H. R. (1995). Isotopic and elemental hydrogeochemistry of a major river system: Fraser River, British Columbia, Canada. *Chemical Geology*, 122(1), 149–169. [https://doi.org/10.1016/0009-2541\(95\)00007-9](https://doi.org/10.1016/0009-2541(95)00007-9)

- Cannon, A. J. (2015). Selecting GCM Scenarios that Span the Range of Changes in a Multimodel Ensemble: Application to CMIP5 Climate Extremes Indices. *Journal of Climate*, 28(3), 1260–1267. <https://doi.org/10.1175/JCLI-D-14-00636.1>
- Carver, M., Weiler, M., Stahl, K., Scheffler, C., Schneider, J., & Naranjo, J. a. B. (2009). Development of a low-flow hazard model for the Fraser basin, British Columbia. *Mountain Pine Beetle Working Paper - Pacific Forestry Centre, Canadian Forest Service, No.2009-14*. <https://www.cabdirect.org/cabdirect/abstract/20103033141>
- Chhetri, B. K., Galanis, E., Sobie, S., Brubacher, J., Balshaw, R., Otterstatter, M., Mak, S., Lem, M., Lysyshyn, M., Murdock, T., Fleury, M., Zickfeld, K., Zubel, M., Clarkson, L., & Takaro, T. K. (2019). Projected local rain events due to climate change and the impacts on waterborne diseases in Vancouver, British Columbia, Canada. *Environmental Health*, 18(1), 116. <https://doi.org/10.1186/s12940-019-0550-y>
- Dashtgard, S. E. (2011). Neoichnology of the lower delta plain: Fraser River Delta, British Columbia, Canada: Implications for the ichnology of deltas. *Palaeogeography, Palaeoclimatology, Palaeoecology*, 307(1), 98–108. <https://doi.org/10.1016/j.palaeo.2011.05.001>
- Dashtgard, S. E., Venditti, J. G., Hill, P. R., Sisulak, C. F., Johnson, S. M., & La Croix, A. D. (2012). Sedimentation Across the Tidal-Fluvial Transition in the Lower Fraser River, Canada. *The Sedimentary Record*, 10(4), 4–9. <https://doi.org/10.2110/sedred.2012.4.4>
- de Wit, M. J. M., van den Hurk, B., Warmerdam, P. M. M., Torfs, P. J. J. F., Roulin, E., & van Deursen, W. P. A. (2007). Impact of climate change on low-flows in the river Meuse. *Climatic Change*, 82(3), 351–372. <https://doi.org/10.1007/s10584-006-9195-2>
- Easton, M. D. L., Kruzynski, G. M., Solar, I. I., & Dye, H. M. (1997). Genetic toxicity of pulp mill effluent on juvenile chinook salmon (*Onchorhynchus tshawytscha*) using flow cytometry. *Water Science and Technology; London*, 35(2–3), 347–355.
- Environment and Climate Change Canada. (2011, October 31). *Environment and Climate Change Canada*. <https://climate.weather.gc.ca/>

Gilhousen, P. (1990). *Prespawning mortalities of sockeye salmon in the fraser river system and possible causal factors*. International pacific salmon fisheries commission*.

Gustard, A., Bullock, A., & Dixon, J. M. (1992). *Low flow estimation in the United Kingdom*. Institute of Hydrology.

Hay, L. E., & McCabe, G. J. (2010). Hydrologic effects of climate change in the Yukon River Basin. *Climatic Change*, 100(3), 509–523. <https://doi.org/10.1007/s10584-010-9805-x>

IPCC. (2020). https://ipcc-data.org/guidelines/pages/gcm_guide.html

Islam, S, Déry, S. J., & Werner, A. T. (2017). Future Climate Change Impacts on Snow and Water Resources of the Fraser River Basin, British Columbia. *Journal of Hydrometeorology*, 18(2), 473–496. <https://doi.org/10.1175/JHM-D-16-0012.1>

Islam, S, Hay, R. W., Déry, S. J., & Booth, B. P. (2019). Modelling the impacts of climate change on riverine thermal regimes in western Canada's largest Pacific watershed. *Scientific Reports*, 9(1), 11398. <https://doi.org/10.1038/s41598-019-47804-2>

Jost, G., Weber, F., & Geo, P. (2013). *Potential impacts of climate change on bc hydro-managed water resources*. 28.

Kerkhoven, & Gan, T. Y. (2011a). Unconditional uncertainties of historical and simulated river flows subjected to climate change. *Journal of Hydrology*, 396(1), 113–127. <https://doi.org/10.1016/j.jhydrol.2010.10.042>

Kerkhoven, & Gan, T. Y. (2011b). Differences and sensitivities in potential hydrologic impact of climate change to regional-scale Athabasca and Fraser River basins of the leeward and windward sides of the Canadian Rocky Mountains respectively. *CLIMATIC CHANGE*, 106(4), 583–607. <https://doi.org/10.1007/s10584-010-9958-7>

Krishnappan, B. (2000). In Situ Size Distribution of Suspended Particles in the Fraser River. *Journal of Hydraulic Engineering*, 126(8), 561–569. [https://doi.org/10.1061/\(ASCE\)0733-9429\(2000\)126:8\(561\)](https://doi.org/10.1061/(ASCE)0733-9429(2000)126:8(561))

Li, S. S., Millar, R. G., & Islam, S. (2008). Modelling gravel transport and morphology for the Fraser River Gravel Reach, British Columbia. *Geomorphology*, 95(3), 206–222. <https://doi.org/10.1016/j.geomorph.2007.06.010>

MacLean, K. (2009). *Map_basin_overview_2009.pdf*.
https://www.fraserbasin.bc.ca/_Library/Maps/map_basin_overview_2009.pdf

McLean, D. G. (1990). *The relation between channel instability and sediment transport on Lower Fraser River* [University of British Columbia].
<https://doi.org/10.14288/1.0302167>

Ministry of Environment, Lands, and Parks. (1997). *Water Quality Assessment and Objectives for the Fraser River From Moose Lake to Hope*.
https://www.for.gov.bc.ca/hfd/LIBRARY/FFIP/BCMoE1997_A.pdf

NASA. (2020). <https://www.nccs.nasa.gov/services/data-collections/land-based-products/nex-gddp>

Neilson-Welch, L., & Smith, L. (2001). Saline water intrusion adjacent to the Fraser River, Richmond, British Columbia. *Canadian Geotechnical Journal*, 38(1), 67–82. <https://doi.org/10.1139/t00-075>

Pachauri, R. K., Mayer, L., & Intergovernmental Panel on Climate Change (Eds.). (2015). *Climate change 2014: Synthesis report*. Intergovernmental Panel on Climate Change.

Pacific Climate Impacts Consortium. (2020).
<https://www.pacificclimate.org/data/statistically-downscaled-climate-scenarios>

PCMDI. (2020). <https://pcmdi.llnl.gov/>. <https://pcmdi.llnl.gov/mips/cmip5/availability.html>

Rempel, L. L., Richardson, J. S., & Healey, M. C. (1999). Flow Refugia for Benthic Macroinvertebrates during Flooding of a Large River. *Journal of the North American Benthological Society*, 18(1), 34–48. <https://doi.org/10.2307/1468007>

Rice, S. P., Church, M., Wooldridge, C. L., & Hickin, E. J. (2009). Morphology and evolution of bars in a wandering gravel-bed river; lower Fraser river, British Columbia,

Canada. *Sedimentology*, 56(3), 709–736. <https://doi.org/10.1111/j.1365-3091.2008.00994.x>

Ryu, J. H., Lee, J. H., Jeong, S., Park, S. K., & Han, K. (2011). The impacts of climate change on local hydrology and low flow frequency in the Geum River Basin, Korea. *Hydrological Processes*, 25(22), 3437–3447. <https://doi.org/10.1002/hyp.8072>

Schaake, J. C., & Chunzhen, L. (1989). *Development and application of simple water balance models to understand the relationship between climate and water resources*. 10.

Schnorbus, M., Werner, A., & Bennett, K. (2014). Impacts of climate change in three hydrologic regimes in British Columbia, Canada. *Hydrological Processes*, 28(3), 1170–1189. <https://doi.org/10.1002/hyp.9661>

Sekela, M., Brewer, R., Baldazzi, C., Moyle, G., & Tuominen, T. (1999). Concentration and distribution of chlorinated phenolic compounds in Fraser River suspended sediment. *Aquatic Ecosystem Health & Management*, 2(4), 449–454. <https://doi.org/10.1080/14634989908656982>

Shrestha, R. R., Cannon, A. J., Schnorbus, M. A., & Alford, H. (2019). Climatic controls on future hydrologic changes in a subarctic river basin in Canada. *Journal of Hydrometeorology*, 20(9), 1757–1778. <https://doi.org/10.1175/JHM-D-18-0262.1>

Shrestha, R. R., Schnorbus, M. A., & Cannon, A. J. (2015). A Dynamical Climate Model–Driven Hydrologic Prediction System for the Fraser River, Canada. *Journal of Hydrometeorology*, 16(3), 1273–1292. <https://doi.org/10.1175/JHM-D-14-0167.1>

Shrestha, R. R., Schnorbus, M. A., Werner, A. T., & Berland, A. J. (2012). Modelling spatial and temporal variability of hydrologic impacts of climate change in the Fraser River basin, British Columbia, Canada. *Hydrological Processes*, 26(12), 1840–1860. <https://doi.org/10.1002/hyp.9283>

Smakhtin, V. U. (2001). Low flow hydrology: A review. *Journal of Hydrology*, 240(3), 147–186. [https://doi.org/10.1016/S0022-1694\(00\)00340-1](https://doi.org/10.1016/S0022-1694(00)00340-1)

Thomson, R. E. (1981). *Oceanography of the British Columbia coast*. Dept. of Fisheries and Oceans.

USGS, U. (2005). *Water Resources data—State, 2005*.

https://water.usgs.gov/ADR_Defs_2005.pdf

van Vliet, M. T. H., Franssen, W. H. P., Yearsley, J. R., Ludwig, F., Haddeland, I., Lettenmaier, D. P., & Kabat, P. (2013). Global river discharge and water temperature under climate change. *Global Environmental Change*, 23(2), 450–464. <https://doi.org/10.1016/j.gloenvcha.2012.11.002>

Wang, J. Y., Whitfield, P. H., & Cannon, A. J. (2006). Influence of Pacific Climate Patterns on Low-Flows in British Columbia and Yukon, Canada. *Canadian Water Resources Journal / Revue Canadienne Des Ressources Hydriques*, 31(1), 25–40. <https://doi.org/10.4296/cwrj3101025>

Whitfield, P. H. (2008). Improving the Prediction of Low Flows in Ungauged Basins in Canada in the Future. *Canadian Water Resources Journal*, 8.

Wilby, R. L., & Harris, I. (2006). A framework for assessing uncertainties in climate change impacts: Low-flow scenarios for the River Thames, UK. *Water Resources Research*, 42(2). <https://doi.org/10.1029/2005WR004065>

World Meteorological Organization (Geneva). (2008). *Manual on low-flow estimation and prediction*. WMO.

WSC. (2020).

https://wateroffice.ec.gc.ca/report/historical_e.html?stn=08MF005&dataType=Annual+Extremes¶meterType=Flow&mode=Graph&y1Max=1&scale=normal&year=2016&page=historical